POLITECNICO DI MILANO

Master of Science in Mechanical Engineering

Major in Ground Vehicle Engineering

POLITECNICO
MILANO 1863

TORQUE VECTORING CONTROL STRATEGIES FOR ELECTRIC VEHICLES WITH MULTIPLE MOTORS

Mechanical Engineering Department

Supervisors: Prof. Basilio Lenzo
Prof. Edoardo Sabbioni

Graduation Thesis by:
Andrea Mangia, 873799

Academic year 2018-2019

Ai veri amici

“Gli uomini non hanno più tempo per conoscere nulla. Comprano le cose già fatte nei negozi. Ma siccome non esistono negozi che vengono amici, gli uomini non hanno più amici. Se vuoi un amico, addomensticami!”

(Antoine de Saint-Exupéry)

Abstract

Road vehicles are going through one of the deepest transformation in their history. Pushed by progressively restrictive regulation on pollutant emission, electric vehicles are developing fast with almost all the main automotive companies proposing at least one full electric vehicle. This gives the possibility to develop new technologies such as Advanced Driver-Assistance Systems (ADAS) that are systems developed to automate, adapt and enhance vehicle systems for safety and better driving. One of the most interesting is *Torque Vectoring*, that consists in differentiating the torque on each wheel bringing to improve the vehicle performances in different aspects like dynamics, efficiency and safety. Electric vehicles ease the application of this technique since different motor and transmission configurations are possible, as the case of 4 independent motors, one for each wheel, that has been considered in this study. At the same time this controller is composed of different parts and the integration of all of them presents a certain degree of complexity. Another issue is the estimation of the vehicle state since this kind of controller requires typically different quantities and parameters of the vehicles. Estimation of those were not considered in this study to not excessively extend the area of focus, however the solution presented has a certain level of robustness to estimation errors. The study proposes a solution for this kind of controller showing how to integrate the different parts and how the vehicle behaviour can be influenced with different setting of the controller. This results in the implementation of the so called *driving modes*, selectable by the driver. Numerical tests show how each mode is a trade-off between performance and efficiency.

The research presented was developed at Sheffield Hallam University (UK), under the supervision of prof. Basilio Lenzo.

Acknowledgments

My heartfelt thanks are due to Professor Basilio Lenzo; my main supervisor of this thesis, for all his support during my time at Sheffield Hallam university. During my research he was an inspiring guide with his methodology of approach and advice, letting me to develop my work autonomously. Without him I could never have completed my research. Working besides him enriched me not only from a professional but also from a personal point of view.
In addition, I would like to thank Professor Edoardo Sabbioni who provided me with the vehicle model and the tyre data. His support was also important during the writing of the thesis to perfect each chapter and obtain better and clearer explanations.
My thanks are also due to Professor Federico Cheli who gave me the opportunity to develop my thesis abroad.
I would also like to mention Professor Giovanni Lutzemberger for the support and the data he provided me regarding the electric motor. It was a small but fundamental contribution.

A special thanks is due to to all my friends with whom I shared my time of study. We always supported each other and shared unforgettable moments.
Finally, I would like to mention my family who supported me morally and economically throughout my study period. Their help was fundamental to overcome the most difficult moments.

Contents

List of Figures

List of Tables

List of Symbols

Symbol	Quantity	Unit (SI)
a_x	Longitudinal acceleration of the centre of gravity of the vehicle	$\mathrm{m\,s^{-2}}$
a_y	Lateral acceleration of the centre of gravity of the vehicle	$\mathrm{m\,s^{-2}}$
a_y^*	Maximum extension of the linear region of the understeer characteristic	$\mathrm{m\,s^{-2}}$
$a_{y,MAX}$	Maximum achievable lateral acceleration of the understeer characteristic	$\mathrm{m\,s^{-2}}$
a	Front semi-wheelbase	m
b	Rear semi-wheelbase	m
c_1	Coefficient of the yaw index controller	–
c_2	Coefficient of the yaw index controller	–
C_x	Drag coefficient	
$C_{\alpha i}$	Axle tyre lateral stiffness	$\mathrm{Nm\,rad^{-1}}$
d_1	Coefficient of the Pacejka-MF	–
d_2	Coefficient of the Pacejka-MF	–
F_i	Tyre force of the i-th wheel	N
F_x	Longitudinal force on the centre of gravity of the vehicle	N
F_y	Lateral force on the centre of gravity of the vehicle	N
F_z	Vertical force on the centre of gravity of the vehicle	N
$F_{z,0}$	Reference vertical force of the tyre	N
$F_{z,ij}$	Vertical force on the i-th wheel	N
$F_{z,stat,ij}$	Vertical force on the i-th,j-th wheel in static conditions	N
g	Acceleration of gravity	$\mathrm{m\,s^{-2}}$
h	Centre of gravity height of the vehicle	m
I_Y	Yaw index	$\mathrm{rad\,s^{-1}}$
J_z	Moment of inertia about vertical axis	$\mathrm{kg\,m^2}$

K_{us}	Understeer coefficient	$\mathrm{rad\,m^{-1}\,s^2}$
k_i	Gain of the control system	$-$
L	distance of the P point from the centre of gravity of the vehicle in the driver model	m
l	Wheelbase	m
M_z, $M_{z,TV}$	Yaw moment introduced by torque vectoring	$\mathrm{N\,m}$
m	Total mass of the vehicle	kg
P_b	Base power of the motor power losses function	kW
R	Steering radius of the vehicle	m
R_w	Wheel radius	m
r	yaw rate	$\mathrm{rad\,s^{-1}}$
r_{MAX}	Maximum value of yaw rate in the control system	$\mathrm{rad\,s^{-1}}$
r_{ref}	Reference yaw rate	$\mathrm{rad\,s^{-1}}$
T	Torque of the motor	Nm
T_b	Base torque of the power losses function	Nm
T_{tot}	Total torque of the motors	Nm
t_r	Reaction time of the driver	s
v_x	Longitudinal speed of the centre of gravity of the vehicle	$\mathrm{m\,s^{-1}}$
$v_{x,i}$	Longitudinal speed of the i-th wheel hub	$\mathrm{m\,s^{-1}}$
$v_{x,i}^S$	Longitudinal slip speed of the i-th wheel hub	$\mathrm{m\,s^{-1}}$
v_y	Lateral speed of the centre of gravity of the vehicle	$\mathrm{m\,s^{-1}}$
$v_{y,i}$	Lateral speed of the i-th wheel hub	$\mathrm{m\,s^{-1}}$
$v_{y,i}^S$	Lateral slip speed of the i-th wheel hub	$\mathrm{m\,s^{-1}}$
V	Speed of the centre of gravity	$\mathrm{m\,s^{-1}}$
w	Track width	m
X_G	Longitudinal position of the centre of gravity for the global reference system	m
x	Longitudinal displacement of the centre of gravity of the vehicle	m
x_i	Longitudinal coordinate of the i-th wheel	m
Y_G	Lateral position of the centre of gravity for the global reference system	m
y	Lateral displacement of the centre of gravity of the vehicle	m
y_i	Lateral coordinate of the i-th wheel	m
z	Vertical displacement of the centre of gravity of the vehicle	m
z_i	Vertical displacement of the i-th wheel hub	m

α_i	Slip angle of the i-th tyre	rad
β	Sideslip angle of the centre of gravity of the vehicle	rad
β_i	Sideslip angle of the i-th axle of the vehicle	rad
β_{MAX}	Maximum value of the sideslip reference generator and control system	rad
β_{ref}	Reference sideslip angle	rad
γ_i	Camber angle of the i-th tyre	rad
ΔT_{LR}	Left-Right side variation of the motor torque	Nm
δ_{dyn}	Dynamic steer angle of the wheel	rad
δ, δ_i	Steer angle of the wheel	rad
δ_{kin}	Kinematic steer angle of the wheel	rad
δ_{sw}	Steering wheel angle	rad
ζ_{I_Y}	Decreasing coefficient for the steady state controller	–
η	Efficiency of the motor transmission	–
θ_i	Rotation of the i-th wheel about hub axis	rad
κ_i	Slip ratio of the i-th tyre	–
μ	Friction coefficient	–
σ_L, σ_R	Distribution coefficient of the motor torque of left and right side	–
τ	Motor transmission ratio of the i-th wheel and motor	–
τ_{sw}	Steering transmission rate	–
ψ	Yaw angle of the vehicle	rad
Ω_i	Angular speed of the i-th motor	$\mathrm{rad\,s^{-1}}$
Ω_b	Base angular speed of the motor power losses function	$\mathrm{rad\,s^{-1}}$
ω_i	Angular speed of the i-th wheel	$\mathrm{rad\,s^{-1}}$

Symbol	Meaning
CAN-bus	Controller Area Network bus
LQR	Linear Quadratic Regulator
NEDC	New European Driving Cycle
PID	Proportional Integral Derivative
SSC	Steady State controller
TV	Torque Vectoring
VDC	Vehicle Dynamic Controller
YI	Yaw Index

Chapter 1

Introduction

Road vehicles are going through one of the deepest transformation in their history. Pushed by progressively restrictive regulation on pollutant emission, electric vehicles are developing fast with almost all the main automotive companies proposing at least one full electric vehicle. At the same time the development of electronic is making available more powerful, cheaper computing systems and sensors that already have wide application in the automotive sector.

This is giving the possibility to implement new technologies and functions on road vehicles such as Advanced Driver-Assistance Systems (ADAS) that are systems developed to automate, adapt and enhance vehicle systems for safety and better driving.

However electric vehicles presents some problems that are limiting their diffusion, notably the limited autonomy and recharging time. The main advantages of an electric motor with respect to to a traditional internal combustion engine are the lower cost (both in term of purchase and maintenance) and its compactness. Consequently the application of multiple, independent actuators is now a viable solution, with different configurations that can be applied. Each motor can be controlled independently by requiring a different torque to each motor. This permits to to easily apply a control technique called **Torque Vectoring**, that consist exactly in applying different torque to different wheels creating a yaw moment that is able to influence the vehicle dynamics. By the use of sensors different data estimating the vehicle state can be gathered and, with proper algorithms, elaborated to allocate a specific torque to each wheel. The algorithm can be developed to achieve different optimisation objectives, including enhance vehicle *stability, performances and energy efficiency*. Potentially it could substitute some safety technology that are nowadays widely diffused on road cars, like Anti-lock Braking System (ABS) and Electronic Stability Control (ESC).

1.1 The Torque Vectoring control technique

This study focuses on the Torque Vectoring control technique. Torque vectoring consists basically in differentiating the torque on each powered wheel and its main advantage is to impose on the vehicle a yaw moment by differentiating torques on left and right side. As a consequence it is possible to influence the yaw dynamic of the vehicle (i.e. the behaviour of the vehicle to rotation about its vertical axes.) and in general improve its controllability.
This control techniques is already applied to commercial vehicles also with internal combustion engines. However in this cases its application is limited by the fact that there is a single motor whose torque have to be distribute to the wheel. Multiple motors is not a viable solution unless in case of hybrid solutions, in which electric motors supports the internal combustion engine. The compactness and cheapness of an electric motor permits to have a multiple motor vehicle with different configuration, making easier the application of Torque Vectoring since motors are controlled separately.
A notable example of Torque Vectoring applied with an internal combustion engine is the case of differential braking, where the brakes are used to decrease the torques on some wheels, producing a yaw moment. However this solution does not represent an ideal solution since it needs to dissipate part of the energy produced through brakes representing a non optimal solution from the efficiency point of view.
Other solutions are represented by the use of active differentials which does not represent an economic solution, limiting its use to high priced vehicles. In this study was thus selected a full electric vehicle.

1.2 General overview

Since this technique shows to have an easier application and wider advantages with electric vehicle it will be this case. Specifically the configuration analysed is the 4 wheels - 4 motors configuration where each wheel is controlled by a motor, that are all identical. This permits to analyse better the possibilities of Torque Vectoring being possible to differentiate the torque between right and left side but also between front and rear axle, which does not arise a yaw moment but may introduce other advantages.
A lot of research material is available for this kind of technology (Google Scholar research of the words "Torque Vectoring" provides almost 10'000 results) but at the same time each research paper tend to focus on a specific aspect of this controller rather than a complete solution, consequently it is one of the objective of this study to provide a solution for each part of the controller that are described in chapter 2, showing how their design is not completely independent from each other.

A Torque Vectoring controller takes as input the state of the vehicle and the driver's commands allocating the torque in a proper way, to optimise and improve a certain aspect considered in the criteria of distribution. In this study is showed how the controller can include different control objectives integrated in the controller. The two objectives considered are *efficiency* and *performance* of the vehicle between that there is a trade-off. The Torque Vectoring controller aims to set the vehicle behaviour on different optimal points of the trade-off line of these control objectives. This arises the creation of the so called driving modes, that permit to vary the setting of the controller and in consequence the effects in term of efficiency and performance.

Summarises the novelties introduced by this research are:

- Give a general overview of a Torque Vectoring controller showing how their design is not completely independent from each other.
- Showing how it is possible to integrate efficiency and performance control objectives in the controller showing how there is a trade-off line between them.
- Implementation of the driving modes in a Torque Vectoring controller showing how in case the energy efficiency is prioritised some part of the controller are not used or changes their logic.

1.3 Description of the work

The develop of the controller is preceded by a *paper review* regarding applications of the Torque Vectoring control technique, typically focusing on specific aspects of the control logic. Then is proposed a solution for each part of the controller to reach the declared objectives enunciated in the previous section, proposing new innovative approach where needed.
The proposed solution of the controller is developed for a 14 D.O.F. vehicle model, implemented on the PC programme MATLAB & Simulink, that is the main instrument used in the analysis. The program permitted also to carry on numerical simulations to test the proposed solution. Observation and comments on the results of the simulations complete the analysis process.

1.4 Thesis structure

The thesis is structured in the following manner:

In *Chapter 2* there is the resume of the paper review, where are explained the various part of the controller and some of the solution proposed by the literature.
In *Chapter 3* are illustrated the models used to design the controller and carry on the simulations, mentioning which modification were needed to make it suitable for the analysis.
The proposed solution of the controller is explained in *Chapter 4*.
Chapter 5 explains the simulations used to validate the controller and shows the results obtained.
Conclusions in *Chapter 6* summarise the purposes and results obtained by this thesis, along with some future perspective and possible further research.

Chapter 2

State of the art

Seen the number of papers regarding Torque Vectoring, it is evident how this control technique is very promising for future applications, especially with diffusion of electric vehicles. At the same time the complexity of this control technique makes arise various issues, notably estimations of vehicle state and definition of the control objectives to implement in the control system, in other words, the characteristic of the vehicle that the controller have to enhanced. Typically these are represented by performances and efficiency. By paper review results how solutions for control systems that aim to improve the dynamics performances of the vehicle results quite different with respect to to solutions that wants to maximise energy efficiency. However these two global objectives do not necessarily exclude each other as it is demonstrated in chapter 4. Mostly of the literature do not integrate these two aspects, rather focusing only on one of these two. Objective of this study is show that may be set a certain trade-off between efficiency and performance using Torque Vectoring by proper setting and configuration of the controller. This arise the implementation of the so called driving modes.
Figure 2.1 shows the typical structure of a Torque Vectoring controller according to main of the scientific literature. It is formed by three different main blocks: *Reference Generator*, *High Level controller* and *Low Level controller*.

In case the objective is to influence the dynamic behaviour of the vehicle a reference quantity is computed, based on the state of the vehicle (typically is in term of yaw rate but other quantity may be considered as explained in section 2.1). Then it is routed to an high level controller that computes a certain desired yaw moment M_z to follow the reference. At the same time a driver interpreter generate the desired total torque T_{tot} developed by motors that determines the desired longitudinal force and acceleration of the vehicle. These are sent to a low level controller that distributes the torque to each motor to obtain the desired total torque and yaw moment T_{tot} and M_z. It is important to note

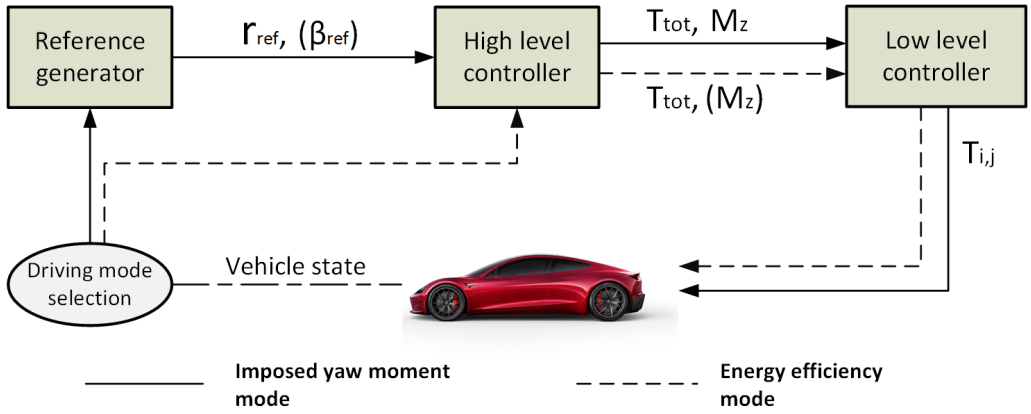

Figure 2.1: Typical structure of a Torque Vectoring controller

how in case of 4 electric motors the actuating system is redundant, as to obtain these two values is sufficient to differentiate the total torque on each side and still some consideration may be done to distribute the torque and obtain the desired T_{tot} and M_z. Conveniently this should be established aiming to energy minimisation [26].
Instead if the primary objective is to optimise the energy consumption only, no yaw reference have to be defined but algorithms calculate the optimal yaw moment that minimise energy consumption [14], or alternatively motor torques are directly defined in the low level controller applying an optimal distribution of the torques to obtain the total torque required by the driver. The optimal yaw moment is therefore defined implicitly defined [4], [12], [26], [5], [15]. These alternatives are analysed in section 2.3.

In a real vehicle is reasonable that these two cases of optimisation will be present, switching from one to the other by the definition of the so called driving modes, selectable by the driver [7]. So will be present a driving mode that can be called *"Energy Efficiency"*, that aim to optimise the energy consumption only. The other driving modes (ex. *"Normal"*, *"Sport"*) aim to influence somehow the dynamic behaviour of the vehicle by following a certain reference imposing a yaw moment explicitly. Each of these mode defines some characteristic or parameters of the controller, determining different behaviours for different Driving Modes.
So the Torque Vectoring controller design can be divided into these sub-problems:

- Definition of the Reference Generator
- Definition of the High Level controller
- Definition of the Low Level controller

2.1 Reference generator

The reference generator is the block that takes as input the driver's command along with measured or estimated vehicle states and by combining these information gives in output a certain yaw rate reference to follow. Then the controller tries to follow this reference by applying Torque Vectoring. For [17] and [7] the design of the reference generator modifies the cornering response of the vehicle to:

1. to reduce the understeer gradient with respect to the passive vehicle (i.e. the same vehicle plant without the TV controller)
2. to extend the region of linear cornering response
3. to extend the range of possible lateral accelerations for the available tire-road friction conditions

It is also fundamental that the state of the vehicle is considered as some of them are correlated with physical limits of the vehicle and because the driver's intention may fall outside those limits.

Most of the reference generator are based on tuning the understeer characteristic, in particular by setting a certain understeering coefficient K_{us} [23], [10], [5], [7], [15], [26].

An alternative significant formulation is found in [17], [28] where the reference is set by defining two thresholds r_h and r_s, the first dependent basically on driver's input and the second on friction limit considerations. The reference value is the weighted average of these two values, whose weights depends on the value of sideslip angle β, compared again to other two thresholds. For low value of β the reference will be equal to r_h, while for increasing values it approaches r_s till saturation, over a certain limit value β_{lim}. This is a notable example of how the sideslip angle β is considered in the reference generator as a correction of the yaw rate reference r_{ref} and it is not an output of this block. Is opinion of the authors that proposes this solution fundamental to keep into account also of this quantity.

Among the formulation relying on K_{us}, is particularly interesting the one firstly formulated in [6] and recalled by different papers. It is based on an experimental formulation of the understeer characteristic between the dynamic steer and the lateral acceleration. This is defined by setting three parameters: (i) the understeer gradient K_{us}, (ii) the lateral acceleration limit of the linear zone a_y^* and (iii) the maximum acceleration $a_{y,MAX}$. What the author propose is basically to try to extend the linear behaviour of the vehicle (where

$\delta_{dyn} = K_{us} a_y$) as well as the maximum absolute lateral acceleration. The author also points in [8] how these parameters has a physical meaning and that is an important characteristic for a reference generator. Indeed results difficult to tune a reference generator, whose parameters has no physical meanings.

By different setting of the reference generator can be obtained different vehicle behaviour as it was realised in [7]. The results are the so called driving mode that can be selected by the driver itself to adapt the vehicles behaviour as desired (i.e. improving the fun-to-drive, enhance energy efficiency or improve safety for low friction conditions).

2.2 High Level controller

The high level controller takes the references with drivers input and traduce them in commands of total torque required T_{tot} and yaw moment M_z. A Torque Vectoring controller is particularly sensible to the error estimation of the vehicles state. Indeed if excessive, the command produced may results in incorrect control of the vehicle due to incorrect reference generation that may lead to vehicle instability. In [25] the problem is dealt by introducing the a *Yaw Index* (YI) controller, along with a *Linear Quadratic Regulator* (LQR). The LQR shows to have good performances in steady state cornering conditions, where estimations are typically more reliable. If transient conditions are detected the YI produces a correction that avoid excessive increase of β angle and always tend to stabilise the vehicle. This second contribute is based on reliable estimations only that are commonly available in a CAN-bus of a vehicle. In this case the LQR requires a reference also on the sideslip angle and the controller try to follow both. These two control references, yaw rate and sideslip angle are indeed in contrast and the control action generated is a mediation of the two, depending on the set-up of the controller. An alternative way to guarantee robustness is to associate a sliding mode controller with the LQR, as in [11], [13], [24] and [3]. These needs also the same references.

PID controller are instead to be avoided as they do not guarantee any robustness. However in [19] is proposed an H_∞ *loop shaping* controller along with a PI controller, where the author bears to guarantee robustness and better performances with respect to a sliding mode controller.

2.3 Low Level controller

Being the efficiency always considered in each driving mode of the vehicle, it is important to define which physical phenomena (i.e. which power losses) are relevant and so to be

considered in the control torque allocator. In the case of petrol engine the relevant losses are mainly due to combustion efficiency, that prevails on other source of losses. Electric motors have an overall higher efficiency compared to internal combustion motors and consequently also other power losses became relevant, notably due to longitudinal and lateral slips of the tyres [7], and rolling resistance losses. Besides motor losses other source of energy dispersion are inverter losses, transmission losses and battery losses. The problem then is to determine which losses consider to make the optimisation.
In [14] are considered losses due to slip, rolling resistance, aerodynamic force, motor, inverter and transmission. These are computed with analytic function and in particular the slip losses are computed using a single track model with linear tyre model, showing how these are function of vehicle parameters, lateral acceleration and M_z, with a minimum for for yaw moment different from zero, and concordant to the yaw rate. [12] studies the distribution of the torque between front and rear axle on a vehicle that is proceeding on a straight line. Also in this case the losses are modelled with an analytic function of the copper losses and iron losses of the motors. The minimisation is performed by determining a distribution ratio of the torque k between front and rear axle, showing how Torque Vectoring is effective not only in cornering conditions and as the distribution of the torque between front and rear axle can brings relevant improvements.

Most solution proposed for the low level controller fail by needing estimator of quantities that are still not accurate or rely on quite expensive instruments. An effective solution was presented by [4] which considers only losses due to motor, inverter, transmission and longitudinal slips, along with the hypothesis of 4 identical and independent motors. The losses are modelled with a cubic polynomial function of the torque, whose coefficients are dependent on motor speed (but more state quantity may be included to improve model precision, like motor temperature) and the proposed solution to distribute the torque is analytic, dependent on the value of the coefficients. Effectiveness of a cubic function to be used for this purpose is confirmed in [18]. In [20] is used an equivalent formulation, a cubic function of torque and speed proving how this formulation has solid physical basis, since losses are directly or indirectly connected to these two quantities. The advantage to model the losses in this way rely also on not being dependent on low reliable estimation but only on motor angular speeds, and other parameters easy to measure directly or to estimate. However, a more general solution should be provided as a vehicle with 4 identical motor is not a granted technical solution (i.e. motors on front and rear axle may be different). This is the purpose of [16] where the coefficients are scaled so to permits to model different motors between front and rear axle.

In [4] slip losses are proved to be minor compared to motor and inverter one. In [5] and

[6] different efficiency optimisation functions are considered an compared showing how to optimise slip losses (or quantities related to it, such as standard deviation of longitudinal tyre sip) is slightly advantageous or equivalent to optimise input power losses, depending on motor technology. Vantages regard not only energy efficiency but also comfort, being the distribution of the torque in function of the vehicle state more regular.
However, to optimise slip losses is not actually viable as not good estimator are present nowadays, thus may be counter effective to consider them as well. Moreover to optimise motor and slip losses are not two completely different objective as optimising one lead to decrease the other and on the contrary conditions that leads to high motor losses are the same for slip losses (ex. high torque differences between motors). This explains results of [5] and [6].
Regarding battery losses, these are correlated mainly to the state of charge, with a little dependency on power required [1]. This falls outside the limits of analysis for this study, and may be neglected also because by minimising power losses it minimises also power input and consequently battery losses.

The problem of faced in a low level controller is basically a matter of torque distribution as the overall torque that influence the longitudinal acceleration is basically determined by the driver's input (acceleration and brake pedals). This is explicit with the formulation proposed in [15] where the torque at each wheel is determined by the overall torque required and 3 distribution factors. These are virtually two if a specific yaw moment is imposed. This is due to the fact that the configuration considered has a redundant system of 4 electric motors, so to determine the 4 torques are needed 4 equations or, in other words, 4 principles/constraints that determine how to distribute the torque on each wheel. As said one of them is the overall torque required, that is determined by interpreting driver's input (if this would be determined by energy efficiency the solution would be trivial, with all torques set to 0). Then if the objective is to improve the energy efficiency only, this is made by setting all the 3 factors with this purpose. Alternatively if the vehicle have to follow a certain reference the yaw moment have to be imposed and it is an output of the high level controller and consequently the distribution factors to be determined by energy efficiency in the low level controller are two, with the third implicitly determined by the yaw moment. Similar approaches are found in [3] and [22].

The determination of the optimal yaw moment is implicit if the energy efficiency algorithm is implemented directly in the low level controller with reference generator and high level controller that determines the yaw moment are excluded. However an alternative approach in which a function of the energy consumption with respect to the yaw moment and vehicle

state is possible and may be implemented, thus in this case the yaw moment is determined in the high level controller. However still in this case the logic to determine the yaw moment is completely different form the one used in case the dynamic of the vehicle is influenced by Torque Vectoring.
In the process of allocation some constraints must be considered to have a feasible solution. These are due to both motor limits and traction capacity limits. For [26] the limits are due to (i) actuator limits, (ii) actuator failure, (iii) friction limits and (iv) slip limitation. In [6] are considered also (v) battery power limitation and (vi) maximum braking friction coefficient.

Resuming while in the high level controller algorithm are concerned to interpret and follow drivers' desire and input the low level controller acts to allocate the torque (i) trying to respect high level commands and (ii) minimising power consumption for the remaining degrees of freedom.

Chapter 3

Models for dynamic simulations

3.1 Vehicle model: 14 *dofs* model

The Controller was developed and tested with a 14 degrees of freedom (DOFs) vehicle model. The model represents a segment D passenger car, as the proposed solution is meant to be applied on a vehicle who has not high performance motors and thus demonstrating that TV control technique can be applied successfully under these conditions.
The DOFs of the system (Figure 3.1) are:

- 6 dofs for the carbody: 3 displacements (x,y and z) and 3 rotations (yaw ψ, pitch λ and roll ρ)
- 4 dofs for wheels vertical displacements (z_i)
- 4 dofs for wheel rotation about hub axis (θ_i)

Vehicle parameters have been reported in Table 3.1. Contact forces between tyres and road are modelled according to MF-tyre model (Pacejka, 2012) [21], including combined slip effect and relaxation lengths. Suspension compliance is accounted by means of a look-up Table in order to speedup the simulation. The vehicle model was previously validated according to experimental tests performed with a correspondent real instrumented car. The results of the real vehicle were compared to the output of the model, confirming the consistency between the two [2].

3.1.1 Tyre model

Tyres forces are modelled according to combined slip MF-Tyre model [21].

$$F_i = D_i \sin C_i \arctan\{B_i x - E_i(B_i x - \arctan(B_i x))\} \tag{3.1}$$

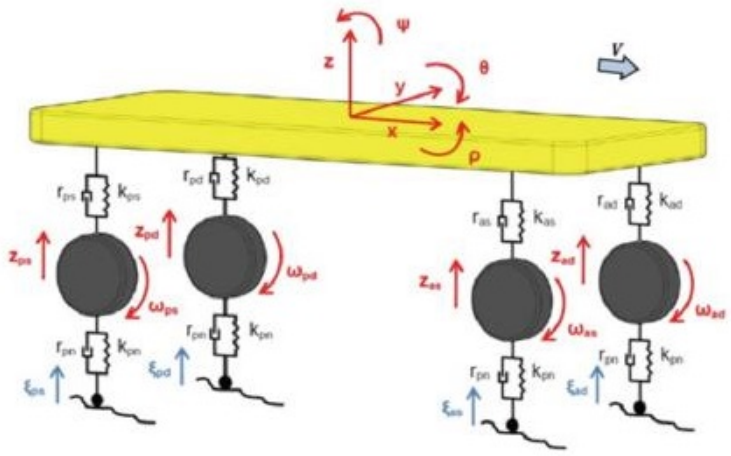

Figure 3.1: Degrees of Freedom of the vehicle model

Table 3.1: Main vehicle parameters.

Symbol	Name and unit	Value
m	Mass (kg)	1580
J_z	Moment of inertia, vertical axis (kg m^2)	2210
a	Front semi-wheelbase (m)	0.977
l	Wheelbase (m)	2.7
τ	Motor transmission ratio (-)	8.92
R_w	Wheel radius (m)	0.336
w	Track width (m)	1.592
h	Center of mass height (m)	0.55
C_x	Drag coefficient (-)	0.9
$C_{\alpha f}$	Front axle tyre lateral stiffness (Nm/rad)	$2.355 \cdot 10^5$
$C_{\alpha r}$	Rear axle tyre lateral stiffness (Nm/rad)	$2.196 \cdot 10^5$

Where x is slip ratio κ for longitudinal forces and slip angle α for lateral forces. B, C, D and E are coefficient determined by experimental test on tyre. MF-Tyre model used accounts for combined slip effect, vertical load dependency and for relaxation length.

slips and slip angles calculation

Slip ratios and slip angles are calculated as follow:

$$\kappa = \frac{v_{x,i} - \omega_i R_W}{v_{x,i}} \tag{3.2}$$

$$\alpha = \arctan\left(\frac{v_{y,i}}{v_{x,i}}\right) \tag{3.3}$$

Where ω_i is the angular speed of the wheels and R_W is the wheel radius. $v_{x,i}$ and $v_{y,i}$ are the lateral and longitudinal speed of each wheel and they are defined as:

$$v_{x,i} = \big(V\cos\beta - ry_i\big)\cos\delta_i + \big(V\sin\beta + rx_i\big)\sin\delta_i \tag{3.4}$$

$$v_{y,i} = -\big(V\cos\beta - ry_i\big)\sin\delta_i + \big(V\sin\beta + rx_i\big)\cos\delta_i \tag{3.5}$$

with the coordinates of the i-th wheel x_i and y_i defined according to Table 3.2.

Table 3.2: Coordinates of each wheel, coherent with sign conventions

Wheel	x_i	y_i
1 = Front left	a	$-\frac{w}{2}$
2 = Front right	a	$\frac{w}{2}$
3 = Rear left	-b	$-\frac{w}{2}$
4 = Rear right	-b	$\frac{w}{2}$

3.1.2 Slip power losses computation

Since the energy efficiency aspect is one of the criteria used to evaluate the effectiveness of the Torque Vectoring controller the power losses of the tyres were computed. Slip losses are defined as the product of the force developed by a tyres for its slip speed v_i^S. These are divided in longitudinal and lateral slip losses $P_{long,i}$ and $P_{lat,i}$, computed as:

$$P_{loss,tyre} = \sum_{i=1}^{4} P_{loss,tyre,i} = \sum_{i=1}^{4} \left(P_{long,i} + P_{lat,i}\right) \tag{3.6}$$

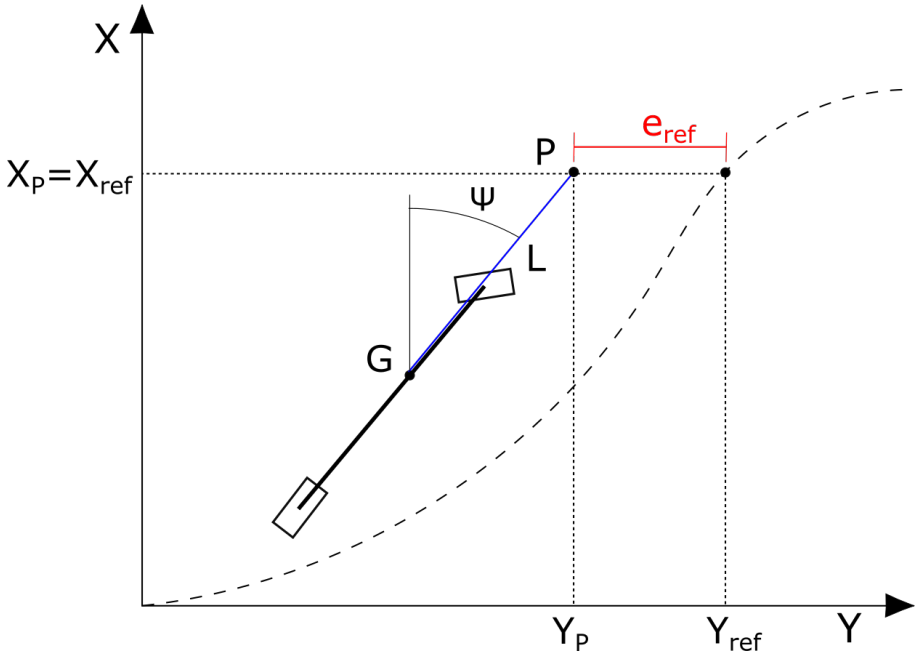

Figure 3.2: Driver model implemented in the vehicle.

where:

$$\begin{aligned} P_{long,i} &= |F_{x,i} v^S_{x,i}| \\ &\simeq \left|F_{x,i}\left[\left(V\cos\beta - r y_i\right)\cos\delta_i + \left(V\sin\beta + r x_i\right)\sin\delta_i - \omega_i R_W\right]\right| \end{aligned} \tag{3.7}$$

$$\begin{aligned} P_{lat,i} &= |F_{y,i} v^S_{y,i}| \\ &\simeq \left|F_{y,i}\left[-\left(V\cos\beta - r y_i\right)\sin\delta_i + \left(V\sin\beta + r x_i\right)\cos\delta_i\right]\right| \end{aligned} \tag{3.8}$$

$\omega_{W,i}$ is the angular speed of the i-th wheel, with rolling radius $R_{W,i}$; $F_{x,i}$ and $F_{y,i}$ are the longitudinal and the lateral tyre forces respectively; $V^S_{x,i}$ and $V^S_{y,i}$ are the slip speeds of the tyres in longitudinal and lateral direction respectively; $\delta_{W,i}$ is the steering angle of the i-th wheel, null for the rear wheels since it is a front steering vehicle. The coordinates of each wheel x_i and y_i are again defined according to Table 3.2.

3.1.3 Driver model

In the vehicle it was integrated a driver model to be used for some manoeuvres where the path to follow was imposed and the driver model acts on the steer to realise it.
The path is defined as a function $Y_R = Y_R(X_R)$, where X_G and Y_G are global coordinates. The steer of the driver is determined with a PD controller of a certain error, defined as:

$$\begin{aligned} e_{ref} &= Y_P - Y_{ref}(X_P) \\ &= \left(y + L\sin\psi\right) - Y_{ref}(y + L\cos\psi) \end{aligned} \tag{3.9}$$

Where the (X_P, Y_P) are the global coordinate of a point that stands in front of the vehicle centre of gravity at a distance L, as showed in Figure 3.2. It is called preview distance and is computed as:

$$L = Vt_r + \frac{1}{2}a_x t_r^2 \tag{3.10}$$

Where t_R is a constant, called reaction time of the driver. This permits to adapt the preview distance to the conditions of longitudinal acceleration and speed. V and a_x are the vehicle speed and longitudinal acceleration.

3.2 Single track model

In a Torque Vectoring application is typically required a reference model of the vehicle to design the controller. This model is the single-track model, that in this study was used to design the Linear Quadratic Regulator (LQR) introduced in section 4.2.2. The model is represented in Figure 3.3.

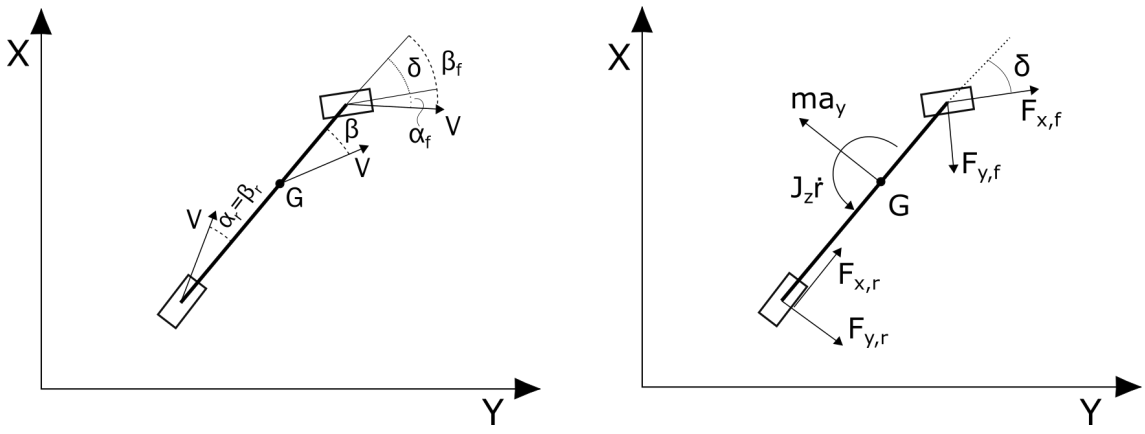

(a) (b)

Figure 3.3: Single track model

By making the equilibrium of forces in lateral direction and for yaw rotation is obtained:

$$\begin{cases} ma_y = \sum_i F_{x,i} \sin\delta_i + \sum F_{y,i} \cos\delta_i \\ J_z\dot{r} = -\sum_i y_i F_{x,i} + \sum x_i F_{y,i} + M_{z,TV} \end{cases} \tag{3.11}$$

Where $M_{z,TV}$ is the yaw moment introduced in the vehicle by Torque Vectoring controller, that is modelled as an input moment. In case of small steer angles δ_i, $\cos\delta_i \approx \delta_i$ and $\sin\delta_i \approx 0$ and considering that in the single track model $y_i = 0$ the equations became:

$$\begin{cases} ma_y \approx \sum F_{y,i} \\ J_z\dot{r} \approx \sum x_i F_{y,i} + M_{z,TV} \end{cases} \tag{3.12}$$

Lateral forces of the tyres are defined as:

$$F_{y,i} = -C_{\alpha,i}\alpha_i = -C_{\alpha,i}\big(\beta_i - \delta_i\big) \tag{3.13}$$

Where the sideslip angle β_i of front axle, rear axle and for the vehicle centre of gravity are defined as:

$$\beta_f = \arctan\left(\frac{v_{y,f}}{v_{x,f}}\right) = \arctan\left(\frac{v_y + ar}{v_x}\right) \simeq \frac{v_y + ar}{v_x} \tag{3.14}$$

$$\beta_r = \arctan\left(\frac{v_{y,r}}{v_{x,r}}\right) = \arctan\left(\frac{v_y - br}{v_x}\right) \simeq \frac{v_y - br}{v_x} \tag{3.15}$$

$$\beta = \arctan\left(\frac{v_y}{v_x}\right) \simeq \frac{v_y}{v_x} \tag{3.16}$$

Again With the hypothesis of small angles. As a consequence the slip angles at front and rear axle are respectively defined as:

$$\alpha_f = \beta_f - \delta = \frac{v_y + ar}{v_x} - \delta = \beta + \frac{a}{v_x}r - \delta \tag{3.17}$$

$$\alpha_r = \beta_r = \frac{v_y - br}{v_x} = \beta - \frac{b}{v_x}r \tag{3.18}$$

As the steering axle is only the front one ($\delta_r = 0$). Consequently forces on each axle are defined as:

$$F_{y,f} = -C_{\alpha,f}\alpha_f = -C_{\alpha,f}\left(\beta + \frac{a}{v_x}r - \delta\right) \tag{3.19}$$

$$F_{y,r} = -C_{\alpha,r}\alpha_r = -C_{\alpha,r}\left(\beta - \frac{b}{v_x}r\right) \tag{3.20}$$

Substituting the equation of the forces and rearranging the equations, the summations found in equation 3.12 became:

$$\sum F_{y,i} = \big(-C_{\alpha,f} - C_{\alpha,r}\big)\beta + \left(\frac{b}{v_x}C_{\alpha,r} - \frac{a}{v_x}C_{\alpha,f}\right)r + C_{\alpha,f}\delta \tag{3.21}$$

$$\sum x_i F_{y,i} = \big(-aC_{\alpha,f} + bC_{\alpha,r}\big)\beta + \left(-\frac{b^2}{v_x}C_{\alpha,r} - \frac{a^2}{v_x}C_{\alpha,f}\right)r + aC_{\alpha,f}\delta \tag{3.22}$$

In compact form:

$$\sum F_{y,i} = Y_\beta\beta + Y_r r + Y_\delta\delta \tag{3.23}$$

$$\sum x_i F_{y,i} = N_\beta\beta + N_r r + N_\delta\delta \tag{3.24}$$

where:

$$\begin{aligned} Y_\beta &= -\big(C_{\alpha f} + C_{\alpha r}\big) \\ Y_r &= -\frac{\big(aC_{\alpha f} - bC_{\alpha r}\big)}{V} \\ Y_\delta &= C_{\alpha,f} \\ N_\beta &= -\big(aC_{\alpha f} - bC_{\alpha r}\big) \\ N_r &= -\frac{\big(a^2C_{\alpha f} + b^2C_{\alpha r}\big)}{V} \\ N_\delta &= aC_{\alpha,f} \end{aligned} \tag{3.25}$$

Considering now the time derivative of sideslip angle defined in equation 3.16 for constant longitudinal speed v_x:

$$\dot{\beta} = \frac{\dot{v}_y}{v_x} \tag{3.26}$$

Lateral acceleration found in equation 3.12 is defined as:

$$a_y = \dot{v}_y - rv_x = \dot{\beta}v_x - rv_x \tag{3.27}$$

Using this definition and equations 3.23 and 3.24, equation 3.11 became:

$$\begin{cases} mv_x\big(\dot{\beta} + r\big) = Y_\beta\beta + Y_r r + Y_\delta\delta \\ J_z\dot{r} = N_\beta\beta + N_r r + N_\delta\delta + M_{z,TV} \end{cases} \tag{3.28}$$

In matrix form the equation 3.28 can be written as function of the state variables sideslip angle β and yaw rate r:

$$\begin{Bmatrix} \dot{\beta} \\ \dot{r} \end{Bmatrix} = \begin{bmatrix} \dfrac{Y_\beta}{mv_x} & \dfrac{Y_r}{mv_x} - 1 \\ \dfrac{N_\beta}{J_z} & \dfrac{N_r}{J_z} \end{bmatrix} \begin{Bmatrix} \beta \\ r \end{Bmatrix} + \begin{bmatrix} \dfrac{Y_\delta}{mv_x} \\ \dfrac{N_\delta}{J_z} \end{bmatrix} \delta + \begin{bmatrix} 0 \\ \dfrac{1}{J_z} \end{bmatrix} M_{z,TV} \tag{3.29}$$

in compact for written as:

$$\dot{x} = \big[A\big]x + \big[D\big]\delta + \big[B\big]M_{z,TV} \tag{3.30}$$

Where $\big[A\big]$ is the control variable coefficient matrix, $\big[D\big]$ is the input coefficient matrix of the steer and $\big[B\big]$ is the input coefficient matrix of the Torque Vectoring control action.

3.3 Motor model

The model is driven by 4 on-board electric motors, modelled from a mechanical point of view. To account for power losses was used the efficiency map to obtain the power losses function, that includes both motor and inverter losses. In Figure 3.4 are represented the motor characteristic curves. Figure 3.5 shows the motor efficiency map.
The power losses were computed with the formula proposed in [20] that is:

$$P_{loss,i}(T_i, \Omega_i) = \sum k_{mn} \left(\frac{T_i}{T_b}\right)^m \left(\frac{\Omega_i}{\Omega_b}\right)^n P_b \qquad m, n = 1, 2, 3 \tag{3.31}$$

Where T_b, Ω_b and P_b are 3 constant values that for this case are 100 Nm, 11000 rpm and 13 kW respectively. Their purpose is to normalise the coefficients, avoiding them to have values excessively small or high, but instead appreciating their real impact on the motor losses. The exponents n and m go from 0 to 3. The selected formulation has solid physical basis as the phenomena of losses are directly or indirectly connected with motor torque and speed [20]. Table 3.3 contains the values of the coefficients for the implemented motor, obtained from the interpolation of the efficiency map that gives the value of η and computing power losses as:

$$P_{loss,i} = T_i \times \Omega_i \times \frac{1 - \eta_i(T_i, \Omega_i)}{\eta_i(T_i, \Omega_i)} \tag{3.32}$$

Table 3.3: Normalised loss coefficients for the motor model

	1	Ω	Ω^2	Ω^3
T^3	0.4086	-	-	-
T^2	-0.0759	0.5232	-	-
T	0.4348	-0.3820	0.2713	-
1	-0.06925	0.4543	-0.2196	0.08132

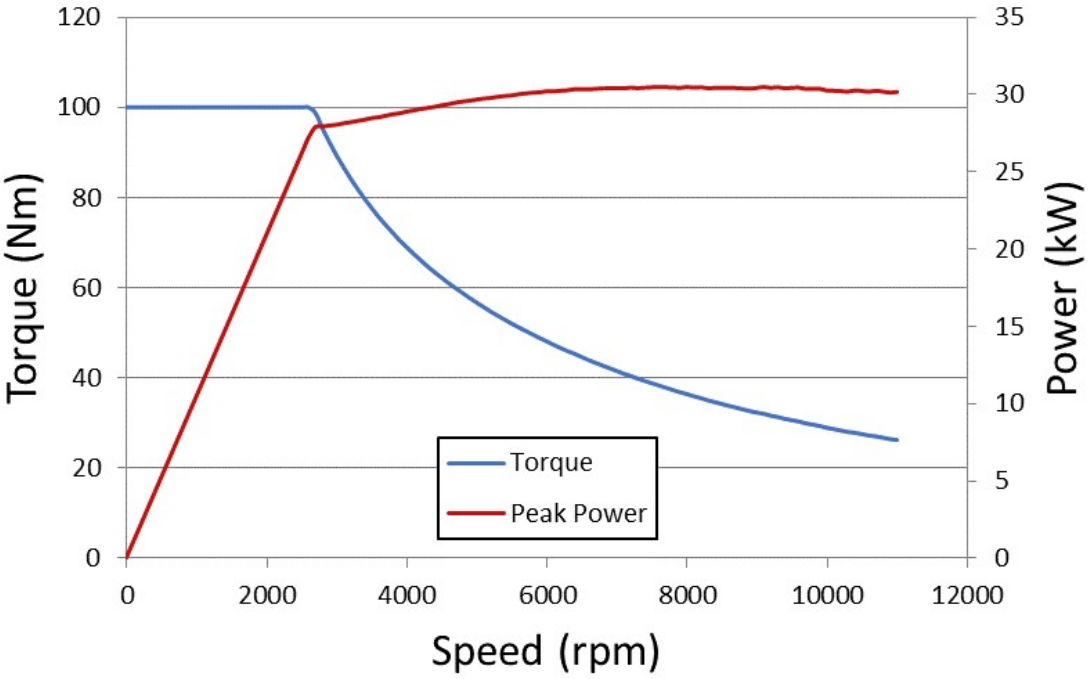

Figure 3.4: Motor characteristic curves. Torque and power in function of the angular speed

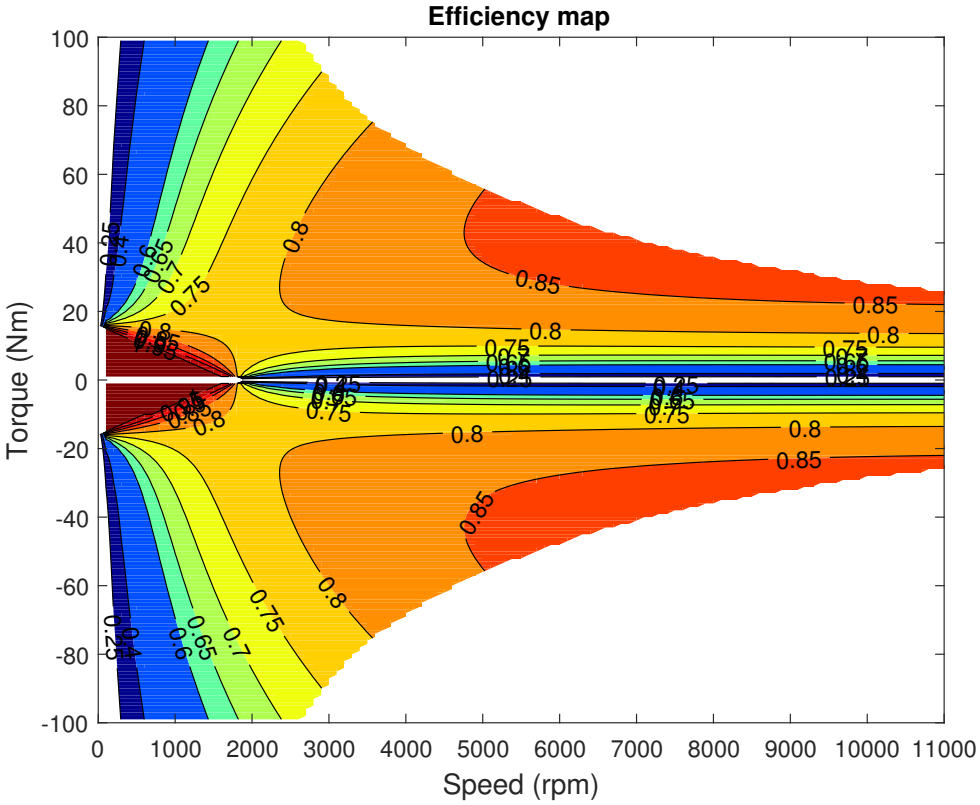

Figure 3.5: Efficiency map of the motor losses.

Chapter 4

Torque Vectoring control strategies

This chapter presents the proposed solution for each of the 3 main blocks described in chapter 2.

These are the same blocks introduced in chapter 2 and are: the *reference generator*, the *high level controller* and the *low level controller*. All these three blocks are active in case the purpose is to influence the vehicle dynamics. The reference generator is the block that gives in output some references, in this case in term of yaw rate and sideslip angle, generated in function of the state of the vehicle and the steer input of the driver. The yaw rate is computed with the specific task to impose a certain understeer characteristic to the vehicle. Sideslip angle is also considered to avoid excessive value of this quantity. The high level controller takes in input these references and tries to realise them producing a desired yaw moment control action M_z. This is the sum of two control logic: the Linear Quadratic Regulator and the Yaw Index controller, the first has good performances in steady state conditions while the second intervenes in case transient conditions are detected. At the same time the high level controller takes driver's input (of brake and throttle pedal) and traduce them in a desired total torque T_{tot}. Finally the low level controller distributes the torque to each wheel trying to respect the desired yaw moment and total torque, by differentiating the torques on each side. The longitudinal distribution of the torque on each side is made with an efficiency criteria. In case the objective is to use Torque Vectoring to maximise energy efficiency the reference generator block is not active, while the high level controller generate only a desired T_{tot}. The low level controller uses an efficiency logic to distribute the torque between left and right side, as well as the longitudinal distribution. This happens since the criterion used to optimise energy consumption are completely different by the one used to influence vehicle dynamic, as showed in section 4.3. In the controller are developed the so called driving modes that set some parameters in the reference generator and high level controller and selects the

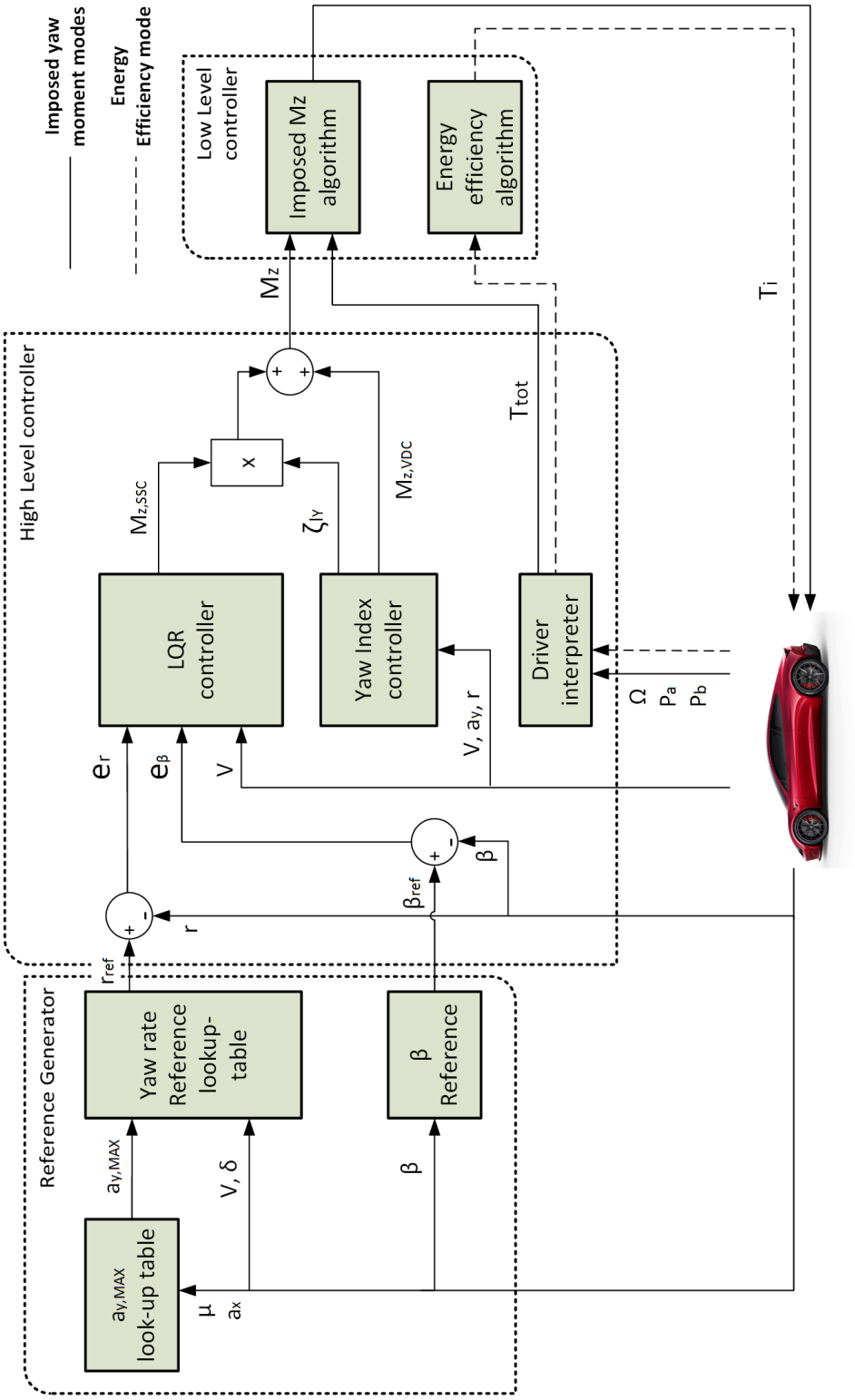

Figure 4.1: Scheme of the proposed controller showing each part of it.

appropriate torque distribution strategy. In case of efficiency optimisation only, the low level torque distribution strategy is the appropriated one and the other parameters are not assigned as not used in this specific control logic.

4.1 Reference generators

The reference generator is based on the solution proposed in [7]. It consists in defining a certain understeer characteristic curve to the vehicle, that the high level controller then try to make the vehicle to follow. By set of different parameters the curve and thus the behaviour of the car can be differentiated implementing the so called driving mode.

4.1.1 Yaw rate reference: the imposed understeer characteristic

The understeer characteristic is the curve that defines the steady state behaviour of a road vehicle. For (Wong, 2008) [27] in a single track model it is defined as:

$$\begin{aligned} \delta_{sw} &= \delta_{kin} + \delta_{dyn} \\ &= \frac{l}{R} + K_{us}\frac{V^2}{gR} \\ &= \frac{l}{R} + K_{us}\frac{a_y}{g} \end{aligned} \tag{4.1}$$

The two term of equation 4.1 are called respectively kinematic steer δ_{kin} and dynamic steer δ_{dyn}.

It defines that the steer angle required to negotiate a given curve is function of the wheelbase l, the steering radius R, lateral acceleration a_y (or speed V) and the so called understeer coefficient K_{us} that is expressed in radiant. Depending on the value of the understeer coefficient the vehicle, the steady state characteristic of a vehicle may be classified in three categories: *neutral steer*, *understeer* and *oversteer*.

With a $K_{us} = 0$ the second term of equation 4.1 is null thus the steer needed to face a certain curve is not dependent on the lateral acceleration. In the vehicle this is translated in equal sideslip angle at front and rear tyres (i.e. $\alpha_f = \alpha_r$). When approaching corner in steady state conditions the driver have to impose a certain steer angle that depends only on the corner radius R and not on the speed or lateral acceleration of the vehicle. This is indicated as neutral steer.

In case of $K_{us} > 0$ the sideslip angle at front tyres is greater compared to rear. (i.e. $\alpha_f > \alpha_r$). So when approaching a curve the required steer angle increase with the lateral acceleration (or with the square of vehicle speed). Equal steer input would produce a lower steering rate compared to a neutral vehicle (Figure 4.2. This is indicated as an understeer.

In case of $K_{us} < 0$ the sideslip angle at front tyres is smaller compared to rear. (i.e. $\alpha_f < \alpha_r$). So when approaching a curve the required steer angle decrease with the lateral acceleration (or with the square of vehicle speed). Equal steer input would produce an higher steering rate compared to a neutral vehicle. This is indicated as oversteer. With sufficiently high value of lateral acceleration or speed the vehicle may reach a null steering radius which means that the vehicle would face the phenomena of tailspin, and for this reason the oversteer behaviour is recognised as unstable. This speed is called critical speed.

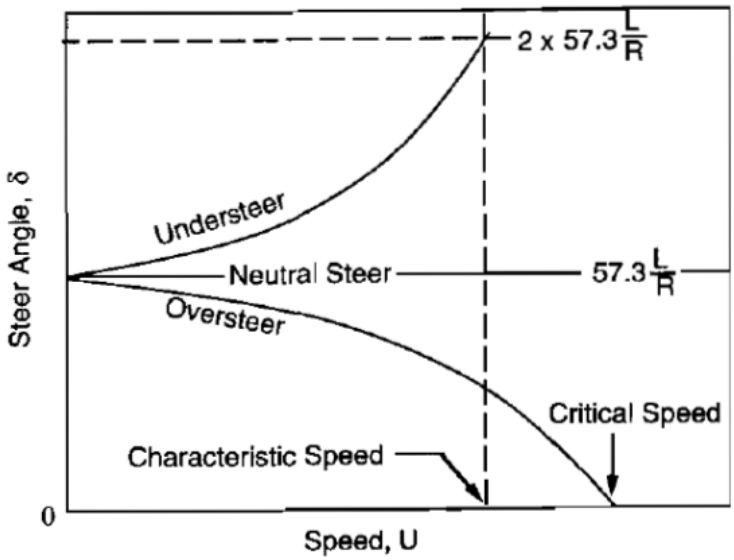

Figure 4.2: Over/understeering behaviour of a vehicle during cornering. Equal steering input produces different turning radius

By defining the second term of equation 4.1 is possible to fix the understeer behaviour of the vehicle and by a proper procedure translate this in a reference yaw rate r_{ref}. By applying Torque Vectoring the vehicle try to follows this reference and as a result it influences the understeer characteristic of the vehicle.
This approach is believed to be the best one because the understeer characteristic that is imposed has basically the same shape of the one of a real vehicle and the parameters to define it have a physical meaning, making easier to tune it. This is done by an experimental formula defined by the parameters: K_{us}, a_y^* and $a_{y,MAX}$

- $\mathbf{K_{us}}$ is the already mentioned understeering coefficient and in this specific case represents the initial slope of the curve.
- $\mathbf{a_y^*}$ is the maximum extension of the linear region of the characteristic
- $\mathbf{a_{y,MAX}}$ is instead the maximum achievable lateral acceleration of the curve.

This characteristic permits a better setting of the reference generator where each parameter influence a specific aspect of the understeer characteristic and so a specific aspect of the vehicle dynamic, as illustrated in Figure 4.3. Specifically the reference generator can (i) extend the linear region, (ii) extend the maximum lateral acceleration and (iii) increase the steering responsiveness of vehicle.

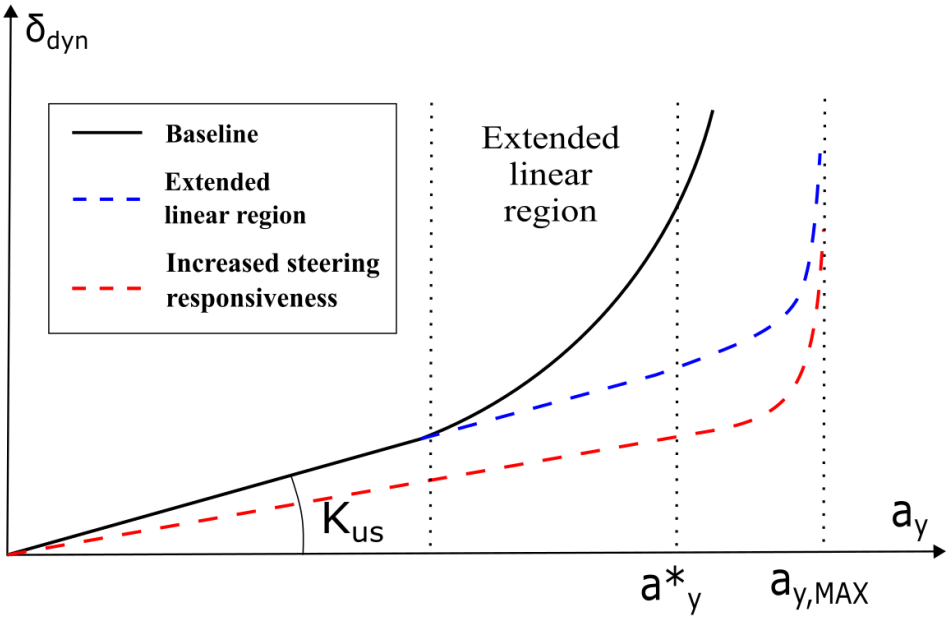

Figure 4.3: Example of reference understeering characteristics for the Torque Vectoring reference generator. The figure shows how a Torque Vectoring controller can vary the understeer characteristic.

By raising a_y^* is possible to extend the linear region while acting on $a_{y,MAX}$ is possible to increase the maximum lateral acceleration that the vehicle can sustain. By setting a lower value of understeering coefficient K_{us} is possible to have a more reactive vehicle, closer to a neutral vehicle (i.e. with $K_{us} = 0$) resulting in a more reactive steering responsiveness. These values are used in equation 4.3.
To impose a curve with a different shape would mean to try to make the vehicle's behaviour unnatural, making very difficult or impossible to follow the reference. On the contrary with this formulation is possible a good definition of the vehicle behaviour. For this motivations this formulation is believed to be the optimal solution.

As said the steering angle is defined by two contributes:

$$\begin{aligned}\delta_{sw}(a_y, V, a_x, \mu) &= \delta_{dyn}(a_y, a_x, \mu) + \delta_{kin} = \delta_{dyn}(a_y, a_x, \mu) + \tau_{sw}\left(l\frac{1}{R}\right) \\ &= \delta_{dyn}(a_y, a_x, \mu) + \tau_{sw}\left(l\frac{r_{ref}}{V}\right)\end{aligned} \tag{4.2}$$

The dynamic angle is computed by inverting the experimental formula 4.3, that defines the previously described understeer characteristic:

$$a_y = \begin{cases} \dfrac{1}{K_{us}\delta_{dyn}} & \delta_{dyn} \leq a_y^* K_{us} \\ a_{y,MAX}(a_x,\mu) + \big(a_y^* - a_{y,MAX}(a_x,\mu)\big) e^{\frac{K_{us}a_y^* - \delta_{dyn}}{(a_{y,MAX} - a_y^*)K_{us}}} & \delta_{dyn} > a_y^* K_{us} \end{cases} \tag{4.3}$$

Each of the parameter that defines this curve were defined in a specific way that slightly differentiate from the paper that propose this reference generator [7]. It suggests that all the three parameters of the curve should be dependent from longitudinal acceleration a_x and friction coefficient μ, without specifying what kind of correlation it was used, thus remaining generic. In this work is proposed a specific definition for these parameters.

Maximum lateral acceleration

The maximum lateral acceleration $a_{y,MAX}$ remains correlated with the friction coefficient because the maximum overall acceleration is strictly related to the maximum friction available, given the second law of the dynamic $F(\mu) = ma$, and with the longitudinal acceleration since the lateral acceleration a_y limit is decreased in case the longitudinal acceleration is not null, standing the relationship $a = \sqrt{a_x^2 + a_y^2}$.
In this study the maximum lateral acceleration is defined in function of the estimated friction coefficient and the load transfer provoked by the longitudinal and lateral acceleration. The friction coefficient for simplification is a constant value that is dependent on the driving mode selected but a more advanced implementation may include an estimator of the friction coefficient that defines this value, that was not included to not exceed the extension of the area of research.
Vertical loads are computed on front and rear wheel, in function of the static loads $F_{z,stat,ij}$, the longitudinal and lateral acceleration, a_x and a_y, as:

$$\begin{aligned} F_{Z,ij} &= F_{z,stat,ij} + \Delta F_{Z,ij} \\ &= F_{z,stat,ij} + \frac{-1^i}{2}\frac{mha_x}{l} + \frac{-1^j}{2}\frac{mha_{y,MAX}}{w}x_i \qquad i,j = 1,2 \end{aligned} \tag{4.4}$$

Where l is the track, w is the wheelbase and x_i are the distribution coefficient of the lateral load transfer on front and rear axle. Vertical loads are used along with the coefficients of the Pacejka Magic Formula that define the D coefficient, d_1, d_2 and $F_{Z,0}$, that represents the maximum force developed from the tyres $F_{tot,ij}^{MAX}$. The longitudinal acceleration defines instead the correspondent overall longitudinal force F_x.

$$F_{y,ij}^{MAX} = \sqrt{\underbrace{\Big[\Big(d_1 + d_2\frac{F_{Z,ij} - F_{Z,0}}{F_{Z,0}}\Big)\Big(F_{Z,stat,ij} - \Delta F_{Z0,ij}\Big)\Big]^2}_{D\ =\ F_{tot,ij}^{MAX}} - \big[F_{x,ij}\big]^2} \tag{4.5}$$

$$F_{x,ij} = \frac{1}{4} m a_x \tag{4.6}$$

d_1 coefficient represents the friction coefficient at the reference load $F_{Z,0}$. The coefficient d_2 represents instead the sensibility of the maximum tyre force to the vertical load variation. Given a set of μ and a_y The maximum lateral acceleration is finally defined as the smaller value between:

1. The lateral acceleration that maximises the lateral force $a_{y,MAX} = \sum \frac{F_{y,ij}^{MAX}}{m}$ solved with the set of equation 4.4, 4.5 and 4.6.

2. The lateral acceleration that null one of the vertical loads transfer computed with equation 4.4

In case (1) the computation is a recursive because a_y is present at both side of the equation and so a proper method of resolution was adopted. However this computation may brings to have a null or negative load on one of the wheel, that is physically impossible, and thus the model used would not be valid. For this reason was introduced case (2), that is also considered a safe condition to avoid the overturning of the vehicle, that would happen for two wheel on both side with null vertical load. The solution is computed offline and implemented in the reference generator as a look-up table with estimated friction coefficient and measured lateral acceleration as input and with maximum lateral acceleration $a_{y,MAX}$ as output.

maximum extension of the linear region and understeer coefficient

To have a smooth transition from the linear to the exponential region of the curve in 4.3, a_y^* is defined as the maximum value of acceleration $a_{y,MAX}$ decreased of 5 m/s^2 (or 0 in case this subtraction would result negative). Setting a constant difference between the two values of accelerations permits to have a constant wideness of the nonlinear area and thus a smooth transition from the two areas. Have to be kept in mind that still a considerable part of the nonlinear area defined with this formulation is in truth almost linear and so the real extension of the linear area is in practice higher than the value that is formally set in the formula with a_y^*. So is established a relationship of the kind $a_y = a_y(a_{y,MAX})$ and, as $a_{y,MAX}$ is correlated with a_x and μ, also a_y^* is indirectly correlated with these quantities. K_{us} is instead a constant, but the value used is dependent on the driving mode selected by the driver.
The resolution of the set of equation composed by 4.2 and 4.3 permits to create an other look-up table, which is function of steer angle, maximum lateral acceleration, speed and

understeer coefficient. This permits to defines the reference yaw rate r_{ref} as shown in Figure 4.4. Figure 4.5 shows the Simulink blocks related to the reference generator.

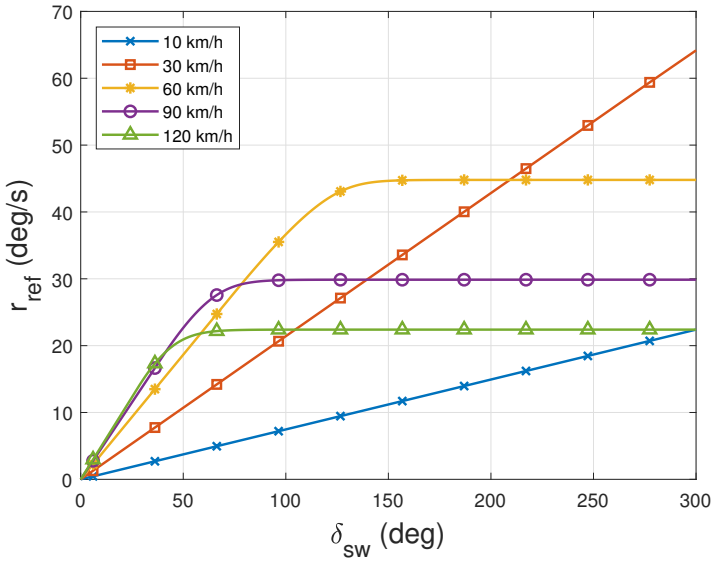

Figure 4.4: Map of the reference yaw rate $r_{ref,S}$ in function of the steer angle for various speed.

As can be observed the shape of the reference is similar to the one of the understeer coefficient (with inverted axis) and it has an initial constant slope that depends on the input parameters previously described, and it is at a certain point saturated, with a smooth transition. In Figure 4.4 is highlighted the dependency with the speed of the reference showing how increasing speed makes the slope of the curve higher but decrease the saturation value as for higher speeds the maximum yaw rate decrease because for equivalent yaw rate (i.e. equivalent curve radius) the lateral acceleration is higher for higher speeds.

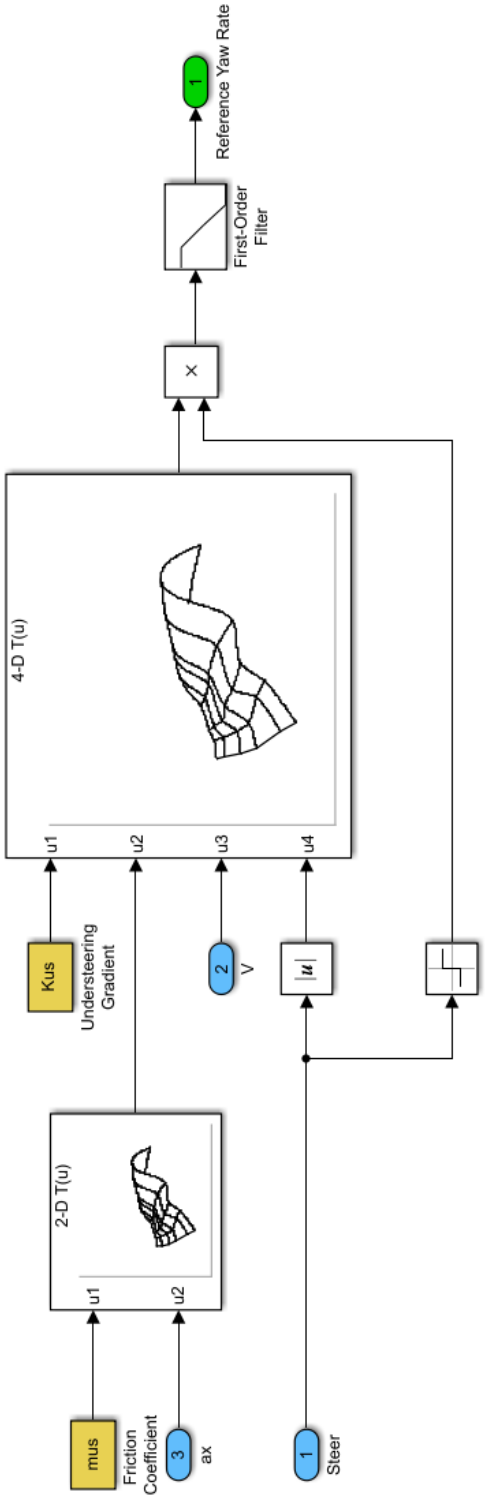

Figure 4.5: Blocks in the Simulink controller related to yaw rate reference generator

4.1.2 Sideslip angle reference

In the reference generator is important to keep into account the value of the sideslip angle β, in order to avoid it reaches excessive values. For this was implemented a simple reference generator β_{ref}, evaluated according to the formula:

$$\beta_{ref} = \beta_{MAX} \times \tanh\left(\frac{\beta}{\beta_{MAX}}\right) \tag{4.7}$$

Where β_{MAX} is a constant.

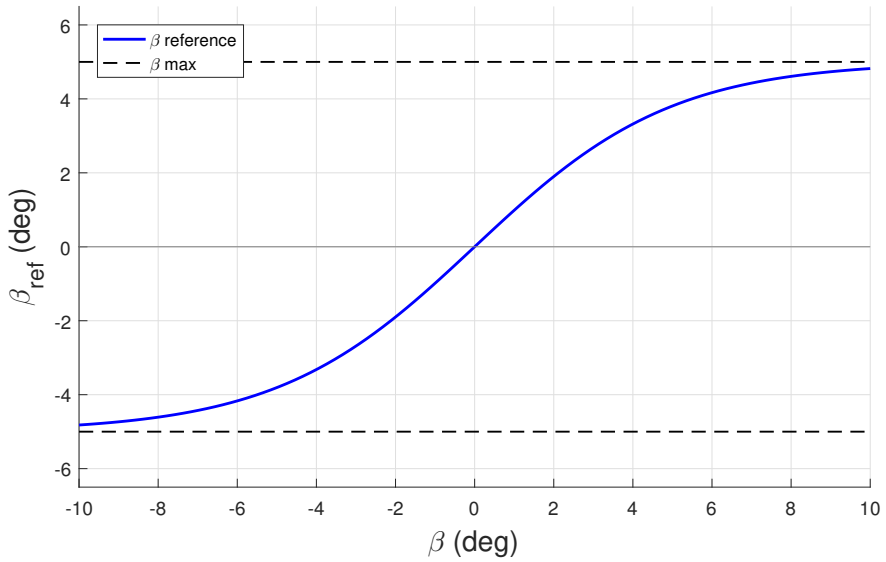

Figure 4.6: Sideslip angle reference. β_{MAX} value is set to 5 deg.

In Figure 4.6 is reported an example of β reference. As is quiet intuitive, the hyperbolic tangent impose a curve similar to the one of the yaw rate reference in Figure 4.4, with a saturation on β_{MAX}. Remembering that for $\beta \approx 0 \rightarrow \tanh\beta \approx \beta$ can be understood how with this formulation the sideslip angle is kept into account only when its value is high while for small sideslip angles $\beta_{ref} \approx \beta$ and the control action related tho sideslip error is almost null.

In the beta reference was introduced also a sign correction in order to have always the correct sign for the yaw moment, Always opposing to the increase of the absolute value of the yaw moment induced by the $M_{z,r}$ contribute due to yaw rate error.

This means to multiply the error for the sign of the yaw rate and beta angle. So the sign of $M_{z,\beta}$ will always be opposite to $M_{z,r}$. Table 4.1 resume this procedure. With the actual formulation of β_{ref}, always stands that $|\beta| > |\beta_{ref}|$, thus the sign of the error is always the opposite of the sign of actual sideslip angle β.

Table 4.1: Cases for the sign of $M_{z,\beta}$, showing how in each case the yaw moment is opposing to the increase of the yaw rate, to oppose excessive values of yaw moment.

		r	β	e_β	$M_{z,\beta} = sign(r)sign(\beta) \times k_\beta\, e_\beta$
Right turn	Oversteering	+	+	-	-
	Understeering	+	-	+	-
Left turn	Oversteering	-	-	+	+
	Understeering	-	+	-	+

4.1.3 Driving modes

As on of the main objective of this study, in the controller were introduced different driving modes, each influencing the vehicle dynamic in different manners. Each mode sets some specific parameters in the controller, in particular the one described in the reference generator, that has an important influence on the vehicle dynamics. In this specific case were developed 4 different modes:

1. Energy Efficiency mode
2. Normal mode
3. Sport mode
4. Low Friction mode

Each mode assign a specific value for K_{us}, estimated μ and β_{MAX} (Table 4.2). It is also meant to select the low level control logic (thus changing the control objectives), as explained in section 4.3.
In *Normal mode* the vehicle has the same understeer coefficient of the Baseline vehicle (i.e. the vehicle without the Torque Vectoring controller) and an estimated friction coefficient equal to 1. β_{MAX} is set to 5 deg. This mode is meant to increase the linear response of the vehicle without increasing the steering responsiveness at low lateral accelerations thus giving a more natural behaviour to the vehicle. This limits the intervention of the controller, containing the power consumption as confirmed in the results (chapter 5).
Passing to *Sport mode* K_{us} is decreased to 3/4 of the Baseline vehicle, determining an increased steering responsiveness also at low lateral accelerations. In this case the level of intervention of the controller is higher thus also the power consumption is expected to be higher. The other parameters are the same of Normal mode.
In *Low Friction mode* only changes the estimated friction coefficient, thus modifying the understeer characteristic imposed by the reference generator.

In all the mode described the yaw moment M_z is defined in the high level controller that tries to follow the references. The torque distribution strategy implemented with these modes in the low level controller thus tires to distribute the torque respecting if possible the desired value.

Radically different is the *Energy Efficiency mode*. As evidenced in the paper review in chapter 2 when the energy efficiency is prioritised in a TV controller the reference generator and the high level controller part that determines the yaw moment are excluded and the torque is determined by different algorithms that considers in their optimisation different quantities, frequently power losses due to motor and tyre slips or the sips itself. This implies that the Control strategy implemented in the low level controller is radically different. No value for K_{us}, μ and β_{MAX} are assigned in this mode and the torque distribution strategy is the specific one for this mode. Both these strategies are explained in section 4.3.

In a real vehicle the mode is supposed to be set through a physical selector or through a digital screen by the driver itself. In this way the driver can change at its pleasure the behaviour of the car. In the model the driving mode is selected before each simulation by a window menu.

Energy Efficiency mode has no assigned values for the reference generator because this block is not active in this specific mode.

Table 4.2: Assigned parameter for each driving mode. Each driving mode use specific value for the reference generator and a low level control strategy

Driving mode	K_{us}	estimated μ	β_{MAX}	Torque distribution strategy
Energy Efficiency	-	-	-	Energy Efficiency
Normal	$K_{us,baseline}$	1	5	Imposed M_z
Sport	$\frac{3}{4}K_{us,baseline}$	1	5	Imposed M_z
Low Friction	$K_{us,baseline}$	0.5	3	Imposed M_z

4.2 High level controller

The high Level controller used on this section is based on the control logic 1 presented in [25].
In general the output of the high level controller are basically two:

- The total required torque $\mathbf{T_{tot}}$.
- The desired yaw moment $\mathbf{M_z}$.

4.2.1 Total required torque

The total torque is dependent on the gas pedal position (p_a) that can be decided from the driver itself or by a cruise control logic. A general solution should include also a dependency on the brake pedal position (p_b), however it was not included for simplicity, since it was not necessary for the study. In the proposed controller it is defined as:

$$\sum_{i=1}^{4} \left[T_{max}(\Omega_i) - T_{min}(\Omega_i)\right] \times p_a + T_{min}(\Omega_i) \tag{4.8}$$

Basically the controller computes the maximum torque (in traction) and minimum torque (in regeneration) for each electric motor in function of the measured rotating speed Ω_k the difference of the two is multiplied for the throttle value, that goes from 0 to 1, and then summed again with the minimum value of torque. The value computed for each motor is summed and this defines the total torque required from the motor T_{tot}. Practically speaking the 0 position of the throttle (completely released) means to require the maximum regeneration torque from each engine and 1 position (full pressed) means to require from each engine the maximum traction torque. Each partial position of the throttle correspond to request a torque within these two limits, proportional to the throttle value itself. In the case of cruise control the throttle is determined by a PI controller on the speed error with respect to a certain reference value $e_{speed} = \left(V - V_{ref}\right)$.

4.2.2 Desired yaw moment

The desired yaw moment control action M_z is defined by the sum of two main contributes: the Steady State Controller (SSC) and the Vehicle Dynamic Controller (VDC):

$$M_z = M_{z,VDC} + \zeta_{I_Y} M_{z,SSC} \tag{4.9}$$

The SSC is meant to be used in steady state conditions while the VDC assures stability in transient conditions, especially in case of fast transient manoeuvres. This choice assures

robustness against estimation errors, fundamental for a Torque Vectoring controller. The coefficient ζ_{Y_I} is meant to decrease the SSC contribute when non steady state conditions are detected and the VDC is active, thus its purpose is to establish when rely more on the SSC or the VDC action, as its analysed is section 4.2.2.

Steady State Control

The SSC contribute is based on a Linear Quadratic Regulator (LQR), that is a typical solution for automotive applications. The reference model is the single track model:

$$\begin{cases} mV\left(\dot{\beta}+r\right) = Y_\beta \beta + Y_r r + C_{\alpha f}\delta \\ J_z \dot{r} = N_\beta \beta + N_r r + aC_{\alpha f}\delta + M_z \end{cases} \tag{4.10}$$

where:

$$\begin{aligned} Y_\beta &= -\left(C_{\alpha f} + C_{\alpha r}\right) \\ Y_r &= -\frac{\left(aC_{\alpha f} - bC_{\alpha r}\right)}{V} \\ N_\beta &= -\left(aC_{\alpha f} - bC_{\alpha r}\right) \\ N_r &= -\frac{\left(a^2 C_{\alpha f} + b^2 C_{\alpha r}\right)}{V} \end{aligned} \tag{4.11}$$

The force estimation is performed using the tyre stiffnesses of front and rear axle, $C_{\alpha f}$ and $C_{\alpha r}$. This choice was selected as at first approximation the cornering stiffnesses are not influenced by friction coefficient variation.
In compact form the equation can be written as:

$$\dot{x} = \left[A\right]x + \left[D\right]\delta + \left[B\right]M_z \tag{4.12}$$

with:

$$x = \begin{Bmatrix} \beta \\ r \end{Bmatrix} \tag{4.13}$$

And the matrix [A], [B] and [D] defined according to section 3.2.
The control input M_z is calculated minimising the following performance index:

$$J = \int_0^\infty \left(x^T \left[Q\right] x + M_z \left[R\right] M_z\right) dt \tag{4.14}$$

where the weight matrix [Q] and [R] are defined as:

$$\left[Q\right] = \begin{bmatrix} \frac{1}{\beta_{MAX}^2} & 0 \\ 0 & \frac{1}{r_{MAX}^2} \end{bmatrix} \qquad \left[R\right] = \left[\rho\right] \tag{4.15}$$

[Q] and [R] respectively penalise state deviation and excessive actuation of forces. It is important to note that the two objectives are in contrast with each other. In the computations it was set β_{MAX} at 5 or 3 deg, according to the driving mode as showed in Table 4.2, while maximum reference yaw rate $r_{max} = \frac{\mu g}{V}$, with friction coefficient according again to selected driving mode.

By solving the equation with a suitable Riccati equation, the matrix of the gains [G] is obtained by an offline computation, with a scheduling on the speed. In this case six speed were used (i.e. 40 km/h, 60 km/h, 80 km/h, 100 km/h, 120 km/h and 140 km/h). The control action of the SSC is thus:

$$M_{z,SSC} = -\Big[G\Big] e_x = \begin{bmatrix} k_\beta \\ k_r \end{bmatrix} \begin{Bmatrix} \beta_{ref} - \beta \\ r_{ref} - r \end{Bmatrix} \tag{4.16}$$

Where k_β and k_r are the gain computed with the described procedure.

The result of this computation, for the case of high and low friction coefficient are reported in Figure 4.7 and 4.8.

The gains have a similar evolution, with a strong dependency with speed as expected and thus confirming the necessity of the scheduling with respect to this quantity. Changing from high to low friction the order of magnitude of the gains related to the yaw rate changes. This happens because the reference maximum yaw rate r_{MAX} used in the weight matrix $\big[Q\big]$ decreases because decreases also the friction coefficient used for its computation, while the same maximum sideslip angle does not change that much. To balance this effect it was defined the maximum sideslip angle β_{MAX} at 3 deg for the Low Friction mode. This avoids to excessively penalise the yaw moment correction due to the sideslip angle error in low friction conditions.

Vehicle Dynamic Control

The VDC aims to stabilise the vehicle in transient conditions. It relies on an index, called Yaw Index I_Y that is correlated with the over/under-steering behaviour of the vehicle and it is based only on estimations that are normally available in a commercial vehicle and, whose approximation is never excessive, since they rely on well established methodologies and instruments. The control action is simply the product for the Yaw Index with a control gain k_Y:

$$M_{z,VDC} = k_Y \times I_Y \tag{4.17}$$

$$I_Y = \frac{a_y}{V} - r \tag{4.18}$$

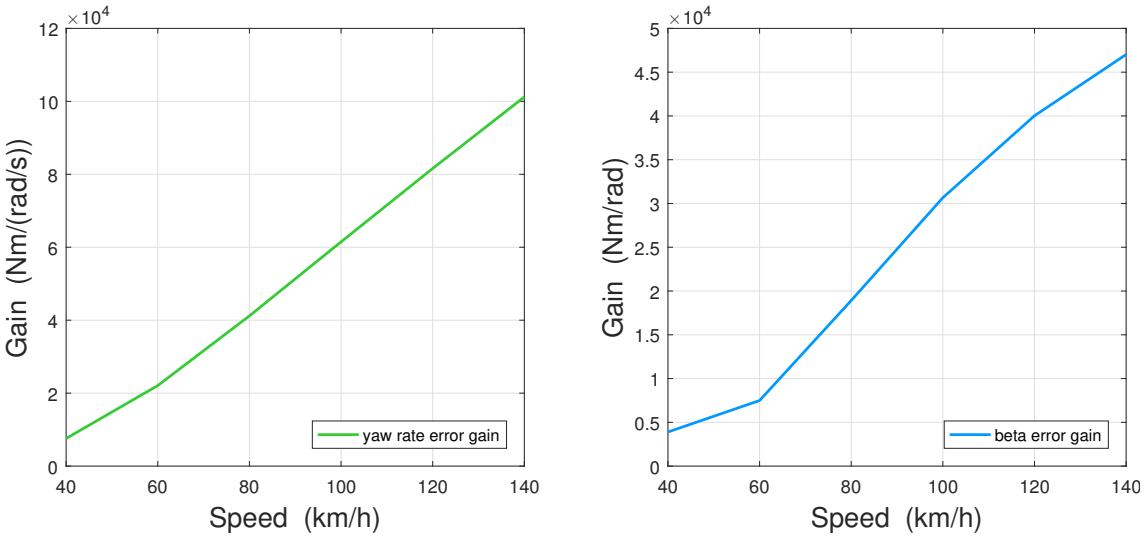

Figure 4.7: LQR gain evolution with respect to speed. High friction conditions.

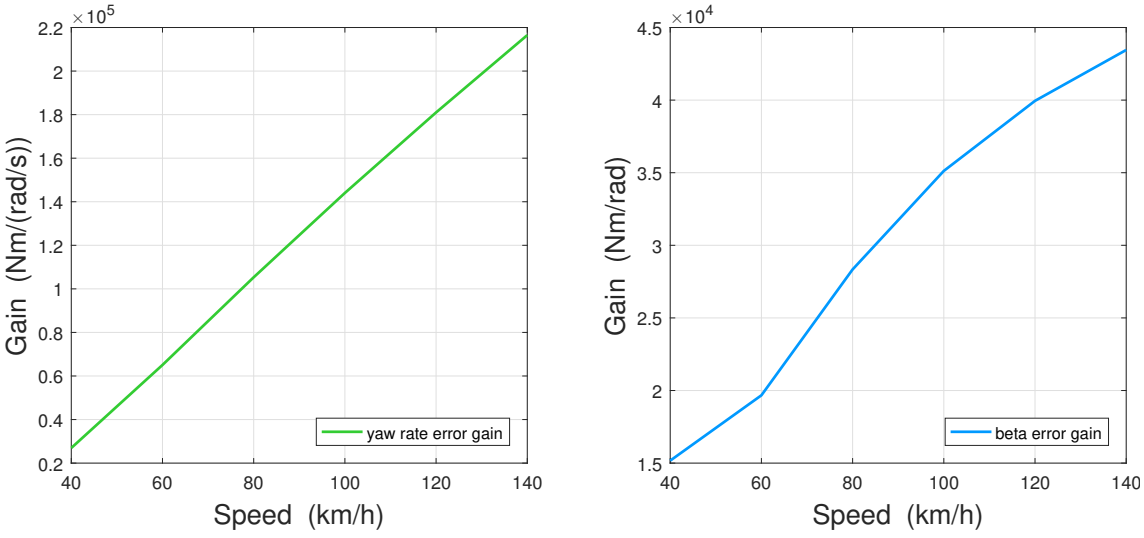

Figure 4.8: LQR gain evolution with respect to speed. Low friction conditions.

The meaning of I_Y can be easily understood considering vehicle cornering condition (Figure 4.9). In steady-state (Figure 4.9 (a)), yaw rate r is equal to the ratio between lateral acceleration a_y and vehicle speed V thus I_Y is null and no yaw moment is needed.

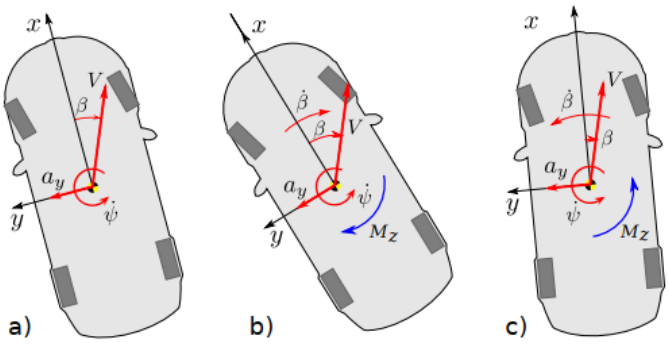

Figure 4.9: Vehicle behaviour in: (a) steady-state, (b) oversteering and (c) understeering

Instead, if the vehicle is in oversteering condition (Figure 4.9 (b)) in a counter-clockwise turn, yaw rate is greater than $\frac{a_y}{V}$, thus I_Y is negative and a negative yaw moment should be applied to prevent vehicle from spinning. On the contrary, if the vehicle is in understeering condition (Figure 4.9 (c)) in a counterclockwise turn, yaw rate is lower than the ratio $\frac{a_y}{V}$, I_Y is positive and a positive yaw moment should be applied to the vehicle to increase its yaw rate (i.e. entering the turn).

VDC tries to ensure vehicle stability keeping yaw index near to zero value. This means that the controller aim is to keep the vehicle in steady-state cornering condition. This prevents an excessive increase of the sideslip angle. In fact, considering a vehicle in a constant speed (V = const) turn, for small sideslip angles β, lateral acceleration can be written as:

$$a_y = V\dot{\beta} + rV \tag{4.19}$$

Rearranging the equation it became:

$$\dot{\beta} = \left(\frac{a_y}{V} - r\right) \tag{4.20}$$

That is exactly the Yaw Index. This means that the control logic generates a yaw moment that prevents sideslip angle from excessive increase, with a corrective control action that opposes to this increase. Indeed if sideslip angle assumes too high values the vehicle could face hazardous situations. An excessive understeer that could happen with a sudden steer of the driver the vehicle could not steer enough to avoid, for example, an obstacle. In case of oversteer it could tailspin, for example in case of μ-split braking.

Table 4.3 reports the behaviour of the VDC in each case, showing how the control action always oppose to the excessive increase of the sideslip angle resumed the behaviour of the control action with respect to the values of each term of the Yaw Index.

Table 4.3: VDC behaviour for different conditions

$\frac{a_y}{V}$	r		I_Y	$\dot{\beta}$		$M_{z,VDC}$
+	+	$\frac{a_y}{V} = r$	0	0	Steady-state	0
+	+	$\frac{a_y}{V} > r$	+	-	Understeer	+
+	+	$\frac{a_y}{V} < r$	-	+	Oversteer	-
-	-	$\frac{a_y}{V} = r$	0	0	Steady-state	0
-	-	$\frac{a_y}{V} > r$	-	+	Understeer	-
-	-	$\frac{a_y}{V} < r$	+	-	Oversteer	+

The SSC contribute $M_{z,SSc}$ is multiplied also for a coefficient ζ_{I_Y}. This is defined as:

$$\zeta_{I_Y} = \frac{1}{2}\big(1 - \tanh\big(c_1|I_Y| + c_2\big)\big) \tag{4.21}$$

Where c_1 and c_2 are two constants. As previously mentioned its function is to decrease the SSC contribute while non steady state conditions are detected and so the VDC is active. To make the two controller work properly together proper value have to be set for c_1 and c_2, thus their influence were analysed.

In Figure 4.10 can be observed how c_1 determines the transition from the SSC controller to the VDC controller with respect to the value of the Yaw Index itself. Have to be remembered that $I_Y \approx \dot{\beta}$ thus the higher is the derivative of the sideslip angle, the more ζ_{I_Y} decreases the SSC contribute. In Figure 4.11 can be noted how c_2 can influence 2 aspects: (i) the smoothness of the curve around $I_Y = 0$ and (ii) the value of the ζ_{I_Y} index at the same point, determining a vertical translation of the curve. Logically for null Yaw Index the value of ζ_{I_Y} should be approximately 1.

So by properly tuning these constant can be set a proper transition from one contribute to the other. The value selected with an explanation are reported in Table 4.4

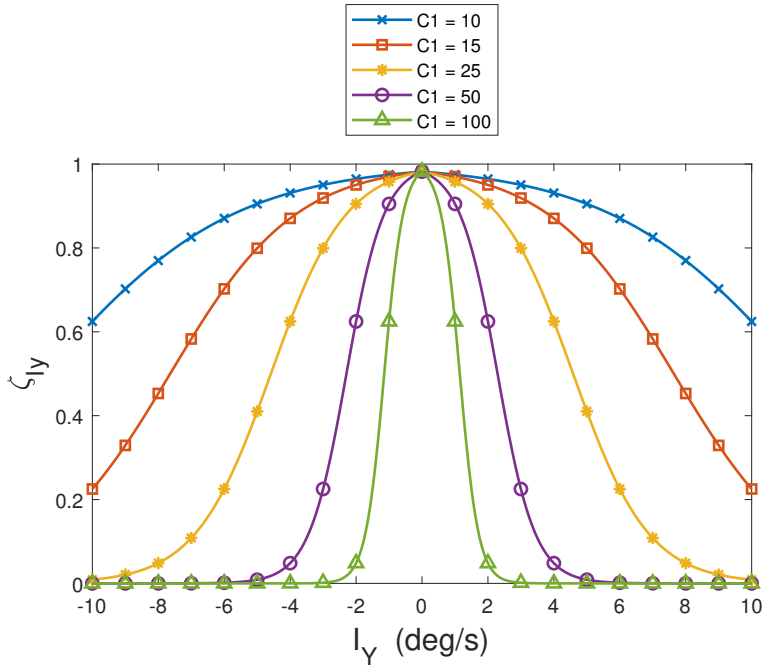

Figure 4.10: Sensitivity analysis of ζ_{I_Y} coefficient with respect to c_1

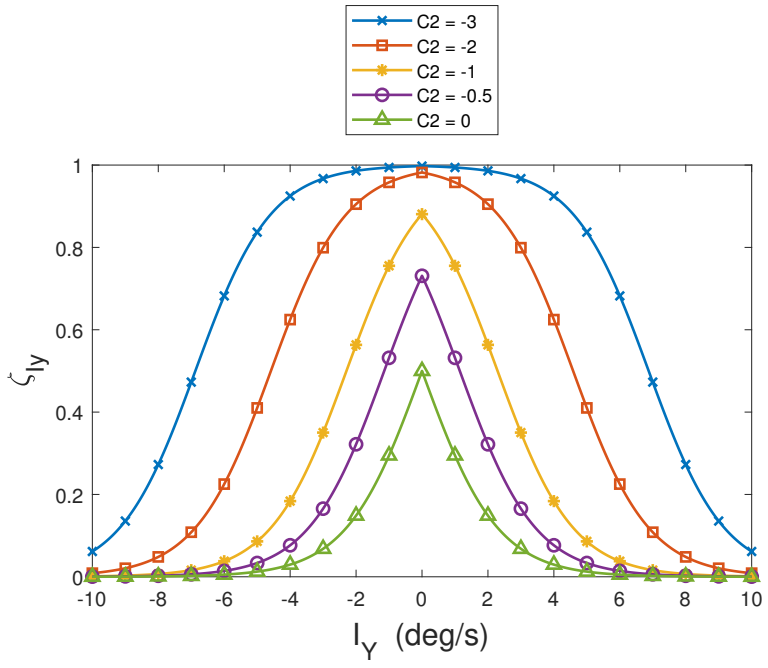

Figure 4.11: Sensitivity analysis of ζ_{I_Y} coefficient with respect to c_2

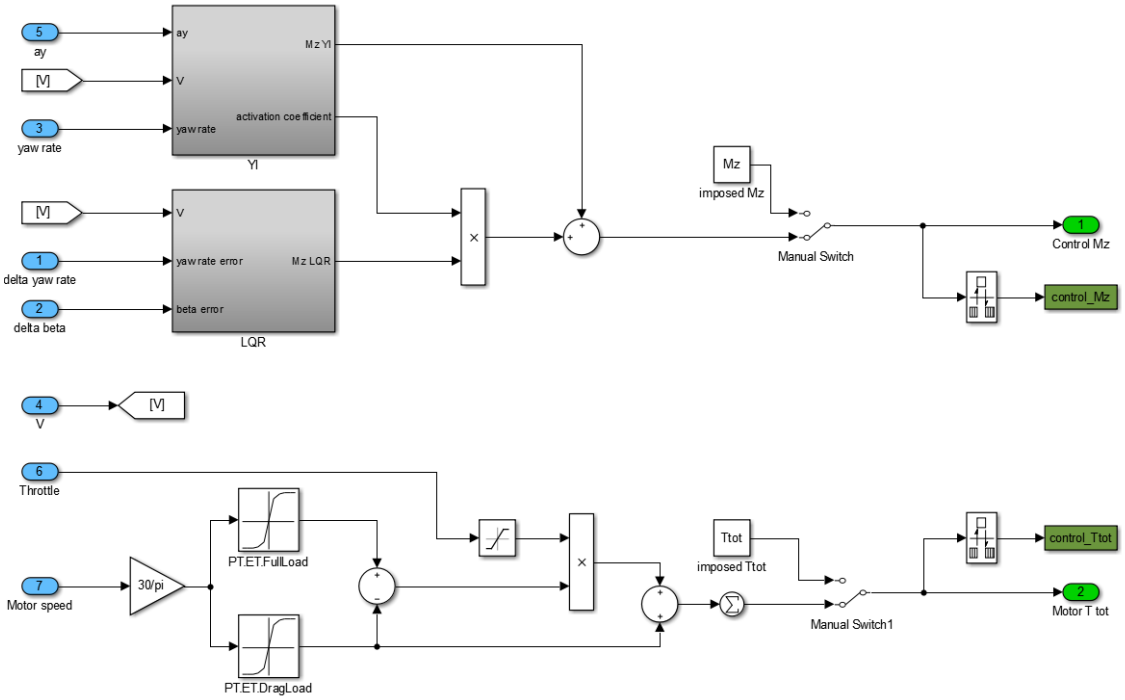

Figure 4.12: Blocks in the Simulink controller related to high level controller. The two outputs of LQR and YI controllers are summed up to define the M_z output. The second output is the total driving torque T_{tot}, based on driver's input of the throttle.

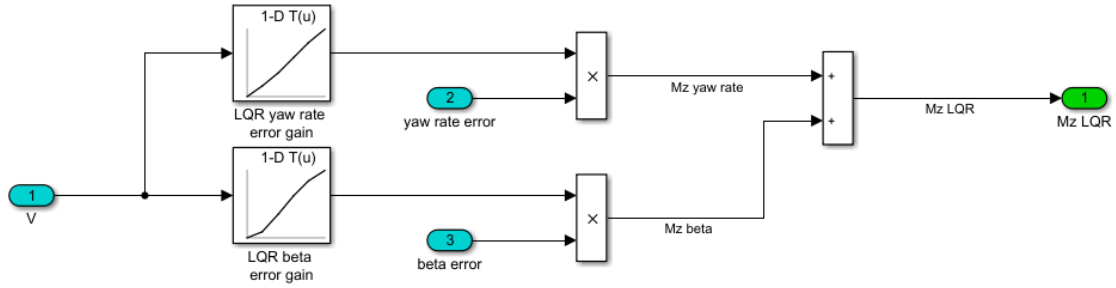

Figure 4.13: Blocks in Simulink related to the Linear Quadratic Regulator (LQR) implemented in the high level controller

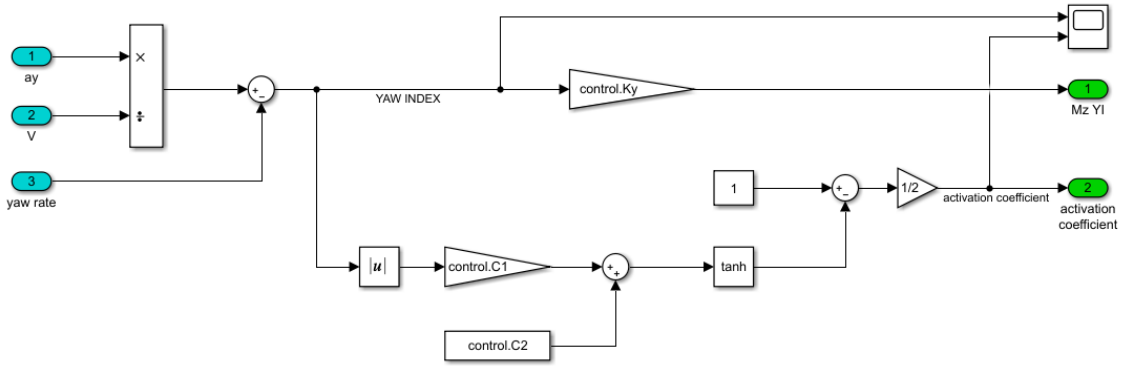

Figure 4.14: Blocks in Simulink related to the Yaw Index (YI) controller implemented in the high level controller

Table 4.4: Values assumed for the VDC control constant

Constant	Value	Motivation
c_1	25	This was set as a compromise between an excessively high or small value. High values provoke a too fast transition from the SSC to the VDC control resulting in excessive oscillation of the M_z that provoke instability due to a too rapid transition from one to the other contribute of M_z. A too small value would make ineffective the VDC control.
c_2	-3	This value permits to have $\zeta_{I_Y} \simeq 1$ for $I_Y = 0$ (no contribute of the VDC controller)
k_Y	1×10^4	This is the proportional gain of the yaw index controller and its main function is to change the magnitude of I_Y to be adapt to M_z.

4.3 Low Level controller

The low level controller receives the output of the high level controller along with some state quantities of the vehicle and try to distribute the torque to realise these commands, trying to make it in the most efficient way. In this controller can be distinguished two different control logic (i.e. torque distribution strategies):

- The algorithm for the Energy Efficiency mode
- The algorithm for the imposed M_z mode

In the first algorithm the control objective is to improve the energy efficiency of the vehicle using Torque Vectoring. In this case the M_z is not imposed by the high level controller but is implicitly determined by the torque distribution algorithm present in the low level controller itself, explained in section 4.3.1.
In the second case the yaw moment M_z, output of the high level controller is also considered as input and the algorithm try to distribute the torque in a way that it is generated exactly the desired yaw moment. However still some optimisation to achieve a better energy efficiency is possible at this stage, as explained in section 4.3.2.
The other input of this block is the total torque required by the driver T_{tot}, that is always considered by the algorithms.

The low level controller works with a certain formulation that evidence all the optimisation parameters, that defines the torque at motor level as:

$$\begin{cases} T_1 = \left(\frac{T_{tot}}{2} + \Delta T_{LR}\right)\sigma_L \\ T_2 = \left(\frac{T_{tot}}{2} - \Delta T_{LR}\right)\left(1 - \sigma_L\right) \\ T_3 = \left(\frac{T_{tot}}{2} + \Delta T_{LR}\right)\sigma_R \\ T_4 = \left(\frac{T_{tot}}{2} - \Delta T_{LR}\right)\left(1 - \sigma_R\right) \end{cases} \tag{4.22}$$

The torques are determined by 4 parameters:

- Total torque T_{tot}
- The torque variation between left and right side ΔT_{LR}
- σ_L and σ_R, that are the distribution coefficients between front and rear wheels for left and right side respectively.

T_{tot}, as mentioned, is always imposed by the high level controller, that interprets the driver desire or is given a by cruise control logic. The formulation selected permits to have always the sum of the torques equals to the selected value for T_{tot}.
ΔT_{LR} is instead determined in the low level controller if it is set the Energy Efficiency mode or it is imposed by the selected M_z coming from the high level controller (so this value is automatically computed by applying a formula, thus no decision is taken from the low level controller regarding this parameter).
σ_L and σ_R are two coefficients whose value is between 0 and 1, where 0 distribute the torque on the rear wheel, while 1 impose it only on the front wheel. These are meant to optimise the energy consumption on each side by distributing the torque in an efficient way, considering the total required torque on the side and the function that models the power losses.

4.3.1 Energy Efficiency mode

As analysed in section 2.3, the main sources of losses are motor-inverter losses and slip losses, consequently the formulation of the strategy that aim to improve energy efficiency focus on the influence of the torque distribution on these quantities. The modelling of the losses is according to section 3.1.2 and 3.3.
If the total torque T_{tot} is kept constant and by varying the left-right torque unbalance ΔT_{LR} the variation of the motor losses is not excessive, at the condition that the motors are all in traction or in regeneration. Figure 4.15 evidences exactly this, where the motor power losses in function of the torque unbalance are reported for different speeds and a constant total torque of 50 Nm. Since $T_{tot} = 50\ Nm$, when $\Delta T_{LR} = \pm 25\ Nm$ then the torque demand on the two sides will be 50 Nm and 0, respectively. So, increasing the magnitude of ΔT_{LR} implies that one side works in traction and the other side in regeneration, with a sudden increase of the overall power losses [9].
The motivation of this behaviour is to be found in the power losses function of the motor (Figure 4.16 and 4.19) which has a discontinuity along the line $T = 0$ passing from traction to regeneration and the other way out. In fact if one side is in traction and the other in regeneration would mean that a part of the power is produced on one side and immediately reabsorbed on the other side, with the result of an inefficient overall power production. This condition should be avoided in the Energy Efficiency mode.

The lateral slip power losses are instead strictly linked with the distribution of the vertical load on each wheel (Figure 4.17), in particular in steady state cornering conditions, with sufficiently high lateral accelerations, the load is higher on the external wheels, that is left side in this case. If the total motor torque T_{tot} is distributed equally on all the wheels

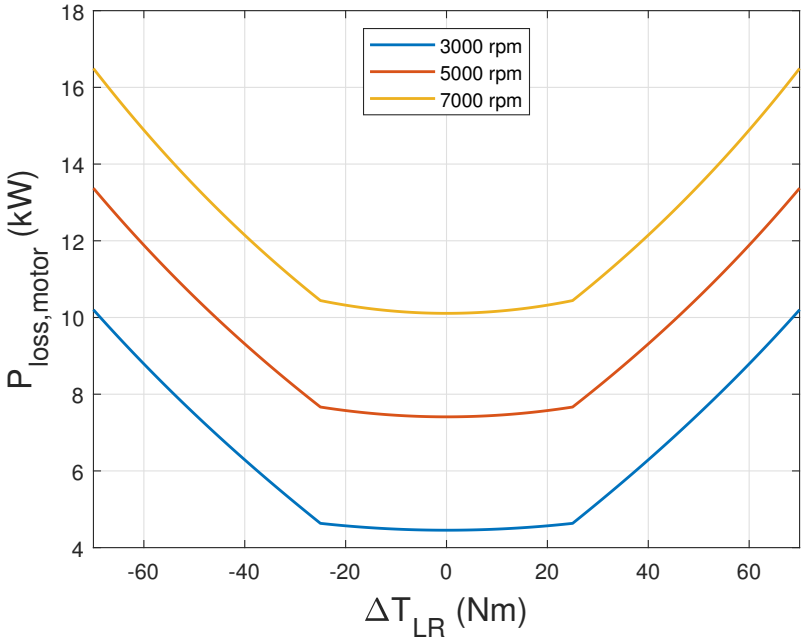

Figure 4.15: Motor power losses in function of different rotating speed. Total torque is 50 Nm. The sudden increase of the losses begins at $\Delta T_{LR} = \pm 25\ Nm$.

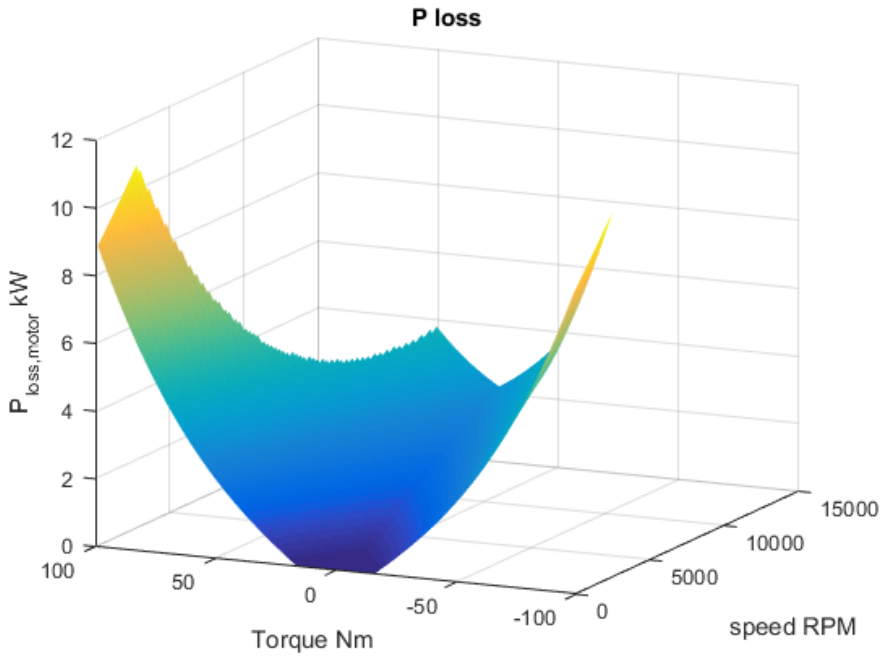

Figure 4.16: Motor and inverter power losses, in function of rotating speed and torque.

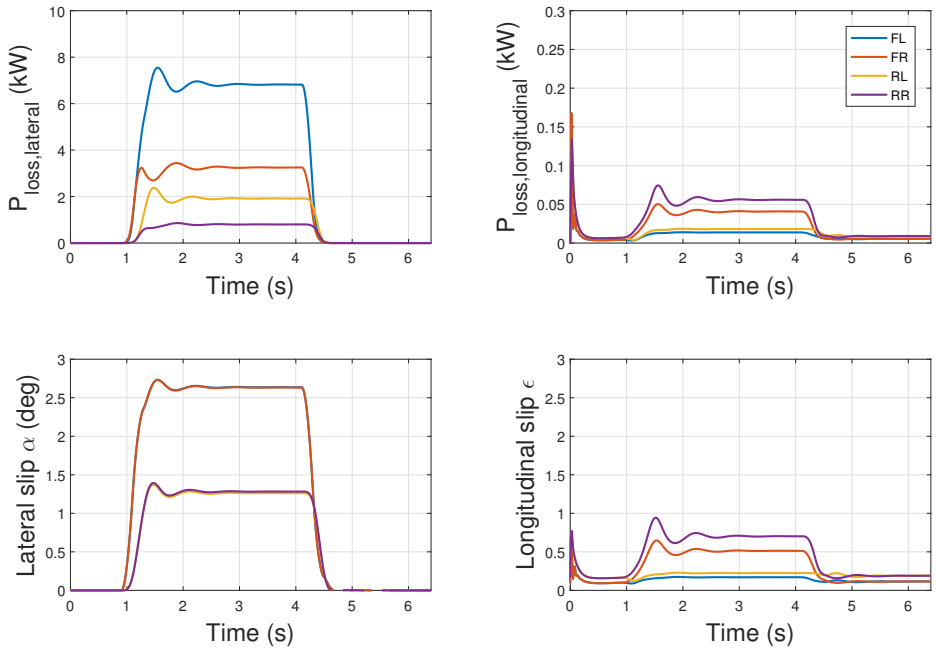

Figure 4.17: Losses and slips in a step steer manoeuvre with equal distribution of the torque on all the wheels. Step steer at 100 km/h with max steer of 40 deg, steering to the right. In the bottom left figure slips on the same axle are superimposed.

on the external tyres the longitudinal slips are smaller, compared to the inner wheels and the same is for the longitudinal slip power losses, that are two order of magnitude smaller compared to lateral slip losses. This happens because the inner wheels are closer to the maximum force that could be developed by the tyres in that conditions (i.e. tyres are in the non linear area), while on the external wheels the load permits to develop an overall higher force. Moreover in steady state cornering conditions the speed is kept constant and so the required longitudinal force developed by motor torques is low, thus producing low longitudinal slip losses.

As a matter of fact the slips and the losses produced by the longitudinal forces during steady state cornering has a little influence on the overall power losses 4.17. It is thus convenient to distribute the torque as much as possible on the external wheels, where the vertical loads and thus the maximum force the tyres can develop is higher. Only if the torque limit of the motors are reached a part of the torque is also distributed on the inner wheels. This would imply a very small increase of the longitudinal slip losses but a more consistent decrease of the lateral slip power losses. This avoids also an excessive motor power losses due to contemporary traction/regeneration of motors.
This under the hypothesis that the vehicle travels corners in steady state or almost steady state conditions (i.e. with null or low longitudinal acceleration). This assures in fact that longitudinal forces are always small. It has to be remembered that still the driving style has also a big impact on the power consumption of the car and if corners are covered also with high longitudinal acceleration, that is the case of a more aggressive driving style, every strategy of energy efficiency optimisation would be nullified anyway. Thus is taken for granted that the driving style of the driver is appropriate to the driving mode.

It was specifically avoided to rely on a specific algorithm that compute the slips on each wheel as this measure would be quite unreliable to compute. And thus they may be counter effective in trying to minimise power losses.

To avoid an unnatural behaviour of the vehicle it was set a threshold on the steer at which the torque unbalance is present. Otherwise a small steer angle would suddenly give an excessive yaw rate. This also permits to not apply the torque unbalance for low lateral accelerations when the load transfer is not high. In this case it was set $\delta_{th} = 20\ deg$.

The algorithm divide the torque allocation process in 2 steps:

1. Computation of the total torque per side, by defining the torque unbalance ΔT_{LR}.
2. Distribution of the torque between front and rear motor, by defining the coefficients σ_L and σ_R.

Computation of the total torque per side

As already affirmed the torque unbalance is not computed with an explicit yaw moment M_z imposed by the high level controller. Instead the algorithm distributes the torque as much as possible on the external side, accounting for the motor limits. In particular the torque unbalance is computed as:

$$\begin{aligned} if \quad & T_{max,ext} \geq T_{tot} \;\&\; abs(\delta) > \delta_{th} \\ & \Delta T_{LR} = sign(\delta)\frac{T_{tot}}{2} \\ else \;\; if \quad & abs(\delta) > \delta_{th} \\ & \Delta T_{LR} = sign(\delta)\left(T_{max,side} - \frac{T_{tot}}{2}\right) \\ else \quad & \Delta T_{LR} = 0 \end{aligned} \tag{4.23}$$

Where the external side is the left one for positive steer angle and the right side for negative steer angles. The maximum torque $T_{max,ext}$ is computed with the torque curve (Figure 3.4), in function of motor speed:

$$T_{max,ext} = T_{max,ext,F}(\Omega_{ext,F}) + T_{max,ext,R}(\Omega_{ext,R}) \tag{4.24}$$

In this way the torque is distributed as much as possible on the external side and only if the overall torque would exceed the maximum torque that the motors can develop on the external side ($T_{max,ext} < T_{tot}$) part of the torque is distributed also on inner side.
Consequently, given the torque unbalance ΔT_{LR}, the imposed yaw moment is:

$$M_z = \frac{\Delta T_{LR} w \eta}{R_w \tau} \tag{4.25}$$

Distribution of the torque between front and rear motor

The longitudinal distribution of the torque on each side is instead made through an optimisation of the motor losses, computed with the function proposed in section 3.3, including the distribution factors that defines the torques. The optimal coefficient is defined as the one that minimises the sum of the losses:

$$\begin{aligned} & min \sum_{i=1,3} P_{loss,i}\big(T_i(\sigma_L), \Omega_i\big) \\ & min \sum_{i=2,4} P_{loss,i}\big(T_i(\sigma_R), \Omega_i\big) \end{aligned} \tag{4.26}$$

The characteristic of the motor power losses function that influence the result of this optimisation function is the second derivative (i.e. its concavity) with respect to the

torque. In case it is always positive thus directed upward the optimal solution is the equal distribution of the torque (i.e. $\sigma_{F,R} = 0,5$), since by changing the distribution of the torque with respect to equal distribution, the losses on one wheel increases more than linearly and on the other decreases less than linearly (Figure 4.18 (a)). As a matter of fact the power losses will always increase with a distribution different than equal distribution. On the opposite if the concavity is negative the ideal solution is to distribute the torque only on one wheel because increasing the torque unbalance brings to increases the losses on one wheel less than linear and on the other to decrease more than linearly, thus the opposite of the previous case (Figure 4.18 (b)). In this second case the solution is to distribute the power on only one wheel thus $\sigma_{F,R}$ can assume the value 0 or 1. In a general case the motor losses function may have both negative and positive concavity, with also the torque limits of the motors that have to be considered. Thus the optimal value of $\sigma_{F,R}$ may be a value between 0 and 1, depending on the amount of torque required and the shape of the curve.

Considering the power losses function of the motor (Figure 4.19), can be observed how the concavity is always positive. This brings to the conclusion that the optimal solution is the equal distribution of the torque on each side. However a case of different solution considering the same losses is reported in [4], where the concavity passes from negative to positive. In the model it is thus implemented simply $\sigma_{L,R} = 0,5$.

In a more general case the optimisation can be faced with an optimisation function using

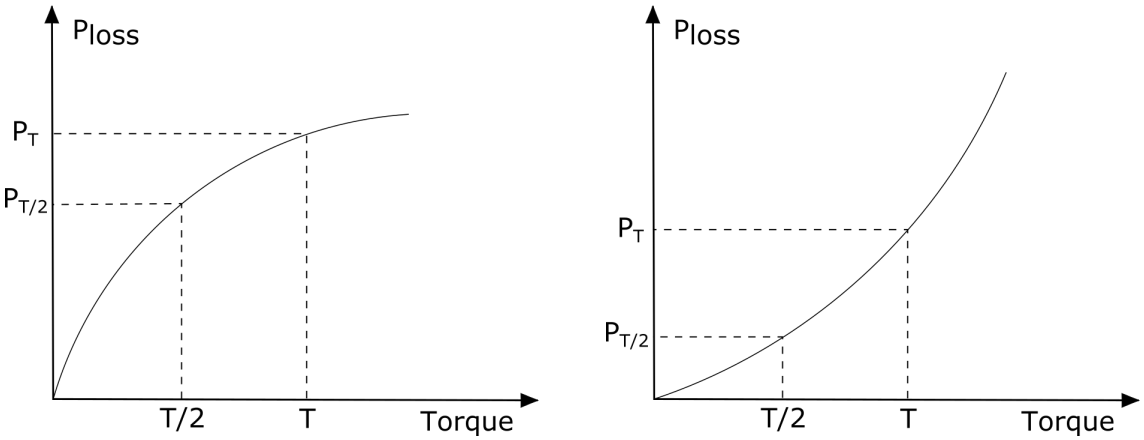

Figure 4.18: Power loss function with different concavities. In case (a) by raising the torque the power losses increases less than linearly and so $P_{loss,T} < 2P_{loss,T/2}$. In case (b) the power losses increases more than linearly by increasing the torque consequently $P_{loss,T} > 2P_{loss,T/2}$.

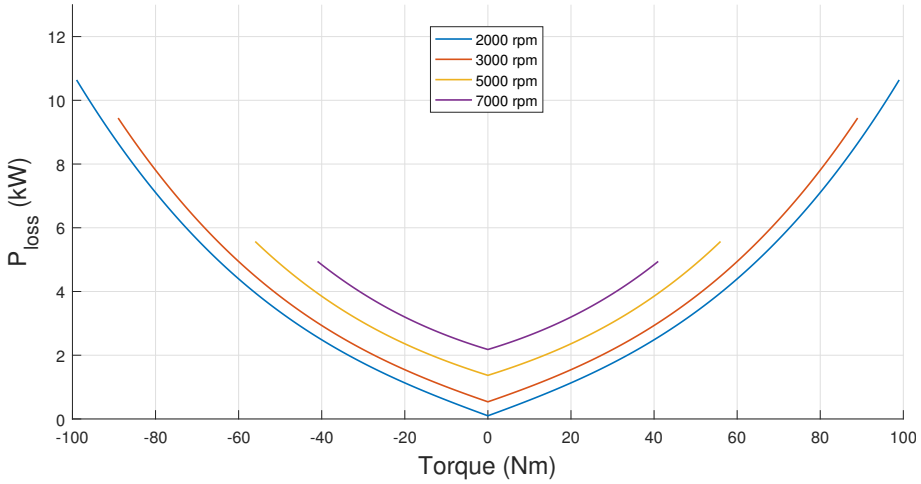

Figure 4.19: Power losses function in function of the torque for different motor angular speeds.

fmincon MATLAB function, with the proper constraints on the torques. This is performed offline, creating a look-up table, with input the speed of the motors and the torque required on each side $T_{side} = \frac{T_{tot}}{2} \pm \Delta T_{LR}$. An online solver would probably requires an excessive computational power to be implemented.

4.3.2 Imposed yaw moment mode

This algorithm is used with the driving modes that aims to influence vehicle dynamics, in this study these are Normal, Sport and Low Friction modes. It is very similar to the previous one, with the only difference that the ΔT_{LR} is computed with a simple formula, so that the yaw moment imposed on the vehicle is the desired one, output of the high level controller:

$$\Delta T_{LR} = \frac{M_z}{2} \frac{R_w \tau}{\frac{w}{2} \eta} \tag{4.27}$$

Where w is the vehicle track and η is the efficiency of the motor transmission. It is worth to notice that this passage is given by a simple formula because ΔT_{LR} is determined by fixing M_z, computed in the high level controller, thus in low level controller is only a matter of a mathematical passage.

The distribution of the torque for each side is instead performed with the same procedure described for the Energy Efficiency mode (section 4.3.1), through the optimisation of the coefficient σ_L and σ_R, thus again in the controller these are set to 0,5. This shows that also in case is imposed a certain understeer characteristic, thus prioritising performance by imposing a certain yaw moment is still possible to keep into account some efficiency criteria in the distribution of the torque also when the main objective is to influence vehicle dynamics.

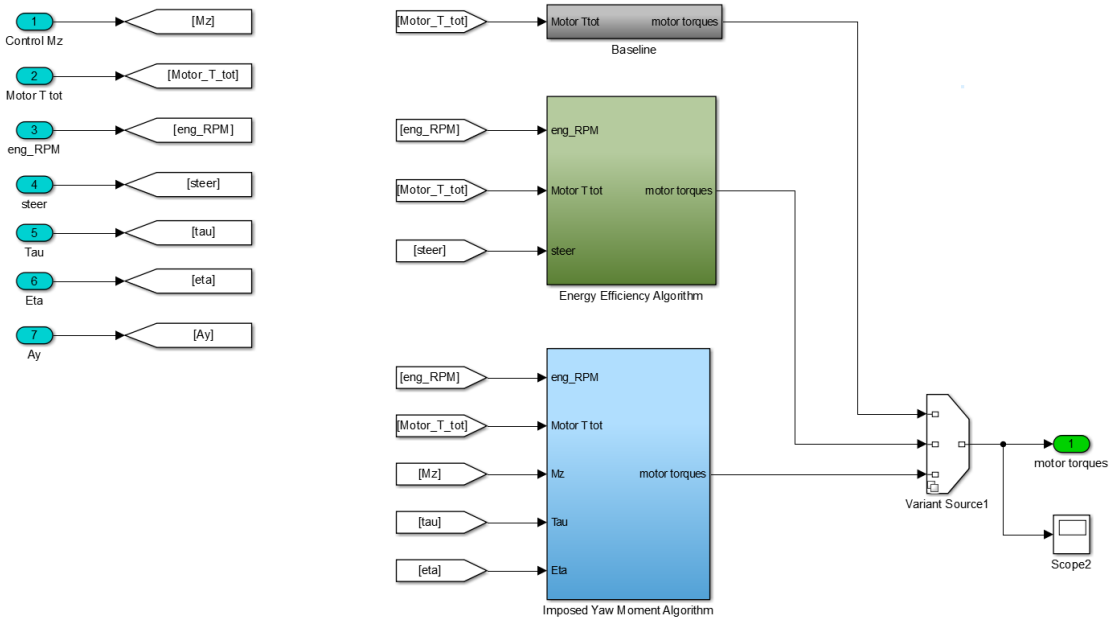

Figure 4.20: Blocks in the Simulink controller related to low level controller. The algorithm is selected depending on the driving mode by a variant sink block.

Chapter 5

Results

The effectiveness of the proposed control strategy was evaluated by means of numerical simulations. Both steady-state manoeuvre and transient manoeuvre were performed, to evaluate the different behaviour of the controller that is able to improve different aspects of the vehicle dynamics. In each case the TV controller is compared to the so called Baseline vehicle that is the same vehicle but with equal torque distributed to all the wheels, and thus with no yaw moment M_z. High friction and low friction coefficient conditions were simulated, with coefficients of $\mu = 1.0$ and $\mu = 0.5$ respectively.

5.1 Steady-state manoeuvre: Steering pad

The steady-state performances of the vehicle were evaluated through a steering pad at constant speed. The car performed a progressive steering, passing from 0 to 60 deg at the speed of 60 km/h (kept with a cruise control logic), in a time of 20 seconds. The purpose of this kind of manoeuvre is to evidence the effectiveness of the high level controller to follow the understeer reference curve that the controller tries to impose to the vehicle.

High friction conditions

In Figure 5.1(a) shows how the controller is able to impose the wanted understeer characteristic in Normal and Sport mode, extending the linear region and the maximum acceleration reached by the vehicle ($8,92\ m/s^2$ for TV vehicle and $8,06\ m/s^2$ for the Baseline). In the case of Sport mode the controller is also able to decrease the slope of the curve, that results in an increase on the responsiveness of the vehicle. This confirms the effectiveness of (i) the reference generator and (ii) the high level controller in following the given reference. Applying the torque vectoring also decrease the sideslip angle of the vehicle, especially at high lateral acceleration, as showed in Figure 5.1(b).

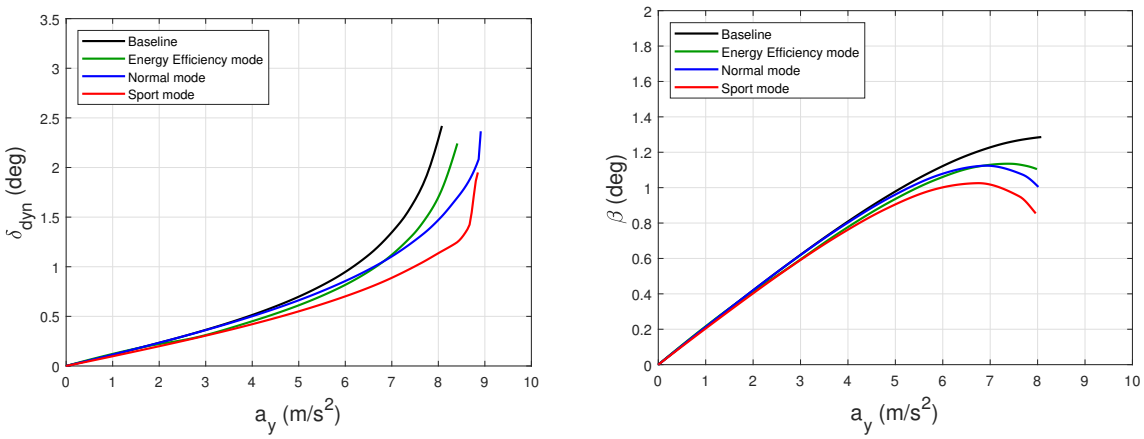

(a) (b)

Figure 5.1: Understeer and sideslip angle characteristic of the vehicle. Comparison of Baseline vehicle with Energy Efficiency mode, Normal mode and Sport mode

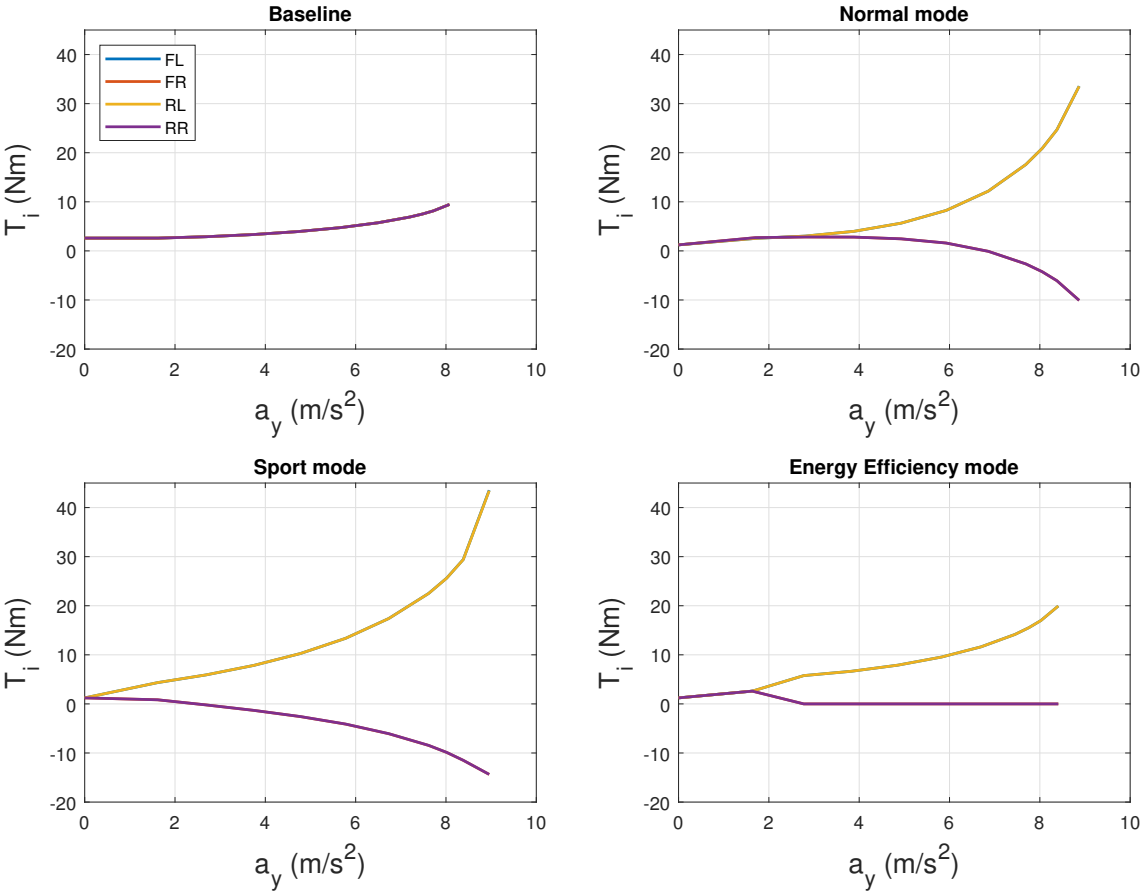

Figure 5.2: Torque evolution for each mode in function of the lateral acceleration. Comparison between Baseline vehicle with Energy Efficiency mode, Normal mode and Sport mode. In the figures torques on each side are superimposed since they are distributed equally.

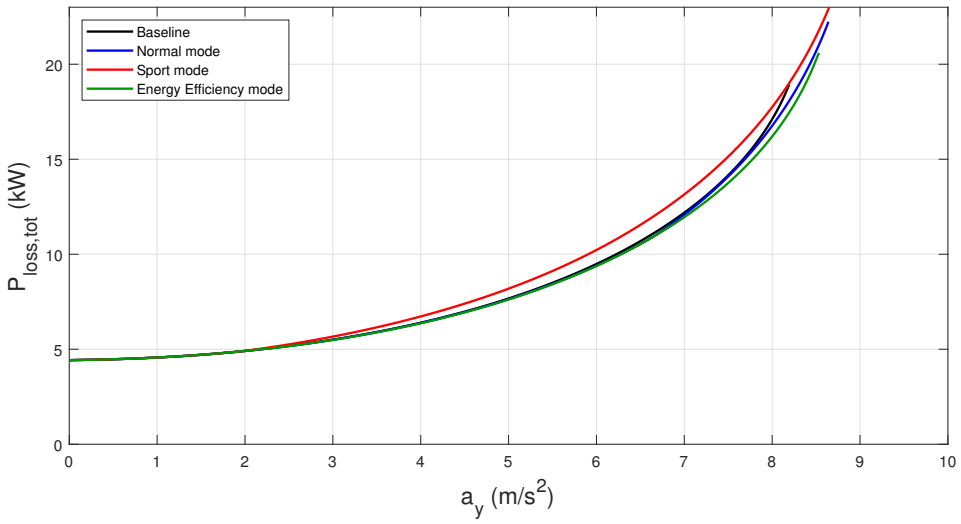

Figure 5.3: Power losses of the vehicle in function of the lateral acceleration, representing the power losses in steady state conditions. Comparison between Baseline vehicle with Energy Efficiency mode, Normal mode and Sport mode.

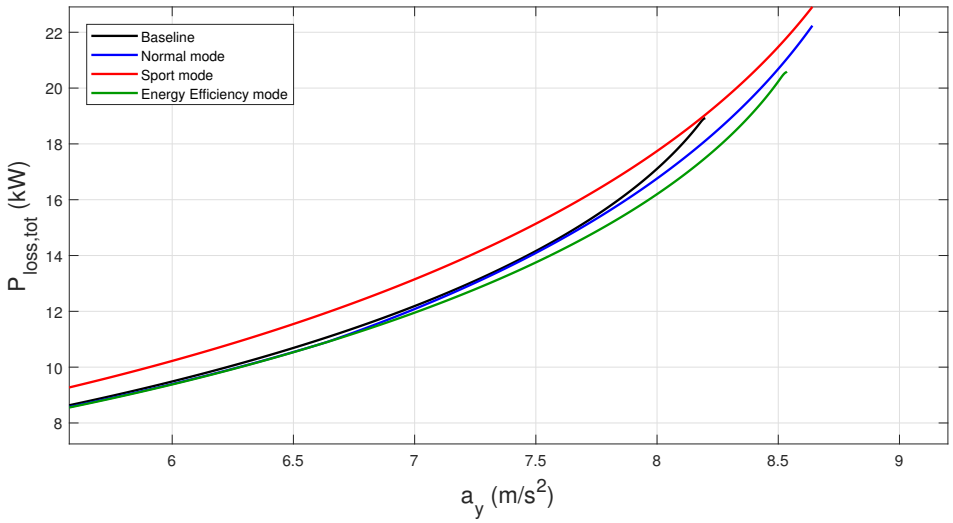

Figure 5.4: Detail of the Power losses represented in Figure 5.3. The power losses in Energy Efficiency mode are always lower than Baseline vehicle and other modes.

In case of Energy Efficiency mode there is no imposed understeer characteristic, however there are some changes on this curve as well, due to the fact that with this mode the algorithm imposes a yaw moment concordant with the yaw rate. Typically this yaw moment is not excessive since the contemporary traction regeneration of the motors is avoided and thus there is a smaller extension of the lateral acceleration with respect to the other modes. However the yaw moment imposed depends on the total torque required by the driver and on the speed of the vehicle that determines the speed of the wheels and thus the torque limits of the motors. This means that also the shape of the understeer characteristic under this mode changes depending on those parameters.

In the torque evolution reported in Figure 5.2 can be compared the different intervention of the controller. In Normal mode the controller act only when the lateral acceleration is over 3 m/s^2 because under this value the imposed understeer characteristic is equivalent to the baseline behaviour. In Sport mode since K_{us} value is decreased respect the baseline vehicle the controller acts for every lateral acceleration. In Energy Efficiency mode the controller acts only when the steer is over the imposed threshold of 20 deg, thus only at a certain acceleration, and then the torque on one side (the right one in this case) is imposed equal to zero. In all the TV controller modes the torque rise more on the left (outer) side because the total torque demanded by the cruise control to keep the speed increases.

Representation of the total power losses $P_{loss,tot}$ in function of the lateral acceleration, reported in Figure 5.3 and 5.4, evidences how the power losses of the Normal mode are similar to Baseline vehicle, while in Sport mode are sensibly higher due to the consistent action of the controller. Moreover power losses in Energy efficiency mode are always under all the other curves, demonstrating the effectiveness of this mode. At the maximum lateral acceleration reached by the Baseline vehicle of 8.2 m/s^2 the power losses in Energy Efficiency mode are 7,6 % lower respect the Baseline itself.

Low friction conditions

Also in low friction conditions the controller is able to influence the understeer characteristic of the controller (Figure 5.5(a)). In this case is set the same understeer coefficient K_{us} of the baseline vehicle for the reference generator as the low friction conditions make already more difficult to follow the reference. Indeed a decrease of the understeer coefficient means to increase the yaw moment control action defined by the high level controller, that is translated in higher force unbalance on the wheels, and consequently some wheels will work closer to the friction limit. As this limit decrease in low friction conditions, an excessive yaw rate would provoke macro slippage of the wheels, making the vehicle unstable.

As expected the increase of lateral acceleration is lower since the vehicle is already in

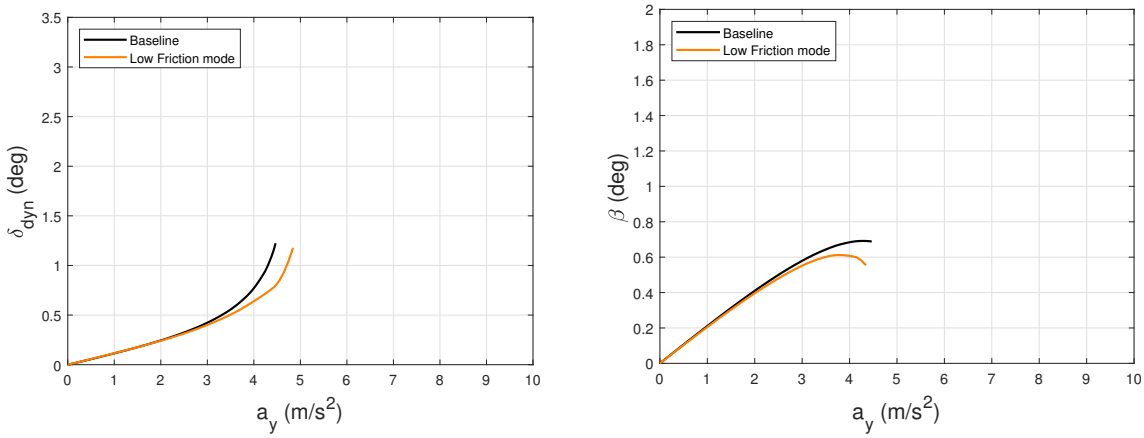

(a) (b)

Figure 5.5: Understeer and sideslip angle characteristic of the vehicle under low friction conditions. Comparison of Baseline vehicle with Energy Efficiency mode, Normal mode and Sport mode

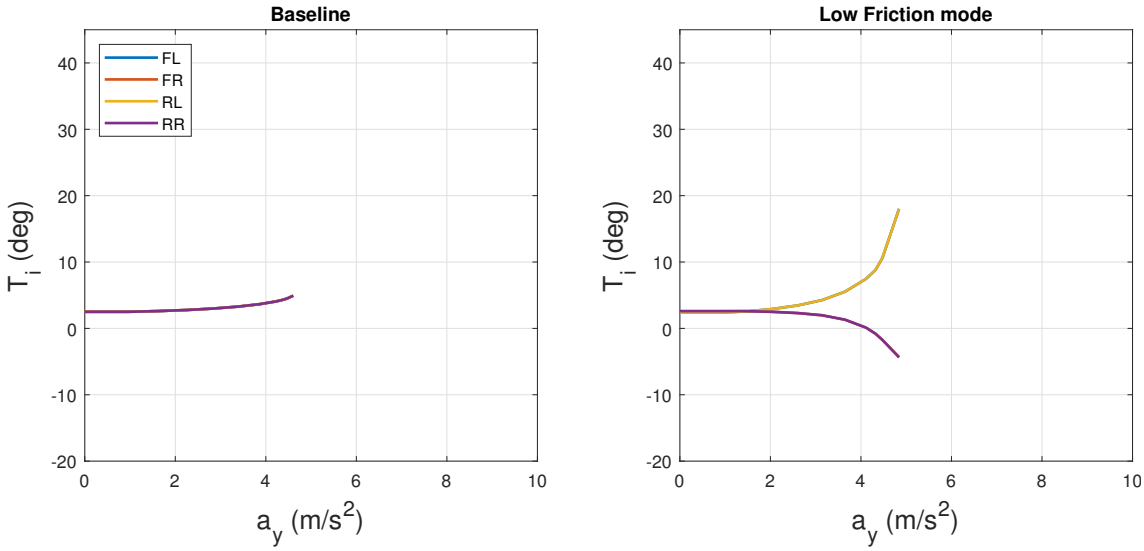

Figure 5.6: Torque evolution under low friction conditions in function of the lateral acceleration. Comparison between Baseline vehicle with Low Friction mode, Normal mode and Sport mode. In the figures torques on each side are superimposed since they are distributed equally.

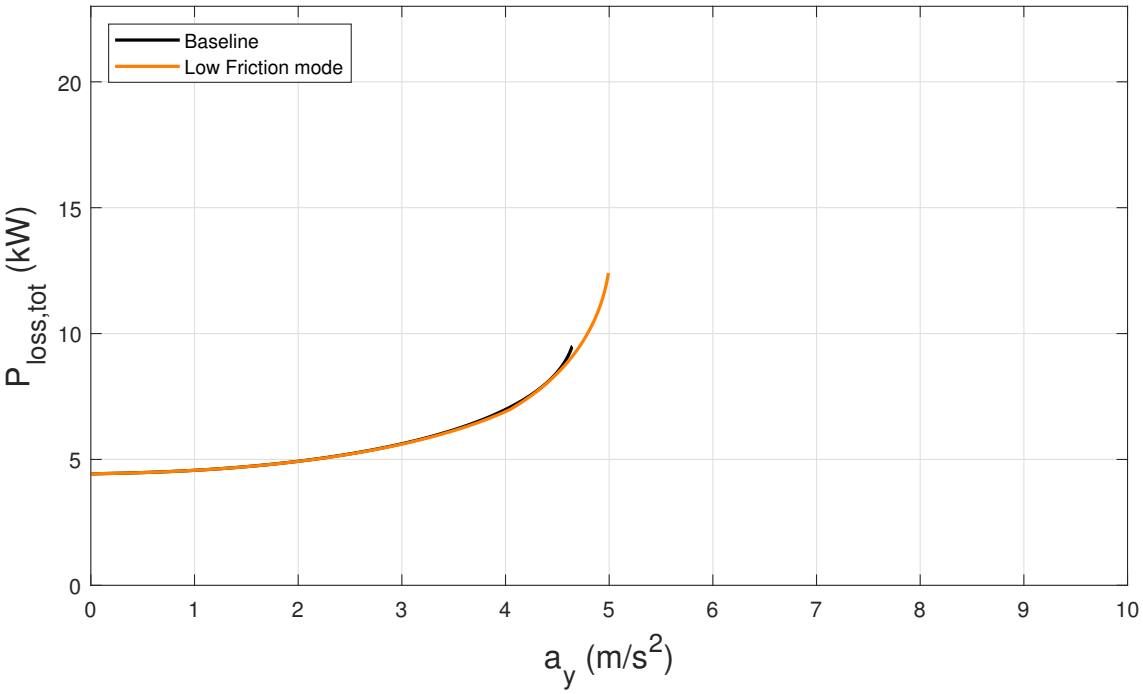

Figure 5.7: Power losses of the vehicle in function of the lateral acceleration under low friction conditions, representing the power losses in steady state conditions. Comparison between Baseline vehicle with Low Friction mode.

limit conditions. The maximum lateral acceleration increase from $4,67\ m/s^2$ to $4,9\ m/s^2$. Despite there is not an increase of the linear area is evidenced how the last part of the curve is improved toward a quasi-linear behaviour.

Also in this case the sideslip angle results slightly decreased with the application of Torque Vectoring, as showed in Figure 5.5(b).

The torque evolution reported in Figure 5.6 shows how the behaviour of the TV controller is similar to the Normal mode with the only difference of the lower friction coefficient and maximum lateral acceleration. The torques tend to have an steeper increase that evidence how the intervention of the controller is more important in low friction conditions, passing from a reduced to a consistent action in term of yaw moment.

Under low friction conditions total power losses $P_{loss,tot}$ of Baseline vehicle and Low Friction mode does not show a relevant difference, as observable in Figure 5.7.

5.2 Transient manoeuvres

5.2.1 Open loop: Step steer

One important advantage of a Torque Vectoring control system is the improvement of the vehicle dynamic in transient conditions. A step steer manoeuvre is suitable to verify this aspect. The manoeuvre is taken at constant speed, maintained with a cruise control logic and the steer is brought from 0 to 40 deg in a short lapse of time, and kept for 3 seconds, before to return to 0 deg. For high friction condition the speed was set to 100 km/h, while for low friction conditions it was 70 km/h. Normal, Sport, Energy Efficiency and Low Friction driving modes have been tested.

Normal mode

The results of this test are reported in Figure 5.8. The most significant effect of the controller can be seen on the yaw rate, where the controller is able to raise this value (from 16 deg/s to $18,1$ deg/s) and significantly decrease the overshoot and the oscillations, thus raising the lateral stability of the vehicle. As a consequence also the lateral acceleration raises, passing to a maximum value of $8,6$ m/s^2 with respect to the $7,7$ m/s^2 of the Baseline vehicle. This result is reached avoiding excessive sideslip angles β, that remains consistently under 1 deg. The cost of the action is a higher motor power losses, that implies in this manoeuvre a 13,5 % higher energy losses with respect to the Baseline vehicle. In this manoeuvre it was compared the motor power losses and not the total power losses since the second one have to be compared only under equal yaw rate or in general equal path followed. Motor power losses comparison shows the different level of intervention of the controller.
During all the manoeuvre the cruise control logic is able to keep the speed without problems. In this case the torques required by the low level controller are not saturated.

Sport mode

In Sport mode the results obtained in the step steer are similar to the Normal mode, with a general improvement in the performances of the vehicle, in particular with an expected increase in the steer responsiveness. Now the maximum yaw rate at equilibrium passes to $18,5$ deg/s. In the first part of the manoeuvre the yaw rate reach 20 deg/s and then has a decrease. This is due to the saturation of the motor torques on the external side (left side in this case) as can be observed in right Figure 5.19. Also the sideslip angle increase with respect to the Normal mode, passing to $2,2$ deg but is kept within the prefixed limits. Lateral accelerations passes to $8,8$ m/s^2 that, referring to the understeer curve obtained

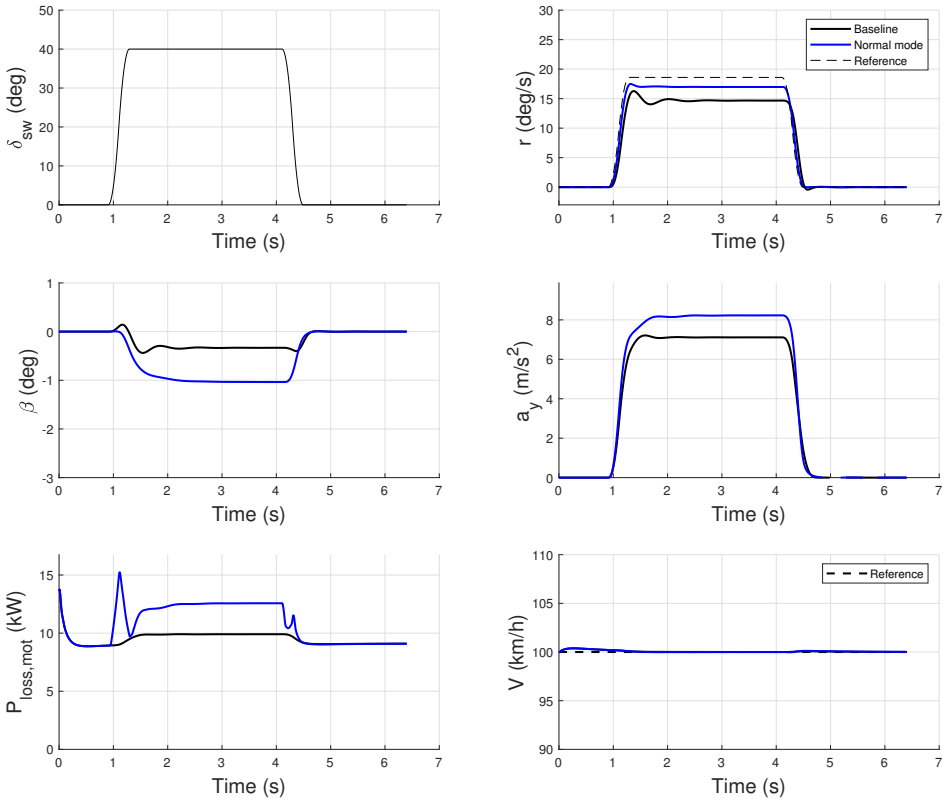

Figure 5.8: Step steer manoeuvre on high friction road. Comparison of Baseline vehicle and Normal mode of the controller.

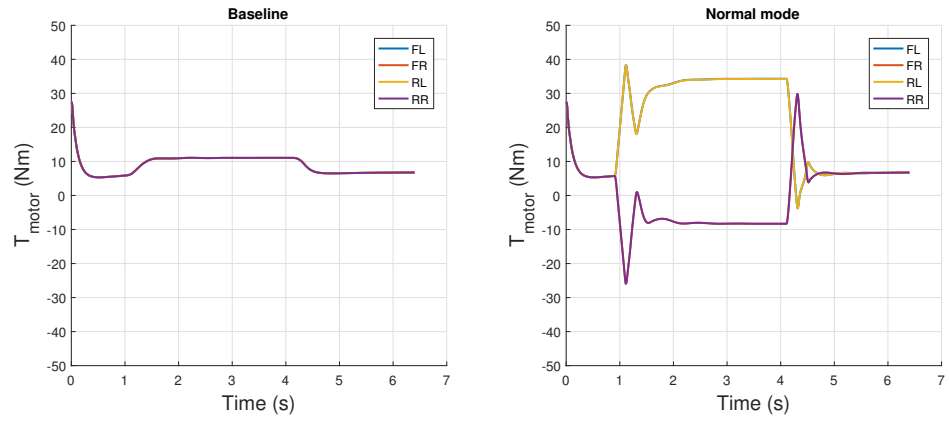

Figure 5.9: Torque evolution of step steer manoeuvre on high friction road. Comparison of Baseline vehicle and Normal mode of the controller. In right figure torques on each side are superimposed since they are distributed equally.

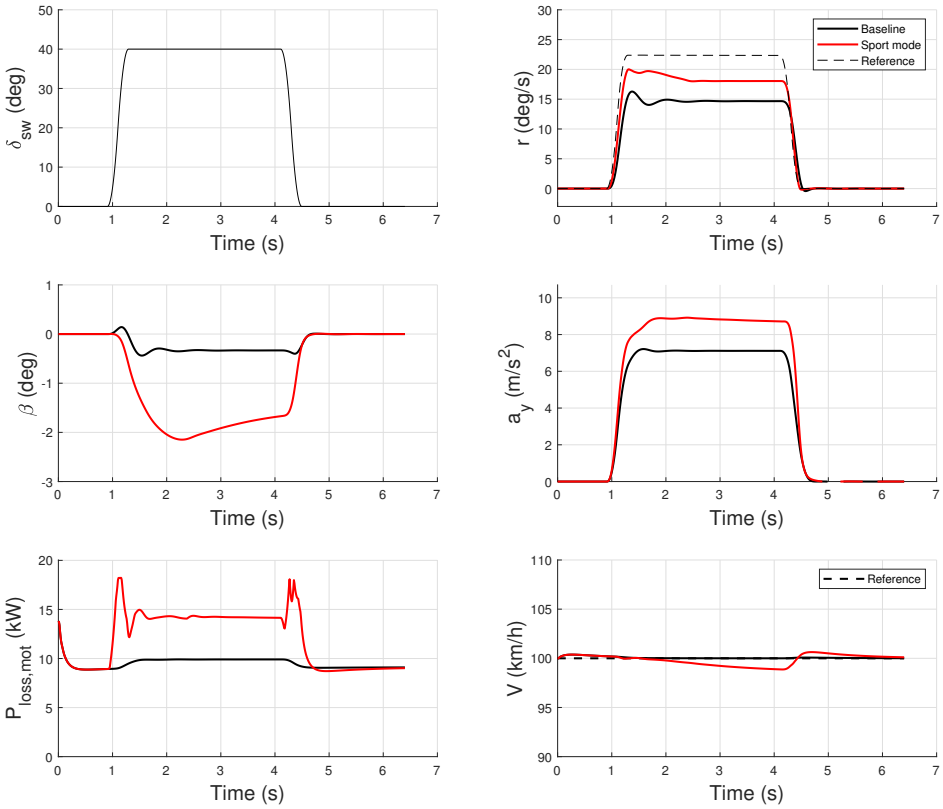

Figure 5.10: Step steer manoeuvre on high friction road. Comparison of Baseline vehicle and Sport mode of the controller.

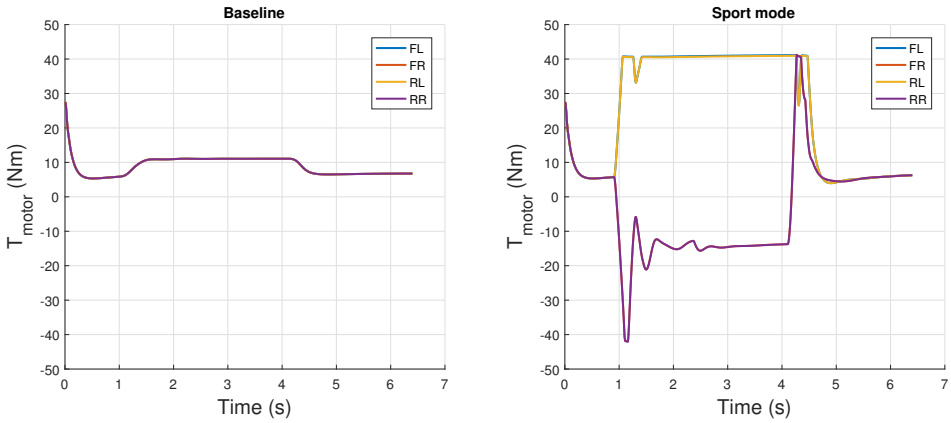

Figure 5.11: Torque evolution of step steer manoeuvre on high friction road. Comparison of Baseline vehicle and Sport mode of the controller. In right figure torques on each side are superimposed since they are distributed equally.

with the spiral test of section 5.1 is at the limit of friction. As a consequence of the higher level of influence imposed to the understeer characteristic of the vehicle also the control action is increased and Figure 5.11 shows how the torques are now saturated to their limits on one the external side. Since the action of the controller is higher motor power losses are 26,8 % higher respect Baseline vehicle.

Energy efficiency mode

In Energy Efficiency mode the vehicle does not follow a certain reference, but it is imposed a yaw moment depending on the total torque required by the driver and the vehicle speed. This means that for a step steer at constant speed it is imposed a constant yaw moment. The result (Figure 5.12) is the increase of the yaw rate, the lateral acceleration and the sideslip angle reached by the vehicle, without a significant improvement of the transient behaviour showing still the same oscillations on those quantities. In this mode the power consumption of the motor is limited with respect to the other modes. The control action in this case is limited and the motor power losses increases of only 2,1 %.

Table 5.1: Comparison of motor power losses variation of each mode respect the Baseline vehicle in steady state conditions.

Mode	Normal	Sport	Energy Efficiency
Power variation of motor losses respect Baseline vehicle (%)	+13,5	+26,7	+2,1

As it was observed, different modes implies different level of intervention of the controller and thus different power consumption. In table 5.1 are reported these consumption. As expected the Sport mode has an higher consumption respect respect the Baseline vehicle but also respect the Normal mode. Energy Efficiency mode is able to keep motor losses lower respect the other modes since the contemporary traction and regeneration of the motors is avoided. In this mode the losses of the motor only are also higher because the energy saving is in the slip losses, as showed in section 5.3.

Low Friction mode

Also in case of low friction the controller is able to improve the performance of the vehicle, increasing the yaw rate that passes from $9,6\ deg/s$ to $13,7\ deg/s$ and reducing the oscillation at equilibrium. Compared to high friction condition the yaw rate and lateral acceleration are lower, as the reference generator adapt to the lower friction conditions and so lower maximum forces that tyres can develop. Sideslip angle increase consistently but

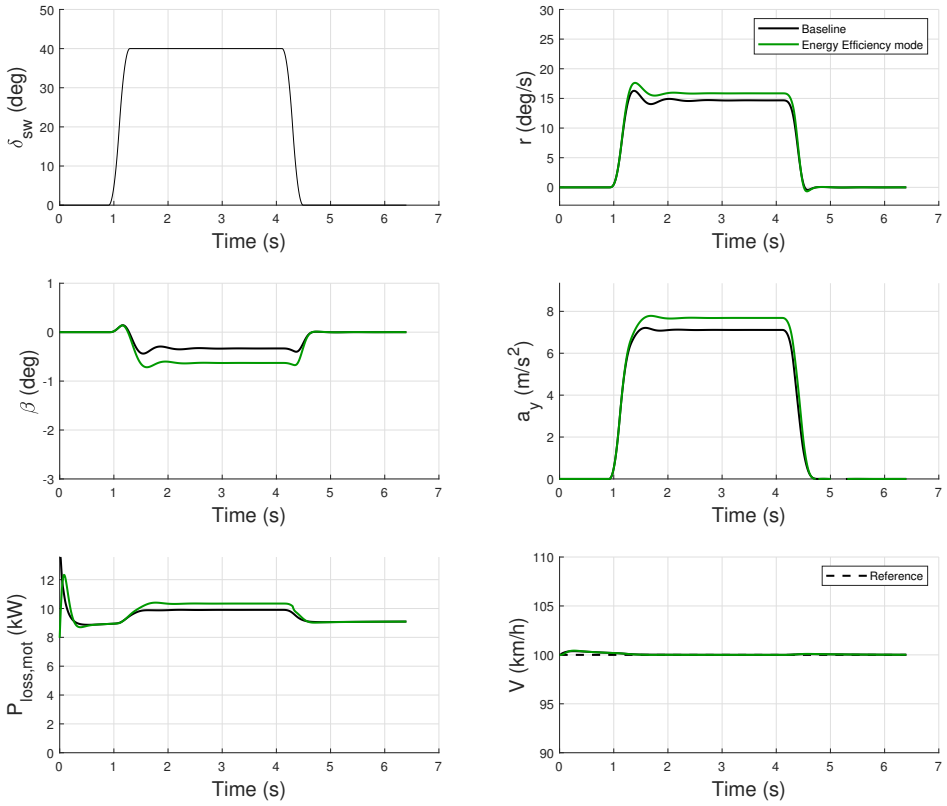

Figure 5.12: Step steer manoeuvre on high friction road. Comparison of Baseline vehicle and Energy Efficiency mode of the controller.

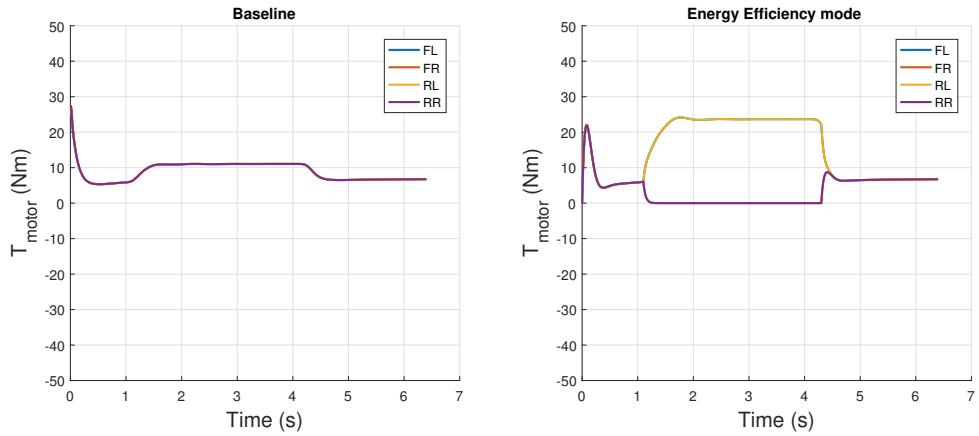

Figure 5.13: Torque evolution of step steer manoeuvre on high friction road. Comparison of Baseline vehicle and Energy Efficiency mode mode of the controller. In right figure torques on each side are superimposed since they are distributed equally.

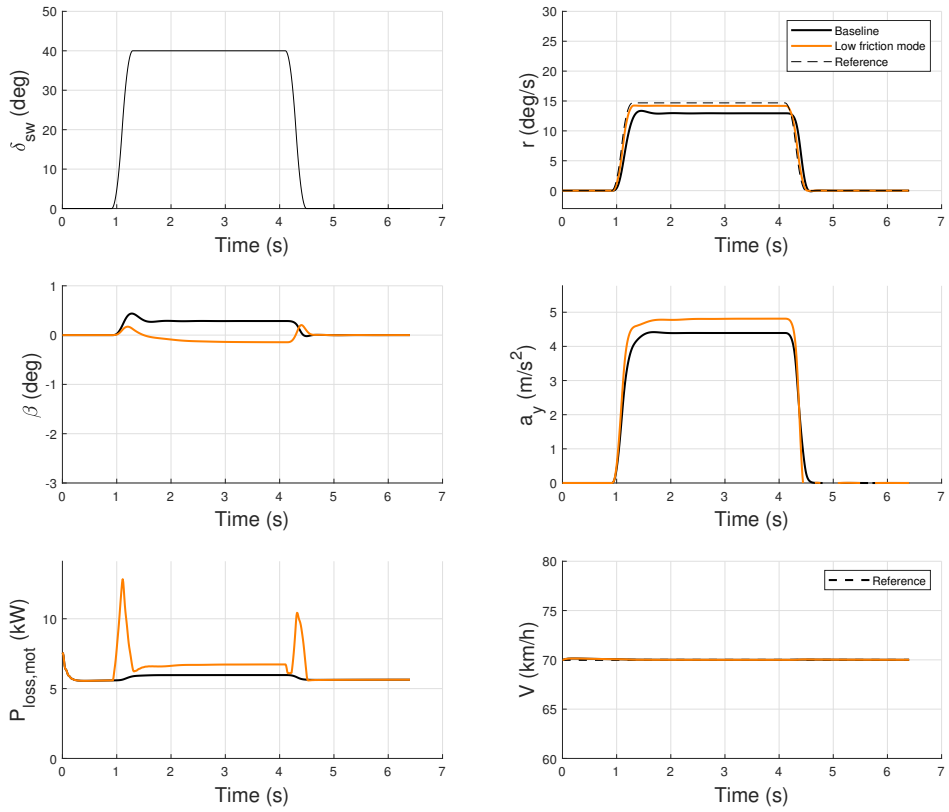

Figure 5.14: Step steer manoeuvre on low friction road. Comparison of Baseline vehicle and Low Friction mode of the controller.

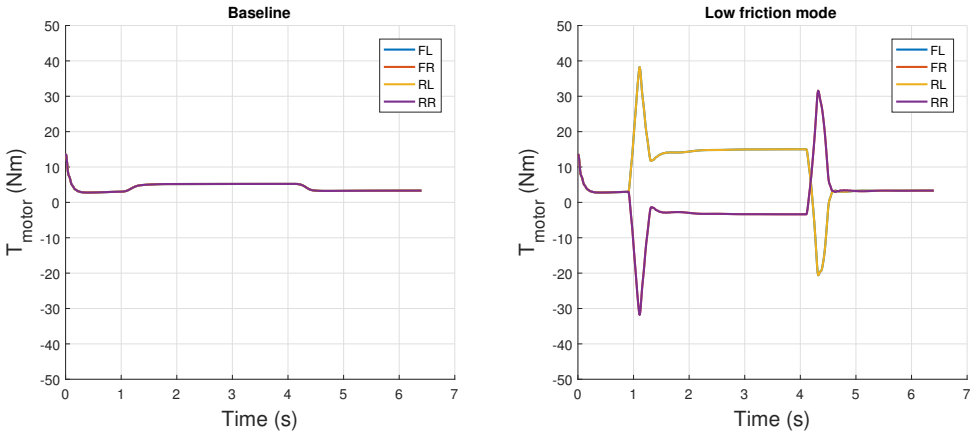

Figure 5.15: Torque evolution of step steer manoeuvre on low friction road. Comparison of Baseline vehicle and Low Friction mode mode of the controller. In right figure torques on each side are superimposed since they are distributed equally.

remains under the limit of 5 deg imposed on the controller, showing how also this value is correctly controlled. The power losses in this mode are higher as the control action is consistent, with an increase in the power losses of almost 10 % with respect to Baseline vehicle. Also lateral acceleration has an increase in its maximum value, passing from $4,6\ m/s^2$ to $5\ m/s^2$. The speed is maintained without problems even in this conditions. Figure 5.15 exhibits two peaks of torque in correspondence of the change of steer, showing the consistent action of the motor to stabilise the vehicle for low friction conditions. Motor power losses are 10,8 % higher in this case showing two peaks in correspondence of the steer changes, when the control action stabilises the vehicle.

5.2.2 Close loop manoeuvre: Double lane change

The behaviour of the vehicle in a more realistic scenario is taken with a double lane change manoeuvre, where a specific path is imposed to the vehicle that is followed thanks to the developed driver model, explained in Section 3.1.3. This is meant to show the real behaviour of the vehicle in a typical manoeuvre that can be taken by a driver. The initial speed is set at 100 km/h in high friction condition and 55 km/h in low friction condition. The gas pedal is kept in rest position during all the time of the manoeuvre, thus the total torque T_{tot} output of the high level controller is zero. Normal, Sport and Low Friction driving modes have been tested. The objective of this test is to show the effectiveness of the high level controller to stabilise the vehicle in limit friction conditions showing the different behaviour of the vehicle for different understeer characteristic imposed by the controller. The capacity to save energy cannot be evidenced in limit friction conditions as explained in Section 5.3 where a specific manoeuvre was designed for this purpose. Energy Efficiency mode was thus excluded by the comparison.

Normal mode

Results related to Normal driving mode are reported in Figure 5.16. In this scenario the vehicle with the Torque Vectoring controller performs better the manoeuvre, following better the reference path. The most evident advantage is in the evolution of the steer input of the driver where the average steer angle is lower passing from 90 deg of the Baseline vehicle to 60 deg in Normal mode. This is perceived by the driver as a better control feeling because the steering wheel have to be rotated less, with a lower steering speed. It is worth to consider that the driver model implemented is simplified and does not does not exactly reproduce the behaviour of a real driver. For example if a real driver has to rotate more the steering wheel and to an higher speed, its accuracy to give the correct steering input to follow a certain path would decreases. As a consequence the real advantage introduced by the TV controller would be even more consistent.

The yaw rate and the sideslip angle have also a better evolution, with less inversions. Moreover, despite the steer input decrease in the first part of the manoeuvre, the yaw rate in the correspondent part has an increased value, again because of the increased linear responsiveness of the vehicle. In the second part of the manoeuvre is clear how the controllability of the vehicle is improved as there are less inversion of the steer and yaw rate.
Regarding the sideslip angle, this is increased during the first part of the manoeuvre but remaining under the prefixed value β_{MAX} set in the controller. In the second part is

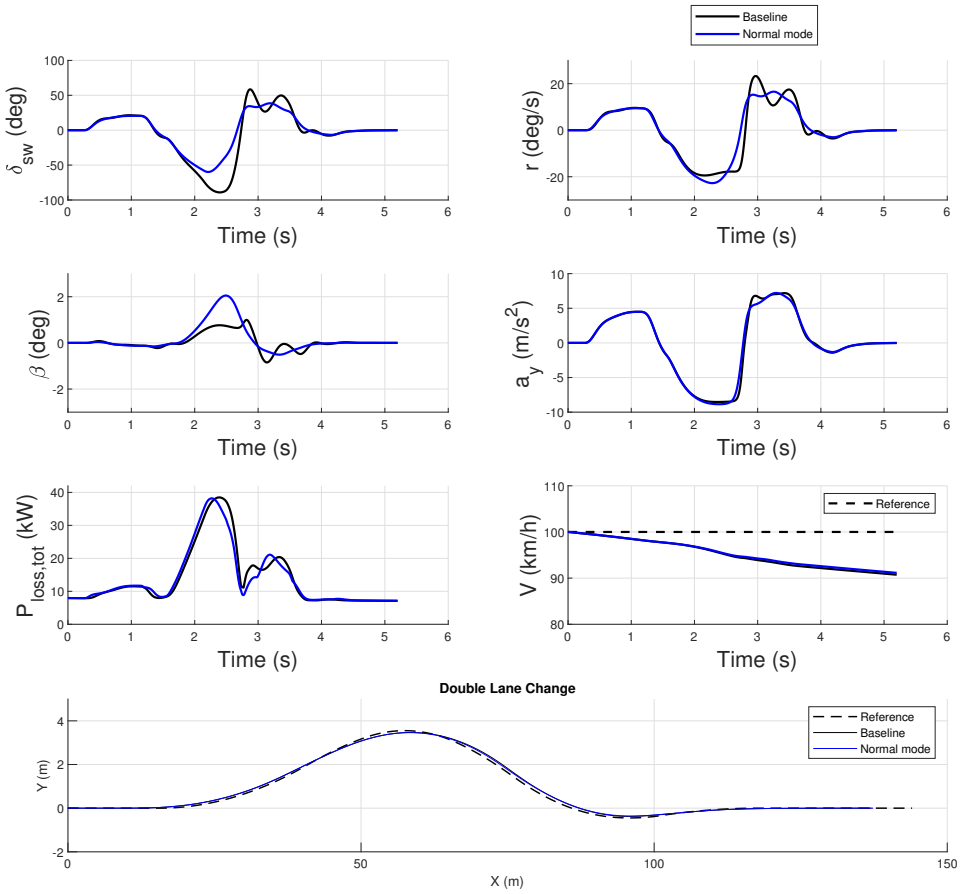

Figure 5.16: Double lane change manoeuvre on high friction road. Comparison of Baseline vehicle and Normal mode of the controller.

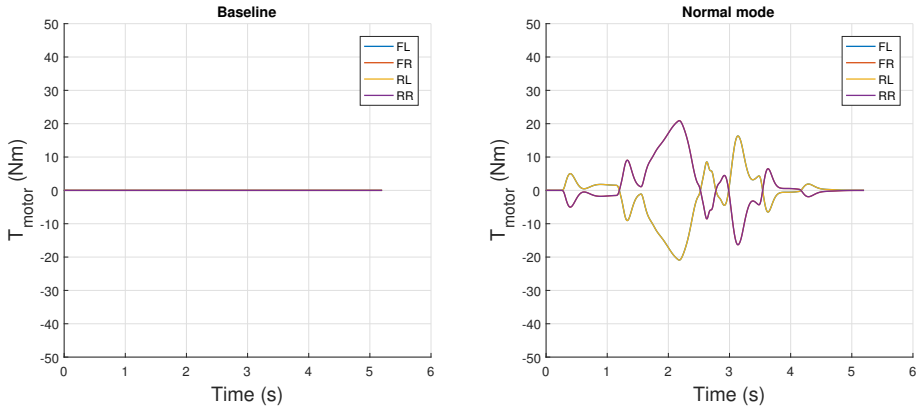

Figure 5.17: Torque evolution for double lane change manoeuvre on high friction road. Comparison of Baseline vehicle and Normal mode of the controller.

present again the smoothing effect as in the other quantities. Lateral acceleration does not increase with the TV controller.

Another interesting effect of the yaw rate controller is the reduction of the total power losses, associated to motor and tyre slips, in the last part of manoeuvre. This is again the effect of the TV controller that stabilises the vehicle reducing the energy losses associated to slips because the steer and thus lateral forces are lower. For this manoeuvre the energy saving was of 1.57 %.
Both the control logic lose approximately 10 km/h during the manoeuvre, with a slightly better result for the TV controller because of the power losses decrease effect described.

Figure 5.17 reports the torques of the motors, that for the Baseline vehicle are obviously null. Regarding the TV controller is worth to report how the motors are not saturated and thus there is still a margin to improve manoeuvrability or to have non null total torque required by the driver. In both cases the manoeuvre is completed by the vehicles with less significant path difference between the two.

Sport mode

In Sport mode the results (Figure 5.18) are similar but with an increased responsiveness of the steer with respect to Normal mode. The steering wheel has now lower peaks, passing to 51 deg (-9 deg with respect to Normal mode) and the yaw rate tends instead to increase in absolute value, with peaks of -23 deg/s and 17 deg/s. The overall energy required for this manoeuvre is now 3,7 % higher with respect to Baseline vehicle, showing how the control action is higher as the variation of the understeer characteristic with respect to the Baseline vehicle is higher (i.e. in Sport mode the controller tries to lower the understeer coefficient $K_u s$). This is also evidenced in the motor torque (Figure 5.19) where the peak values are higher with respect to Normal mode.

Low Friction mode

When the controller is tested in the Low Friction mode, the advantages brought by the controller are quite clear. The Baseline vehicle loses the control in the final part of the manoeuvre while the with TV the reference path is well followed. Steer is again contained, with an evident difference in the peaks of steering wheel, that pass from -230 and 360 deg to -127 and 103 deg. Again despite a lower steer input the yaw rate has an increase in absolute value that has peaks of 22 deg/s in absolute value.

The sideslip angle has an increase again but remaining within the limits. Baseline remains with a β angle under 1 deg in absolute value, while the TV controlled vehicle reach a peak

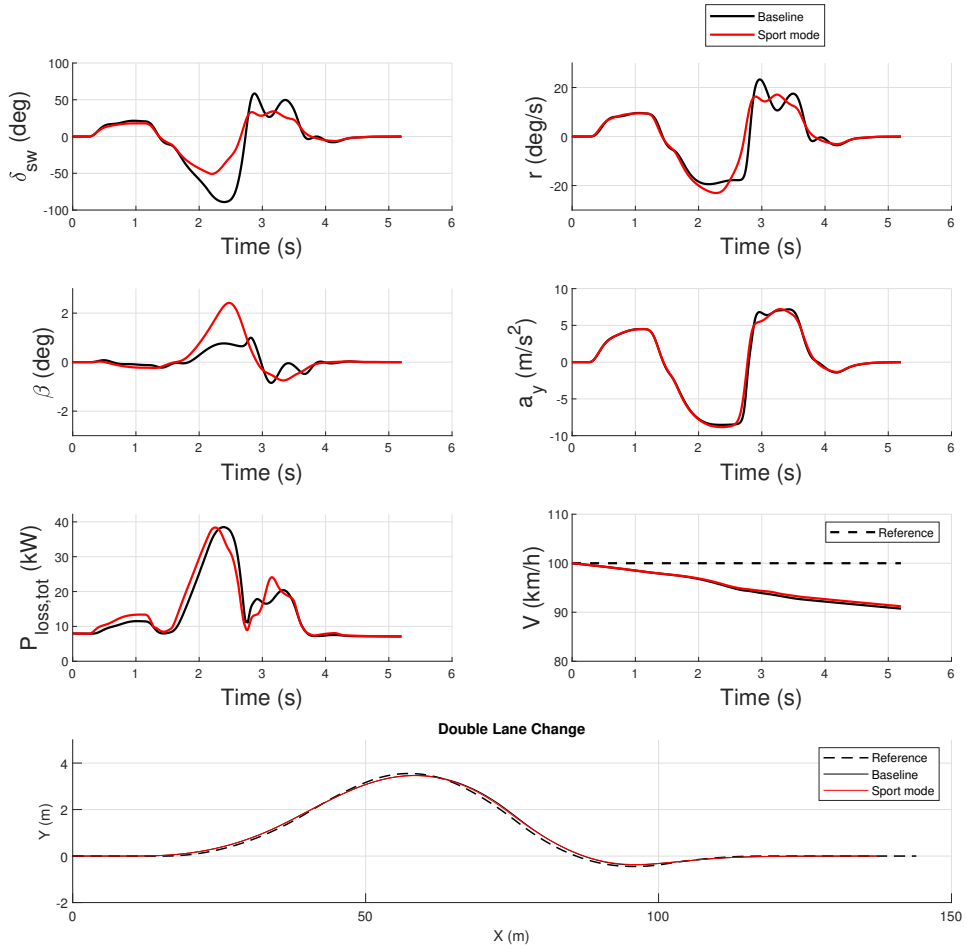

Figure 5.18: Double lane change manoeuvre on high friction road. Comparison of Baseline vehicle and Sport mode of the controller.

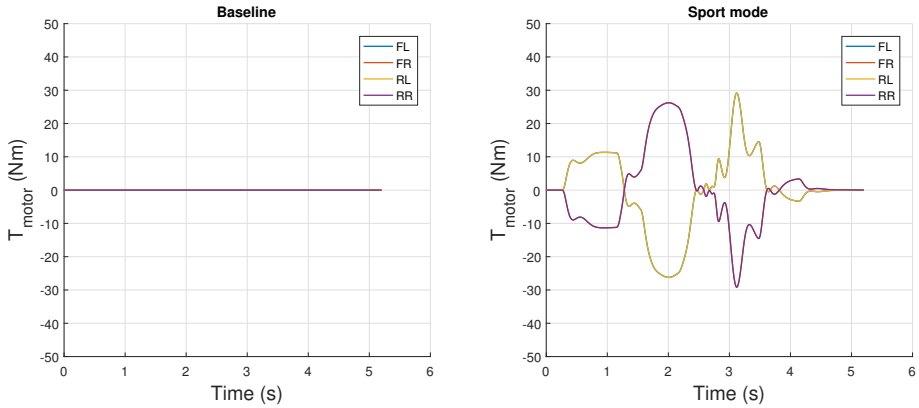

Figure 5.19: Torque evolution for double lane change manoeuvre on high friction road. Comparison of Baseline vehicle and Sport mode of the controller.

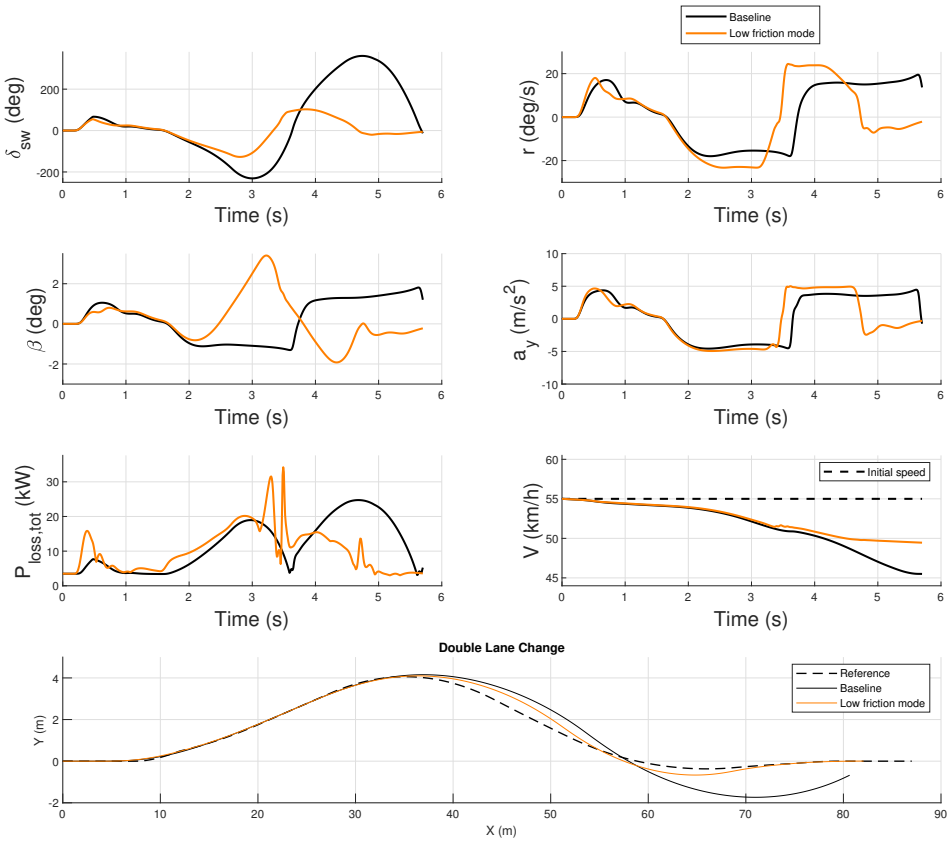

Figure 5.20: Double lane change manoeuvre on low friction road. Comparison of Baseline vehicle and Low Friction mode of the controller.

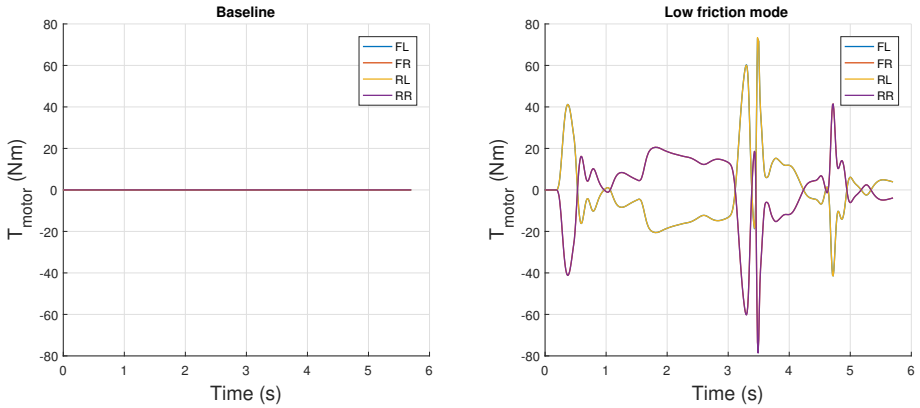

Figure 5.21: Torque evolution for double lane change manoeuvre on low friction road. Comparison of Baseline vehicle and Low Friction mode of the controller.

of 3 *deg*, that is equal to the prefixed maximum of 3 *deg*. Also in this case the stabilisation of the controller permits to decrease the total power losses by 13 %. The advantage of the TV controller is also evident in the speed evolution as the decrease of speed is also quite evident, again for better stability of the vehicle in the second part of the manoeuvre. However between 3 and 4 seconds the losses show some peaks that are also found in the power torque evolution 5.21. This is due to the intervention of the Yaw Index controller that detects an instability as observable from the sideslip angle β evolution. Thus the YI controller decrease the LQR contribute and impose a yaw moment opposite to the yaw rate, to stabilise the vehicle but hinging it to follow the path and the reference yaw rate. Then when the vehicle is stabilised the yaw rate error is bigger and the LQR tries to follow the reference giving a bigger yaw moment. This may be perceived as uncomfortable by the driver and a filter on the yaw moment might be implemented to limit this effect.

5.3 Energy Efficiency mode: energy saving evaluation

To verify the effectiveness of the Energy Efficiency mode, it was simulated another close loop manoeuvre (bottom plot in Figure 5.22) called *Mild Slalom*, where again a specific path is imposed and followed using the driver model illustrated in Section 3.1.3. The manoeuvre was designed to test the energy saving of the Energy Efficiency mode that is compared with Normal and Sport mode. The vehicle have to move to one side with a lateral displacement of 5 meters, going straight for a sufficient time to permits to reach a steady state equilibrium, then it moves to the other side of 10 meters, letting again enough time and finally it turns again of 5 meters. The total torque is kept at a constant value of 50 Nm, giving to the vehicle a slight longitudinal acceleration of $0,4\ m/s^2$. It is typical indeed for a D segment vehicle to face corners with low or null longitudinal acceleration. Initial speed is set to 70 km/h under high friction conditions and it was used the driver model explained is section 3.1.3. This manoeuvre is more appropriate to test the Energy Efficiency driving mode as it is in sub-limit conditions, typical of normal driving conditions, with peaks of lateral accelerations are around 7 m/s^2 that are not in limit conditions of friction, as can be seen in figure 5.1(a). It was not used a standard driving cycle like the NEDC (New European Driving Cycle) because this kind of driving cycle is not designed to account also of benefits of a TV controller, since the vehicle is proceeding straight.

The plots in Figure 5.23 shows the evolution of the power losses, respectively of longitudinal slip, lateral slip and motors. The most relevant power losses are associated with lateral slip, with peaks over 16 kW, and motor losses that are around 8 kW, while longitudinal slip losses are less than $0,2\ kW$ also because the accelerations are supposed to remain low. Applying the Energy Efficiency mode the TV is able to decrease the lateral slip losses since the yaw moment applied decrease cornering resistance and at the same time the increase of motor and longitudinal losses is not excessive. In this manoeuvre the overall energy save is of 1,4 % (right bottom plot in Figure 5.25). The same manoeuvre performed in Normal mode (Figures 5.25 and 5.26) has an energy consumption of 2,8 % higher than Baseline vehicle, thus the energy saving of Energy Efficiency mode with respect to Normal mode is 4,2 %. Setting Sport mode (Figures 5.27 and 5.28) results a consumption higher of 7 %, 9,8 % higher respect Energy Efficiency mode. The increase of performance and the energy consumption have a non linear correlation since to pass from Normal to Sport mode the energy consumption increases of 4.2 %. while the increase of performances is limited.

In Figure 5.24 are showed the differences in term of power consumption of the Energy Efficiency mode with the Baseline vehicle, in term of absolute value and percentage. The energy balance is almost always in favour of the Energy Efficiency mode with peaks of

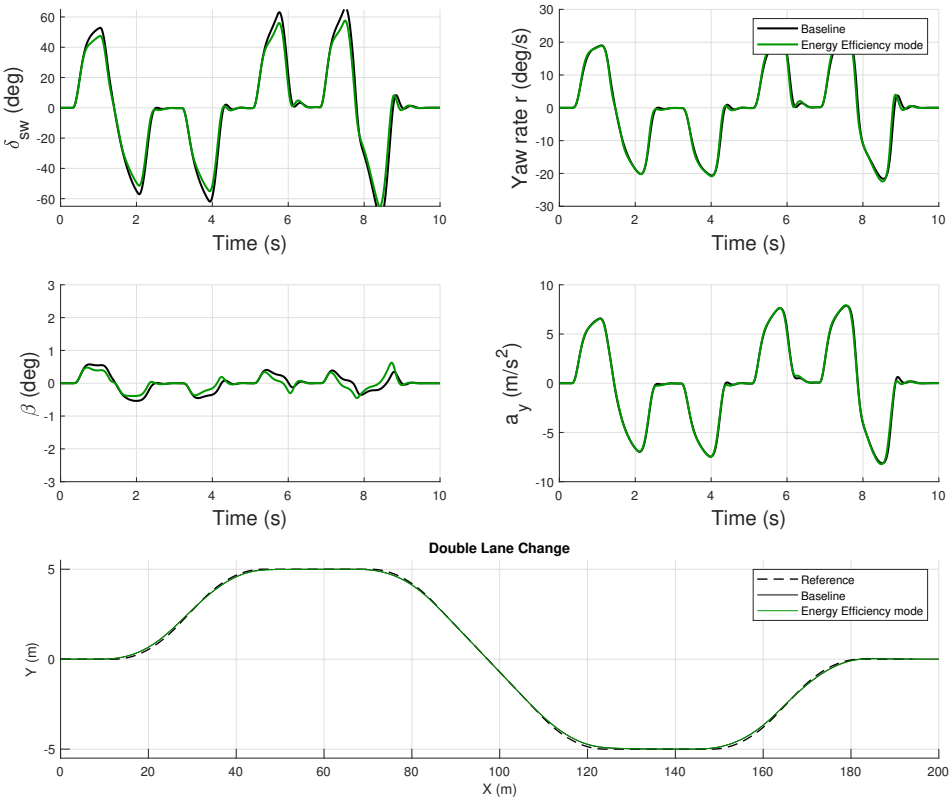

Figure 5.22: Mild slalom to test the Energy Efficiency mode, compared with Baseline vehicle. Initial speed is set to 70 km/h and a the total torque imposed equal to 50 Nm.

energy saving of 2 kW and 7 % respectively. It is important to notice that the two manoeuvre are not perfectly aligned in time so the comparison of energy save in term of absolute value and percentages of Figures 5.24, 5.26 and 5.28 is qualitative. However is clear in upper left plot that the strategy is effective as the lateral slip power losses are always decreased. Is interesting to observe the evolution of the motor power losses in bottom left plot of Figures 5.23, 5.25 and 5.27. In Energy Efficiency mode the increase is less that 1 kW while passing to Normal and Sport mode has Increases of several kW when TV is active. This shows how the efficiency of the motor is a key aspect and with other motor models may be obtained different results.

Also in this manoeuvre is shown how in Energy Efficiency mode the responsiveness of the vehicle has a little improvement as the steer needed to perform the manoeuvre (upper left plot in Figure 5.22) decreases.

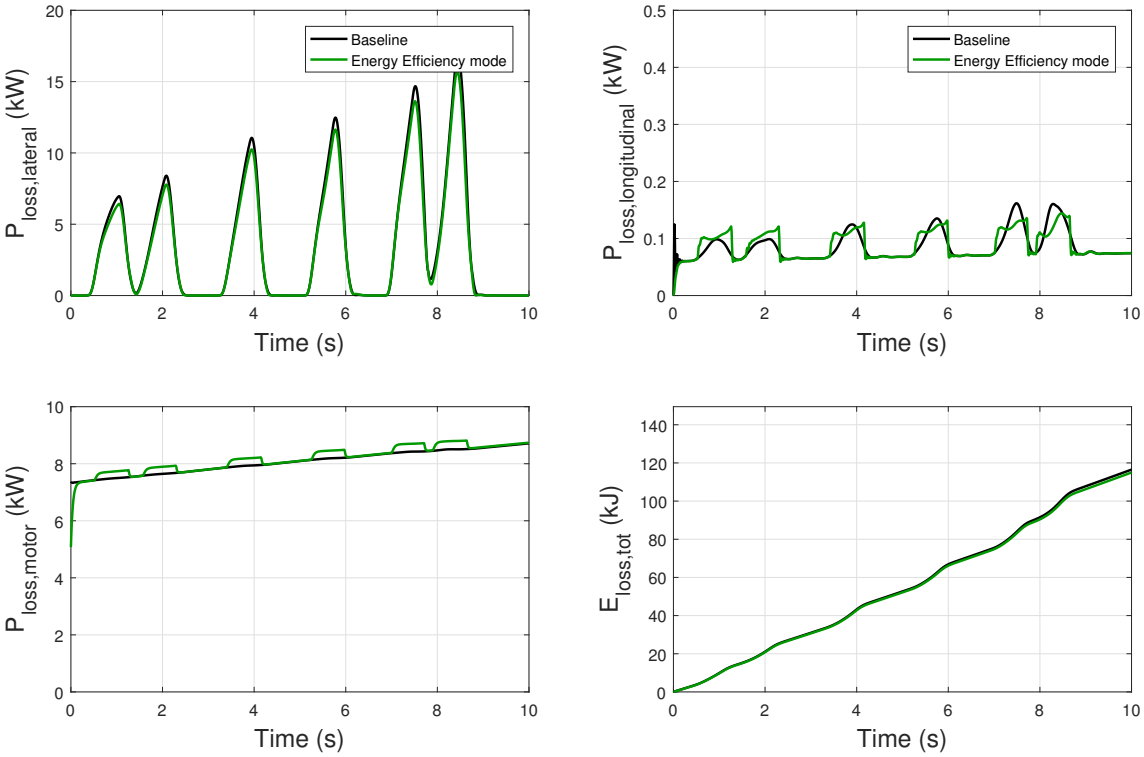

Figure 5.23: Power and energy losses of the mild slalom manoeuvre.

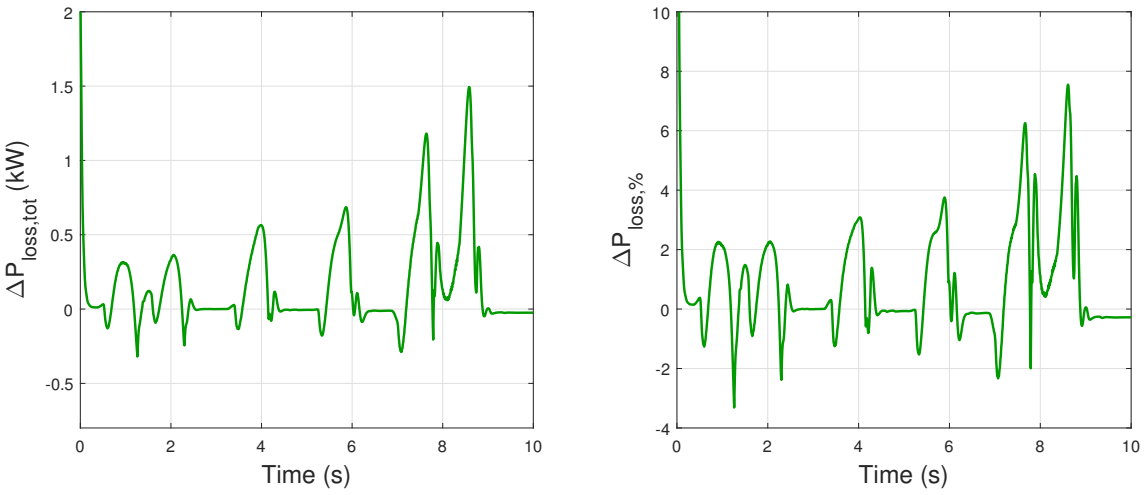

Figure 5.24: Power and energy losses of the mild slalom manoeuvre. Comparison of energy saving in term of absolute power losses and percentage during the manoeuvre.

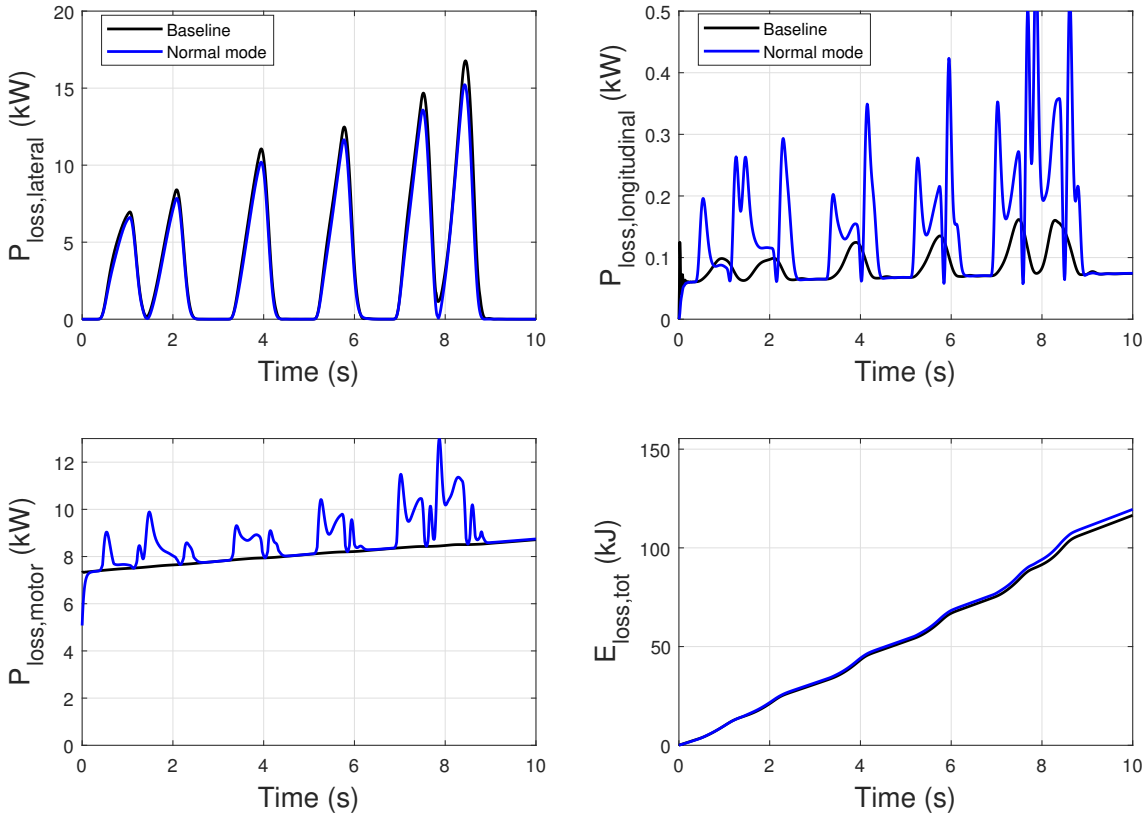

Figure 5.25: Power and energy losses of the mild slalom manoeuvre in Normal mode.

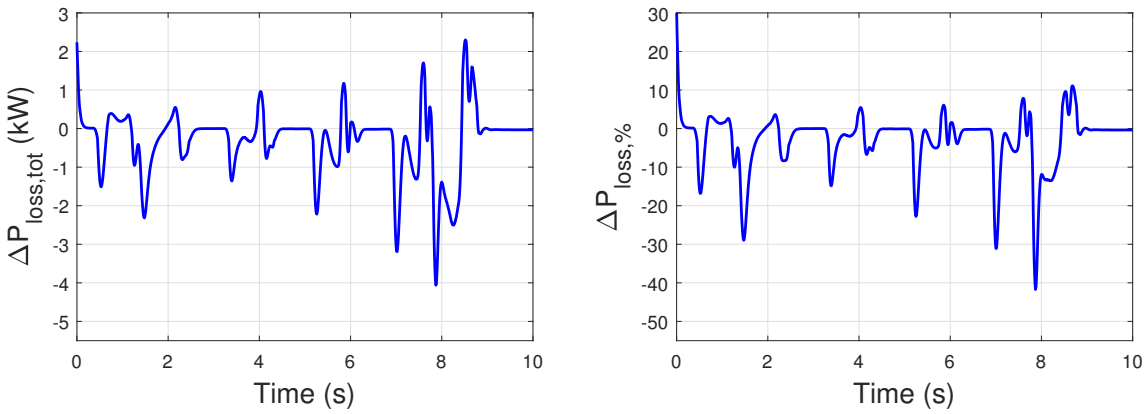

Figure 5.26: Power and energy losses of the mild slalom manoeuvre in Normal mode. Comparison of energy saving in term of absolute power losses and percentage during the manoeuvre.

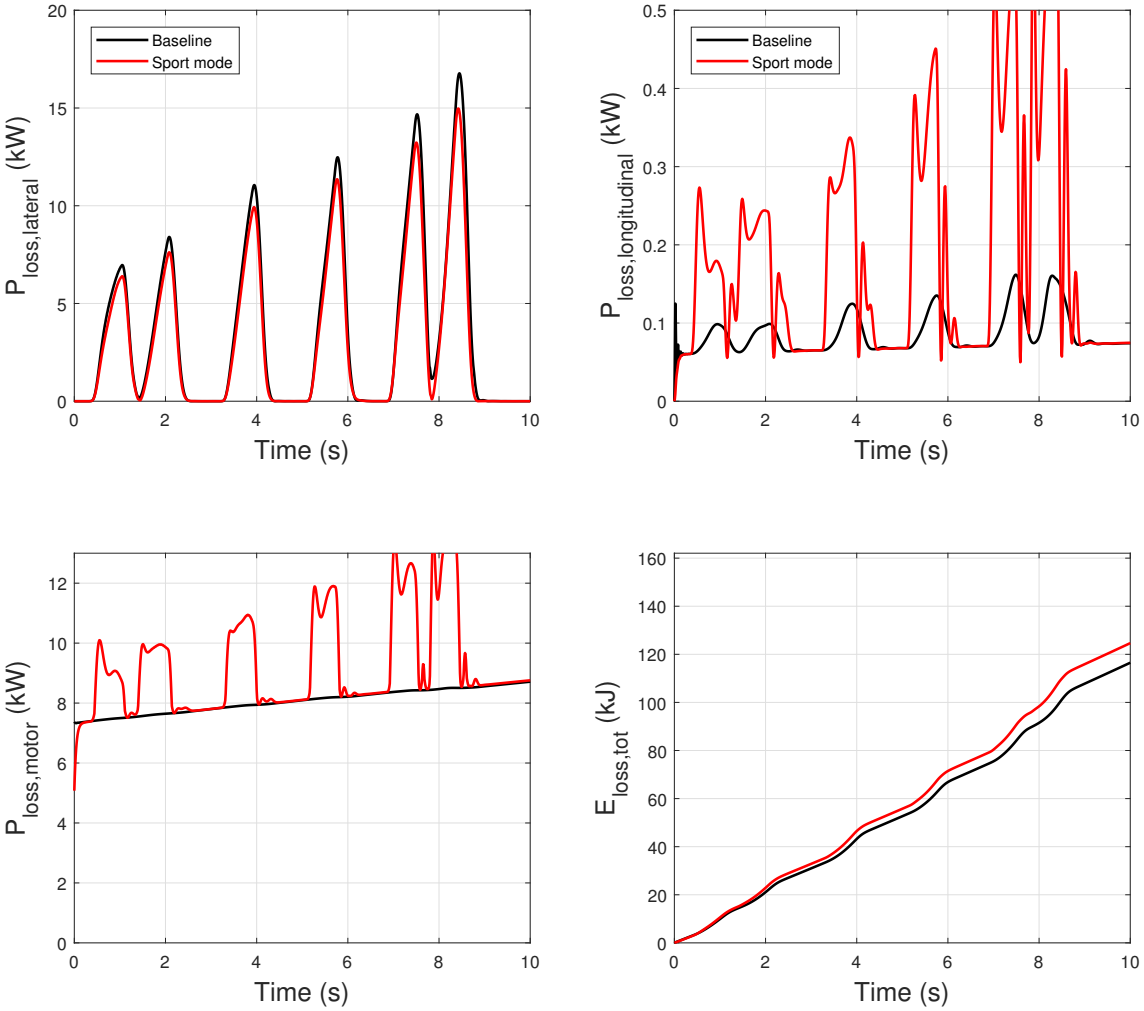

Figure 5.27: Power and energy losses of the mild slalom manoeuvre in Sport mode.

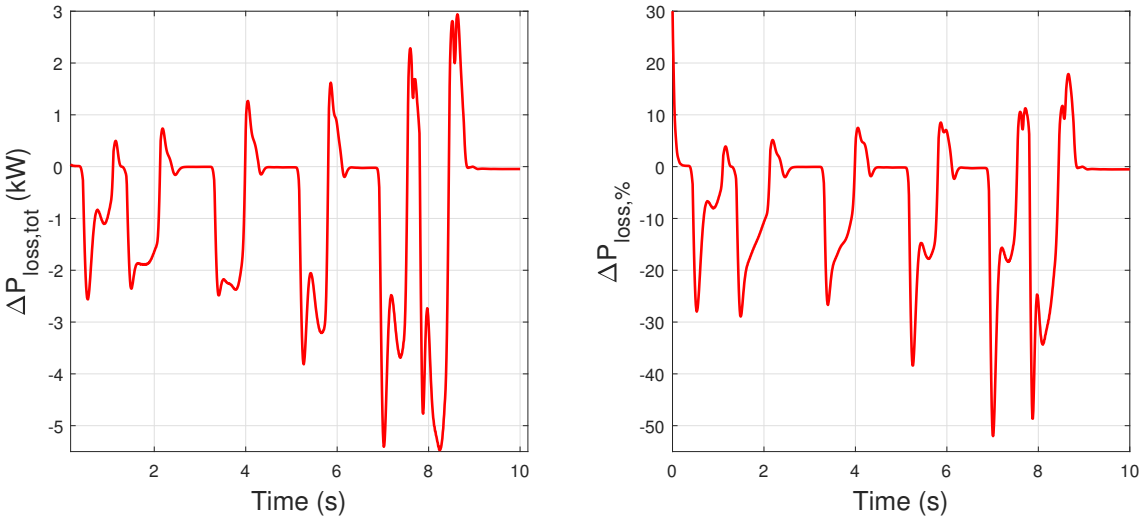

Figure 5.28: Power and energy losses of the mild slalom manoeuvre in Sport mode. Comparison of energy saving in term of absolute power losses and percentage during the manoeuvre.

Chapter 6

Conclusions

The work presented shows a solution of a Torque Vectoring controller that leads to the following conclusions:

1. It confirms the typical control structure of a TV controller but evidence how these are not completely separated and a good controller solution have to well integrates all its parts.

2. It is possible to set algorithms to take into account multiple control objectives, by implementing the so called driving modes. Each mode influences the vehicle dynamic in a different way and with specific control objectives.

3. Specific control strategies are able to use Torque Vectoring to optimise energy efficiency rather than imposing an understeer characteristic, thus potentially extending the range of an electric vehicle. Also in this case there is a little improvement of the performance.

Regarding point 1 it is clear how the reference generator needs to provide a solution that is coherent with the high level controller characteristics. Indeed some high level controllers need both the reference on the yaw rate r and sideslip angel β, while others use only the yaw rate reference and sideslip angle is considered to correct the yaw rate reference itself. A notable example of this second approach is presented in (B. Lenzo, 2017)[17]. Anyway mostly of the scientific literature considers one of these two approaches, showing how an effective solution cannot exclude the sideslip angle. Moreover it was showed how in case energy efficiency is prioritised the reference generator is not necessary. This means also that the characteristic curve of the vehicle in this case is modified but not defined. Also in the low level controller two different logic are implemented for the two cases of imposed yaw moment modes and Energy Efficiency mode. In the proposed controller the Energy Efficiency mode exclude the high level controller part that defines the yaw moment M_z,

however may be possible to compute a correlation that defines the yaw moment minimising losses in function of the vehicle state and thus this kind of solution implies two different high level controller logic (one minimising power losses and the other that try to follow the references), again showing how also in this case the high level controller and the low level controller are not completely separated. The reason of the differences in the controller structure between Energy Efficiency mode and the other modes arise because the method used to define the yaw moment are completely different. In case of efficiency optimisation yaw moment is defined based on energetic consideration on power losses, while in the other cases it is defined by a controller that follow the understeer characteristic, bringing to two different algorithms.

The realisation of different driving modes showed how in the same controller can integrate different algorithms that, with proper setting of parameters can change in different ways the vehicle dynamic and power losses. The two main objectives in a Torque Vectoring controller are the energy efficiency and the vehicle dynamic improvement in term of performance, and each mode implemented sets a different trade-off between them, prioritising one or the other. In Sport and Normal mode the vehicles performance are increased as evidenced in the Steering pad, in the Step-steer and Double Lane Change manoeuvre. These are higher in Sport mode but implies and higher level of intervention of the controller, causing higher power losses. In general the more the understeer characteristic is modified respect the baseline vehicle the more is the energy consumption required. If energy efficiency is prioritised the power losses can be decreased as showed in Mild Slalom and Steering pad manoeuvres. At the same time the performance of the vehicle are increased as showed in Steering pad and Step-steer manoeuvre, because the yaw moment imposed to increase performance is concordant with the yaw rate. Improvements are limited as the increase in term of responsiveness is limited as seen in the Steering pad and the oscillations in transient conditions are not substantially decreased, as evidenced in the Step-Steer.
Figure 6.1 represents exactly the trade-off between energy efficiency and performances, where each mode is on a different position of the optimal line. The Baseline vehicle is not on this line since the solution is not optimal.

When dealing with a Torque Vectoring controller is typical to use it to improve the performance of the vehicle, however it was showed how this kind of controller can be used prioritising only the energy efficiency, decreasing the energy consumption when driving in non limit friction conditions. In this case, still the performances of the vehicle has a little improvement. Increase of efficiency is not assured in case of aggressive driving, however in those conditions the efficiency would be compromised anyway and so any control strategy

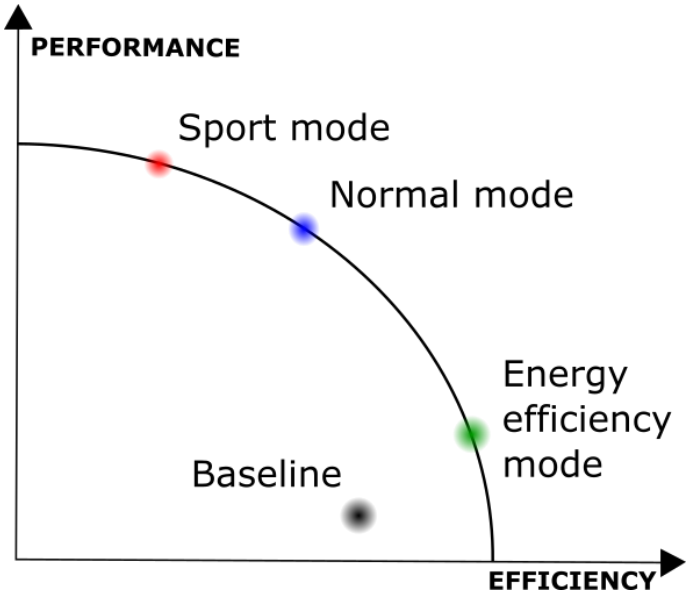

Figure 6.1: Trade-off of each driving mode between performances and efficiency, compared with Baseline vehicle.

regarding power consumption minimisation would be vanished. It was showed also how in Energy Efficiency mode the structure of the Torque Vectoring controller radically changes, where some parts of the controller are not used and others has a different settings.

Bibliography

[1] Massimo Ceraolo, Antonio Di Donato, and Giulia Franceschi. Experimental evaluation of energy efficiency of batteries for hybrid - electric vehicles. University of Pisa.

[2] Federico Cheli, Elisabetta Leo, Stefano Melzi, and F Mancosu. A 14dof model for the evaluation of vehicle's dynamics: numerical–experimental comparison. *International Journal of Mechanics and Control*, 6(2):19–30, 2006.

[3] Long Chen, Te Chen, Xing Xu, Yingfeng Cai, Haobin Jiang, and Xiaoqiang Sun. Multi-objective coordination control strategy of distributed drive electric vehicle by orientated tire force distribution method. *IEEE Access*, 6:69559–69574, 2018.

[4] Giovanni De Filippis, Basilio Lenzo, Aldo Sorniotti, Patrick Gruber, and Wouter De Nijs. Energy-efficient torque-vectoring control of electric vehicles with multiple drivetrains. *IEEE Transactions on Vehicular Technology*, 2018.

[5] Leonardo De Novellis, Aldo Sorniotti, and Patrick Gruber. Optimal wheel torque distribution for a four-wheel-drive fully electric vehicle. *SAE International Journal of Passenger Cars-Mechanical Systems*, 6(2013-01-0673):128–136, 2013.

[6] Leonardo De Novellis, Aldo Sorniotti, and Patrick Gruber. Wheel torque distribution criteria for electric vehicles with torque-vectoring differentials. *IEEE Transactions on Vehicular Technology*, 63(4):1593–1602, 2014.

[7] Leonardo De Novellis, Aldo Sorniotti, and Patrick Gruber. Driving modes for designing the cornering response of fully electric vehicles with multiple motors. *Mechanical Systems and Signal Processing*, 64:1–15, 2015.

[8] Leonardo De Novellis, Aldo Sorniotti, Patrick Gruber, Javier Orus, Jose-Manuel Rodriguez Fortun, Johan Theunissen, and Jasper De Smet. Direct yaw moment control actuated through electric drivetrains and friction brakes: Theoretical design and experimental assessment. *Mechatronics*, 26:1–15, 2015.

[9] Arash M Dizqah, Basilio Lenzo, Aldo Sorniotti, Patrick Gruber, Saber Fallah, and Jasper De Smet. A fast and parametric torque distribution strategy for four-wheel-drive energy-efficient electric vehicles. *IEEE Transactions on Industrial Electronics*, 63(7):4367–4376, 2016.

[10] Ebrahim Esmailzadeh, Avesta Goodarzi, and GR Vossoughi. Optimal yaw moment control law for improved vehicle handling. *Mechatronics*, 13(7):659–675, 2003.

[11] Chunyun Fu, Reza Hoseinnezhad, Alireza Bab-Hadiashar, and Reza N Jazar. Direct yaw moment control for electric and hybrid vehicles with independent motors. *International Journal of Vehicle Design*, 69(1-4):1–24, 2015.

[12] Hiroshi Fujimoto and Shingo Harada. Model-based range extension control system for electric vehicles with front and rear driving–braking force distributions. *IEEE Transactions on Industrial Electronics*, 62(5):3245–3254, 2015.

[13] Tommaso Goggia, Aldo Sorniotti, Leonardo De Novellis, Antonella Ferrara, Patrick Gruber, Johan Theunissen, Dirk Steenbeke, Bernhard Knauder, and Josef Zehetner. Integral sliding mode for the torque-vectoring control of fully electric vehicles: Theoretical design and experimental assessment. *IEEE transactions on vehicular technology*, 64(5):1701–1715, 2015.

[14] Takao Kobayashi, Etsuo Katsuyama, Hideki Sugiura, Eiichi Ono, and Masaki Yamamoto. Direct yaw moment control and power consumption of in-wheel motor vehicle in steady-state turning. *Vehicle System Dynamics*, 55(1):104–120, 2017.

[15] Stefan Koehler, Alexander Viehl, Oliver Bringmann, and Wolfgang Rosenstiel. Improved energy efficiency and vehicle dynamics for battery electric vehicles through torque vectoring control. In *Intelligent Vehicles Symposium (IV), 2015 IEEE*, pages 749–754. IEEE, 2015.

[16] Basilio Lenzo, Giovanni De Filippis, AM Dizqah, Aldo Sorniotti, Patrick Gruber, Saber Fallah, and Wouter De Nijs. Torque distribution strategies for energy-efficient electric vehicles with multiple drivetrains. *Journal of Dynamic Systems, Measurement, and Control*, 139(12):121004, 2017.

[17] Basilio Lenzo, Aldo Sorniotti, Patrick Gruber, and Koen Sannen. On the experimental analysis of single input single output control of yaw rate and sideslip angle. *International Journal of Automotive Technology*, 18(5):799–811, 2017.

[18] Cheng Lin and Zhifeng Xu. Wheel torque distribution of four-wheel-drive electric vehicles based on multi-objective optimization. *Energies*, 8(5):3815–3831, 2015.

[19] Qian Lu, Aldo Sorniotti, Patrick Gruber, Johan Theunissen, and Jasper De Smet. h_∞ loop shaping for the torque-vectoring control of electric vehicles: Theoretical design and experimental assessment. *Mechatronics*, 35:32–43, 2016.

[20] Amin Mahmoudi, Wen L Soong, Gianmario Pellegrino, and Eric Armando. Efficiency maps of electrical machines. In *Energy Conversion Congress and Exposition (ECCE), 2015 IEEE*, pages 2791–2799. IEEE, 2015.

[21] Hans Pacejka. *Tire and Vehicle Dynamics*. Elsevier Science, 3 edition, 2012.

[22] G Parker, J Griffin, and A Popov. The effect on power consumption & handling of efficiency-driven active torque distribution in a four wheeled vehicle. In *The Dynamics of Vehicles on Roads and Tracks: Proceedings of the 24th Symposium of the International Association for Vehicle System Dynamics (IAVSD 2015), Graz, Austria, 17–21 August 2015*, page 97, 2016.

[23] E Siampis, E Velenis, and S Longo. Front-to-rear torque vectoring model predictive control for terminal understeer mitigation. In *The Dynamics of Vehicles on Roads and Tracks: Proceedings of the 24th Symposium of the International Association for Vehicle System Dynamics (IAVSD 2015), Graz, Austria, 17-21 August 2015*, page 153. CRC Press, 2016.

[24] Antonio Tota, Basilio Lenzo, Qian Lu, Aldo Sorniotti, Patrick Gruber, Saber Fallah, Mauro Velardocchia, Enrico Galvagno, and Jasper De Smet. On the experimental analysis of integral sliding modes for yaw rate and sideslip control of an electric vehicle with multiple motors. *International Journal of Automotive Technology*, 19(5):811–823, 2018.

[25] Michele Vignati, Edoardo Sabbioni, and Davide Tarsitano. Torque vectoring control for iwm vehicles. *International Journal of Vehicle Performance*, 2(3):302–324, 2016.

[26] Andy Wong, Dhanaraja Kasinathan, Amir Khajepour, Shih-Ken Chen, and Bakhtiar Litkouhi. Integrated torque vectoring and power management framework for electric vehicles. *Control Engineering Practice*, 48:22–36, 2016.

[27] J. Y. Wong. *Theory of ground vehicles*. Wiley, 4th ed. edition, 2008.

[28] Mattia Zanchetta, Davide Tavernini, Aldo Sorniotti, Patrick Gruber, Basilio Lenzo, Antonella Ferrara, Wouter De Nijs, Koen Sannen, and Jasper De Smet. On the feedback control of hitch angle through torque-vectoring. In *Advanced Motion Control (AMC), 2018 IEEE 15th International Workshop on*, pages 535–540. IEEE, 2018.